NEW 1,3,4-OXADIAZOLE DERIVATIVES AND INVESTIGATION OF THEIR BIOLOGICAL ACTIVITY
Master's Thesis

Sana SAFFOUR

Eskişehir 2022

NEW 1,3,4-OXADIAZOLE DERIVATIVES AND INVESTIGATION OF THEIR BIOLOGICAL ACTIVITY

Sana SAFFOUR

Master's Thesis

Department of Pharmaceutical Chemistry

Supervisor: Prof. Dr. Leyla YURTTAŞ

Eskişehir

Anadolu University

Graduate School of Health Sciences

June 2022

FINAL APPROVAL FOR THESIS

This thesis titled" New 1,3,4-Oxadiazole Derivatives and Investigation of Their Biological Activity" has been prepared and submitted by Sana SAFFOUR in partial fulfillment of the requirements in "Anadolu University Directive on Graduate Education and Examination" for the degree of Master of Science (MS) in Pharmaceutical Chemistry Department has been examined and approved on 28/06/2022.

Committe Members   Signature

Member (Supervisor)   : Prof. Dr. Leyla YURTTAŞ   ……………

Member   : Prof. Dr Ahmet Çağrı KARABURUN   ……………

Member   : Assoc.Prof. Dr. Murat DURAN   ……………

Prof. Dr. Gülşen Akalın ÇİFTÇİ
Director of Graduate School of Health Sciences

ÖZET

Yeni 1,3,4-Oksadiazol Türevleri ve Biyolojik Aktivitelerinin Araştırılması

Sana SAFFOUR

Farmasötik Kimya Anabilim Dalı

Anadolu Üniversitesi, Sağlık Bilimleri Enstitüsü, Haziran 2022

Danışman: Prof. Dr. Leyla YURTTAŞ

1,3,4-Oksadiazol hem endüstriyel hem de farmasötik disiplinlerde geniş çapta işlevselleştirilmiş bir heterosiklik yapı iskelesidir. Son zamanlarda, çeşitli hastalık türlerini tedavi etmek için çok sayıda 1,3,4-oksadiazol içeren yapılar kullanılmıştır. Alzheimer hastalığı (AH), kolinerjik nöronların ölümü ve monoamin oksidaz-B (MAO-B) enziminin artışı ile karakterize karmaşık, çok faktörlü ve ilerleyici bir hastalıktır. Bu tezde, bir dizi yeni 1,3,4-oksadiazol-kinolin hibridi bileşik sentezlenmiş ve asetilkolinesteraz (AChE), bütirilkolinesteraz ve MAO enzimlerinin potansiyel inhibitörleri olarak biyolojik olarak değerlendirilmiştir. Tüm nihai bileşiklerin kimyasal yapıları, ^{1}H-NMR, ^{13}C-NMR ve kütle spektrometrileri kullanılarak doğrulanmıştır. Bileşikler arasında, **5a, 5c** ve **6a**, sırasıyla 0.033 μM, 0.096 μM ve 0.177 μM IC_{50} değerleriyle AChE'a karşı önemli aktivite göstermiştir. En güçlü moleküller olan **5a, 5c** ve **6a**'nın bağlanma modları ve yapı-aktivite ilişkisi, moleküler yerleştirme kullanılarak belirlenmiş ve onaylanmıştır. Bileşik **5a**, AChE'nin hem katyonik anyonik site (CAS) hem de periferik anyonik site (PAS) ile etkileşime girerek ek bir nöroprotektif etki sağlayarak benzersiz bağlanma özellikleri oluşturmuştur. Sentezlenen bileşiklerin fizikokimyasal özellikleri de değerlendirilmiştir.

Anahtar Sözcükler: 1,3,4-Oksadiazol, Kinolin, Alzheimer hastalığı, Antikolinesteraz, Monoamin oksidaz inhibisyonu.

ABSTRACT

New 1,3,4-Oxadiazole Derivatives and Investigation of Their Biological Activity

Sana SAFFOUR

Department of Pharmaceutical Chemistry

Anadolu University, Graduate School of Health Sciences, June 2022

Supervisor: Prof. Dr. Leyla YURTTAŞ

1,3,4-Oxadiazole is a heterocyclic scaffold that is functionalized widely in both industrial and pharmaceutical disciplines. Recently, a large number of 1,3,4-oxadiazole-containing structures have been used to treat diverse types of diseases. Alzheimer's disease (AD) is a complex, multifactorial and progressive disease characterized by the death of cholinergic neurons and upregulation of monoamine oxidase (MAO-B) enzyme. In this thesis, a series of novel 1,3,4-oxadiazole-quinoline hybrids have been synthesized and biologically evaluated as potential inhibitors of acetylcholinesterase (AChE), butyrylcholinesterase and MAOs enzymes. The chemical structures of all final structures were confirmed using IR, ^{1}H-NMR, ^{13}C-NMR and mass spectrometry. Among all the compounds, **5a**, **5c** and **6a** possessed substantial activity against AChE with IC_{50} values of 0.033 µM, 0.096 µM and 0.177 µM, respectively. The binding modes and structural activity relationship (SAR) of the most potent structures **5a**, **5c** and **6a** have been provided and confirmed using molecular docking. Compound **5a** has established unique binding properties by interacting with both catalytic anionic site (CAS) and peripheral anionic site (PAS) of the AChE providing an additional neuroprotective effect. The physicochemical properties of the synthesized structures have been also evaluated.

Keywords: 1,3,4-Oxadiazole, Quinoline, Alzheimer's disease, Anticholinesterase, Monoamine oxidase.

ACKNOWLEDGEMENT

STATEMENT OF COMPLIANCE WITH ETHICAL PRINCIPLES AND RULES

28/06/2022

I hereby truthfully declare that this thesis is an original work prepared by me; that I have behaved in accordance with the scientific ethical principles and rules throughout the stages of preparation, data collection, analysis and presentation of my work; that I have cited the sources of all the data and information that could be obtained within the scope of this study, and included these sources in the references section; and that this study has been scanned for plagiarism with "scientific plagiarism detection program" used by Anadolu University, and that "it does not have any plagiarism" whatsoever. I also declare that, if a case contrary to my declaration is detected in my work at any time, I hereby express my consent to all the ethical and legal consequences that are involved.

Sana SAFFOUR

TABLE OF CONTENTS

LIST OF TABLES

LIST OF FIGURES

LIST OF ABBREVIATIONS

^{13}C-NMR	:	Carbon-13 nuclear magnetic resonance
^{1}H-NMR	:	Proton nuclear magnetic resonance
2D	:	Two-dimensional
3D	:	Three-dimensional
4-PSQ	:	7-Chloro-4-(phenylselanyl) quinoline
5-HT	:	Serotonin
Å	:	Angstrom
AChE	:	Acetylcholinesterase
AD	:	Alzheimer's Disease
AMPA	:	α-Amino-3-hydroxy-5-methyl-4-isoxazolepropionic acid
APP	:	Amyloid precursor protein
Aβ	:	β-amyloid
BACE-1	:	β-secretase
BBB	:	Blood-brain barrier
Bu$_3$P	:	Tributylphosphine
BuChE	:	Butyrylcholinesterase
CAS	:	Catalytic anionic site
CAT	:	Chloramine T
CDI	:	*N,N*-carbonyldiimidazole
ChE	:	Cholinesterase
CS$_2$	:	Carbon disulfide
DA	:	Dopamine
DCC	:	*N,N*-dicyclohexylcarbodiimide
DCE	:	1,2-Dichloroethane
DMC	:	Dimethylimidazolinium chloride
DMF	:	Dimethylformamide
DMSO	:	Dimethyl sulfoxide
EDC	:	1-Ethyl-3-(3-dimethylaminopropyl)carbodiimide
GSK-3β	:	Glycogen synthase kinase-3 beta
HMDS	:	Hexamethyldisilazane
HRMS	:	High-resolution mass spectroscopy

IC$_{50}$	:50% Inhibitory concentration
J	: Coupling constant
M.P	: Melting point
m/z	: Mass/charge
MAO	: Monoamine oxidase
NE	: Norepinephrine
NFT	: Neurofibrillary tangles
NMDAR	: *N*-Methyl-d-aspartate receptors
PAS	: Peripheral active site
PEA	: Phenylethylamine
Ph$_3$P	: Triphenylphosphine
PIDA	: Phenyliodine (III) diacetate
p-TsCl	*: Para*-tosylchloride
ROS	: Reactive oxygen species
TEA	: Triethylamine
THF	: Tetrahydrofuran
TLC	: Thin-layer chromatography
TPSA	: Topological surface area
UV	: Ultraviolet

1. INTRODUCTION

Alzheimer's disease (AD) is a progressive neurodegenerative disease that known to affect the elderly, named after the German psychiatrist Alois Alzheimer the first person who described the disease's hallmarks in 1906. Alzheimer's disease is mainly characterized by abnormal β-amyloid plaque depositions, intraneuronal neurofibrillary tangles (NFT) formation, and neuronal loss [1]. Alzheimer's disease is considered the leading cause of dementia that affects more than 55 million people nowadays around the world according to the World Health Organization [2].

Alzheimer's disease early symptoms arise as memory-related difficulties, apathy and depression proceeding with communication impairment, disorientation, behavioral changes, swallowing and walking difficulties that interfere with the patient's regular activities [3, 4].

Although the disease's etiology is not fully understood, the disease's hallmarks are probably driven by various factors including genetic susceptibility, psychosocial issues, biological factors, vascular disorders including high blood pressure, obesity, diabetes, elevated cholesterol levels, alcohol consumption, and smoking cigarettes [5].

Tremendous efforts have been made with a view to tracking the underlying neuropathological pathways proposing several hypotheses that explain the resulted pathological changes. Assorted studies suggest that β-amyloid (Aβ), the primary component of senile plaques that are defined as lesions in the brain, is the leading cause of pathophysiological alterations and cognitive dysfunction in AD. Aβs, 40-42 amino acid peptides, are produced by transmembrane glycoprotein amyloid precursor protein (APP). Gene mutations cause abnormal APP splitting by secretase enzymes into neurotoxic Aβ oligomers which eventually turn into senile plaques that accumulate in the extracellular regions causing neuronal signal termination, cognitive functions declining and neuronal cell death [3, 6]. It has been also reported that Aβ induces intracellular neurofibrillary tangles formation and neuronal loss by producing reactive oxygen species (ROS) and nitric oxides and inducing neuro-inflammatory cascades [7, 8]. Therefore, secretase enzymes that are included in the APP splitting process are considered potential targets for disease treatment and some inhibitors have reached clinical phases II and III. However, none of them have so far succeeded to reach the market due to their divergent role in homeostasis and other cellular functions thus higher selectivity inhibitors must be developed [9, 10].

Other studies attribute cognitive impairment and memory loss to Tau protein abnormal hyperphosphorylation and neurofibrillary tangles formation that destroy neuronal microtubules causing cell death [11].

It has been also evidenced that monoamine oxidase (MAO) enzymes are responsible for hydrogen peroxide species which are in turn involved in oxidative stress and ROS formation leading to neurodegenerative cascades through lipid, protein and DNA oxidative damage inducement [12, 13]. MAOs are flavin-containing enzymes that have a prominent role in the oxidative deamination of neurotransmitters in peripheral tissues and central nervous system. MAOs are subdivided into two distinct isoforms, MAO-A and MAO-B exhibiting differential substrate and inhibitor specificity with disparate tissue distribution. MAO-A subtype is mainly included in the oxidative deamination of norepinephrine (NE) and serotonin (5-HT) neurotransmitters, and is predominantly found in gastrointestinal, liver, placenta and pulmonary vascular endothelium; whereas MAO-B retains a higher selectivity towards benzylamine and phenylethylamine (PEA) oxidation and substantially located in blood platelets. Catecholamines such as dopamine, epinephrine, norepinephrine and tyramine are considered substrates for both isoenzymes [14, 15].

Moreover, it has been found that MAO-B is upregulated in Alzheimer's-diseased brains and its activity is noticeably increased up to three-fold in particular brain parts, especially in plaque-associated astrocytes [16]. Several MAO-B inhibitors such as selegiline, rasagiline and lazabemide have been used so far, aiming to hinder Alzheimer's disease-associated neurodegenerative process through various neuroprotective mechanisms. It is proposed that MAO-B inhibitors have the ability to improve AD by decreasing free radical formation, preventing environmental pre-toxins activation and exhibiting protective effects against neuronal damage and apoptosis [17]. Therefore, various studies have been conducted aiming to synthesize potent and safe MAO inhibitors [18].

Another prevalent suggestion is the cholinergic hypothesis which established the prominent damage of the cholinergic pathways that play a vital role in neural function, learning and plasticity in the brain. Two cholinesterase enzymes are included in this pathway, acetylcholinesterase (AChE) and butyrylcholinesterase (BuChE) [19].

The primary cholinergic neurotransmitter acetylcholine is mainly hydrolyzed by AChE into acetic acid and choline regulating the level of acetylcholine (ACh) in normal

brains (**Figure 1.1**). However, in AD acetylcholine levels are noticeably reduced in the synaptic gaps due to the higher acetylcholine degradation rate and cholinergic neuronal degeneration resulting in synaptic transmission termination between the neurons [20]. Therefore, acetylcholine deficiency is responsible for memory loss, learning deficits and cognitive function deterioration associated with Alzheimer's disease. Furthermore, cholinergic neurons loss plays an extensive role in other disease aspects worsening that are implicated in progressive Aβ accumulation, inflammation and oxidative stress [3, 21].

Thus, acetylcholinesterase inhibitors are used as first-line pharmacologic interventions to restore acetylcholine levels by prolonging the neurotransmitter duration of action providing a symptomatic treatment for AD [3].

Although butyrylcholinesterase's role is not fully understood, BuChE activity is progressively upregulated in the advanced stages of Alzheimer's disease becoming the main acetylcholine hydrolyzing enzyme [22]. Experimental studies suggested that dual inhibitors of both AChE and BuChE have implicated with higher therapeutic benefits [23]. While other studies proved that BuChE inhibitors are able to hinder amyloid-beta fibril formation and aggregation [24].
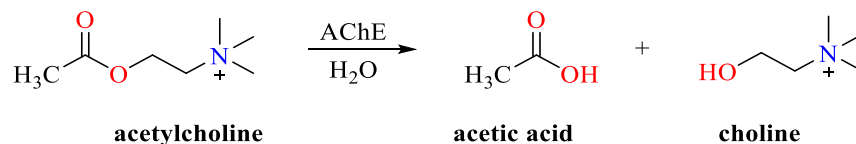
Figure 1.1 *Acetylcholine hydrolysis*

The first approved drug for Alzheimer's disease was tacrine which acted as cholinesterases inhibitor. However, due to its critical hepatotoxicity, it is no longer used [25]. Currently, available agents provide symptomatic relief by increasing levels of acetylcholine via cholinesterase inhibitors including donepezil, rivastigmine and galantamine which are generally prescribed in mild to moderate cases, or by *N*-Methyl-d-Aspartate Receptor (NMDAR) inhibitor memantine that commonly used in moderate conditions as adjunctive therapy along with cholinesterase inhibitors (**Figure 1.2**) [6].

Recently in 2021, the first disease-modifying immunotherapy aducanumab has been approved for mild cognitive impairment or mild Alzheimer's. Although aducanumab is proposed to work by removing abnormal beta-amyloid and reducing the

number of plaques in the brain, the drug's aptitude to slow-down cognitive functions impairment remains uncertain, therefore it should be prescribed with caution [26, 27].
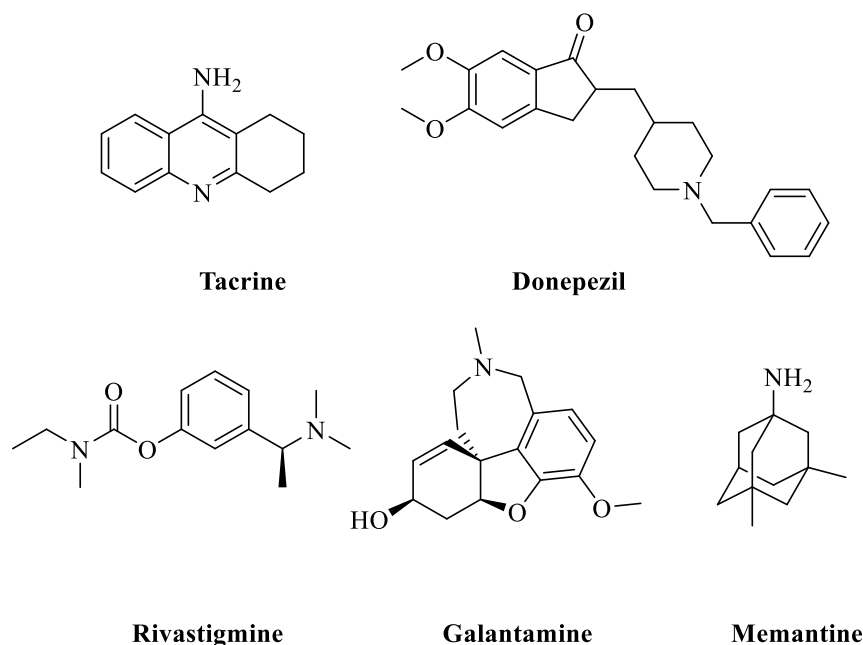
Figure 1.2 *Anti-Alzheimer agents*

On the basis of research that established AChE and BuChE dual inhibition ability to promote therapeutic efficacy, ameliorate cognitive function and evade AChE upregulation [28], several investigations have been carried out to develop highly efficient anticholinesterase analogues [29, 30].

On the other hand, recent research approaches predominately aim to develop and design novel agents that incorporate combinations of bioactive pharmacophores in a single structure that has the ability to show different modes of action minimizing the metabolic load and drug-drug interaction possibilities and improving treatment efficiency [31].

The necessity to develop multi-target agents directed the researchers towards heterocycle-based design to produce effective anti-Alzheimer drugs [32]. According to literature, various heterocycles possess anti-Alzheimer activity including indole [33], coumarin [34], pyridine [35], carbazole [36], piperidine [37], pyrrolidine [38], pyrazole [39], thiazole [40], etc.

One of the most biologically active heterocycles is oxadiazole or furadiazole five-membered ring that bears one oxygen, two nitrogen and two carbon atoms in its

constitution [41]. According to nitrogen atoms' positions, oxadiazole exists in different isomeric forms. However, 1,3,4-oxadiazoles isoform has been considered a vital synthon in the drug design and development process due to its expansive chemical and biological properties. For instance, 1,3,4-oxadiazole derivatives tend to behave as antiviral, antimalarial, anti-inflammatory, antimicrobial, antioxidant, anticancer, anti-convulsant [42-44], etc. Therefore , various 1,3,4-oxadiazole containing agents are found in the market including, raltegravir (antiretroviral), tiodazosin and nesapidil (antihypertensive), zibotentan (anticancer), and furamizole (antibacterial agent) (**Figure 1.3**) [43].
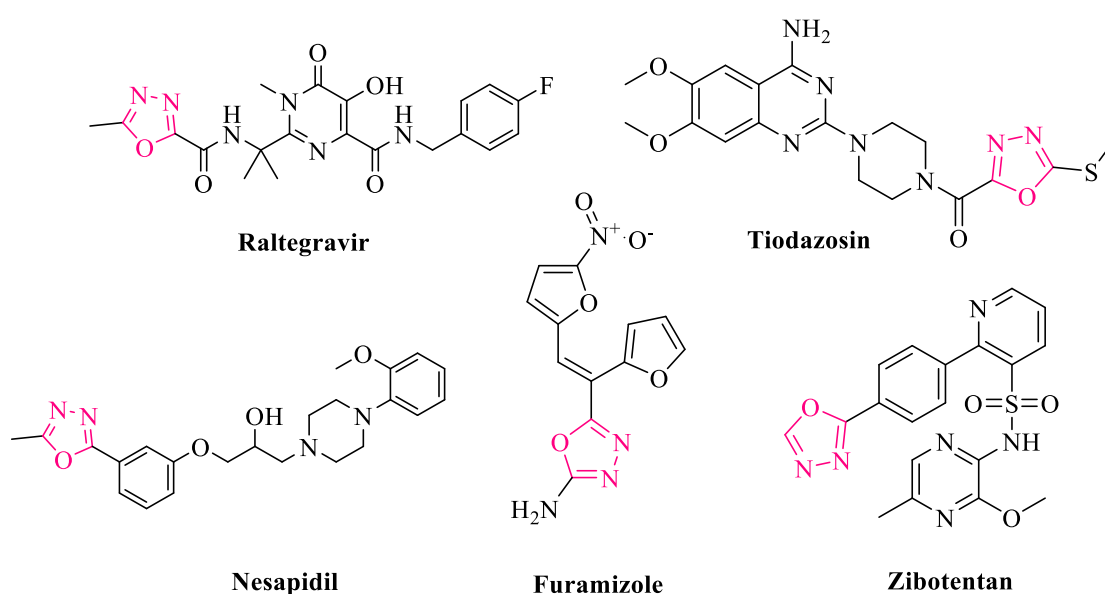
Figure 1.3. *Drugs containing oxadiazole ring*

Recently, 1,3,4-oxadiazole derivatives have demonstrated an outstanding aptness to modulate Alzheimer's disease through several pathways. For instance, various derivatives established a neuroprotective effect against Aβ induced toxicity [45]. Other compounds proved a glycogen synthase kinase-3β (GSK-3β) inhibitory activity which afforded a reduction in tau hyperphosphorylation and β-amyloid production [46-49]. It has also been established that numerous 1,3,4-oxadiazole derivatives retain anticholinesterase [50] and monoamine oxidase inhibitory actions which play an essential role in AD pathogenesis [51, 52].

Another interesting fundamental heterocycle core is quinoline or 1-aza-naphthalene or benzo[b]pyridine ring which is defined as a planner hetero-aromatic structure composed of benzene and pyridine rings fused to each other with a molecular formula of

C_9H_7N [53]. Quinoline exhibits weak base properties and can also participate in both nucleophilic and electrophilic substitution reactions [54].
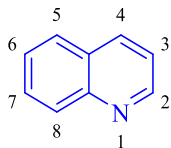
Figure 1.4. *Chemical structure and numbering of quinoline*

Quinoline-containing compounds have generated considerable interest in the medicinal chemistry of heterocyclic compounds due to their wide spectrum pharmacological activity [55]. Among them, quinoline has been found to possess antimalarial [56], antihypertensive, anticonvulsant [57], anti-inflammatory [58], anticancer [59], antibacterial [60], antifungal [61], antioxidant activities [62], etc.

Quinoline is a part of several clinically approved drugs in the market including the cholesterol-lowering agent pitavastatin, the antineoplastic tipifarnib, the antibacterial ciprofloxacin and the antiretroviral saquinavir (**Figure 1.5**).
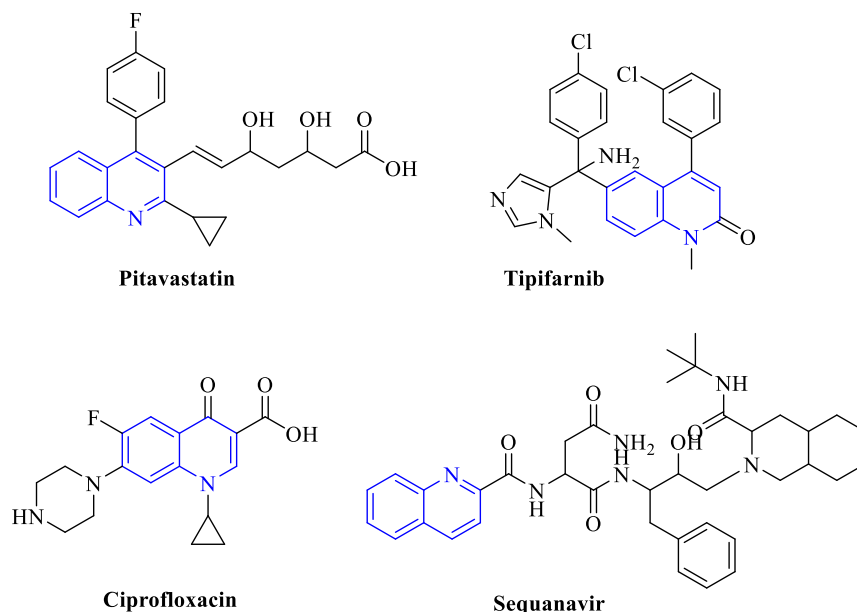
Figure 1.5. *Drugs containing quinoline ring*

Based on the previous research, we attempted to synthesize several compounds incorporating quinoline and 1,3,4-oxadiazole cores in their skeleton to pursue a better

therapeutic profile in the continuation of the ongoing investigations on Alzheimer's diseases related to simultaneously targeting cholinesterase/ monoamine oxidase enzymes inhibition. Furthermore, we intended to further analyze the most potent candidates *in-silico* by applying molecular docking technique to predict the relevant ligand-receptor binding clues.
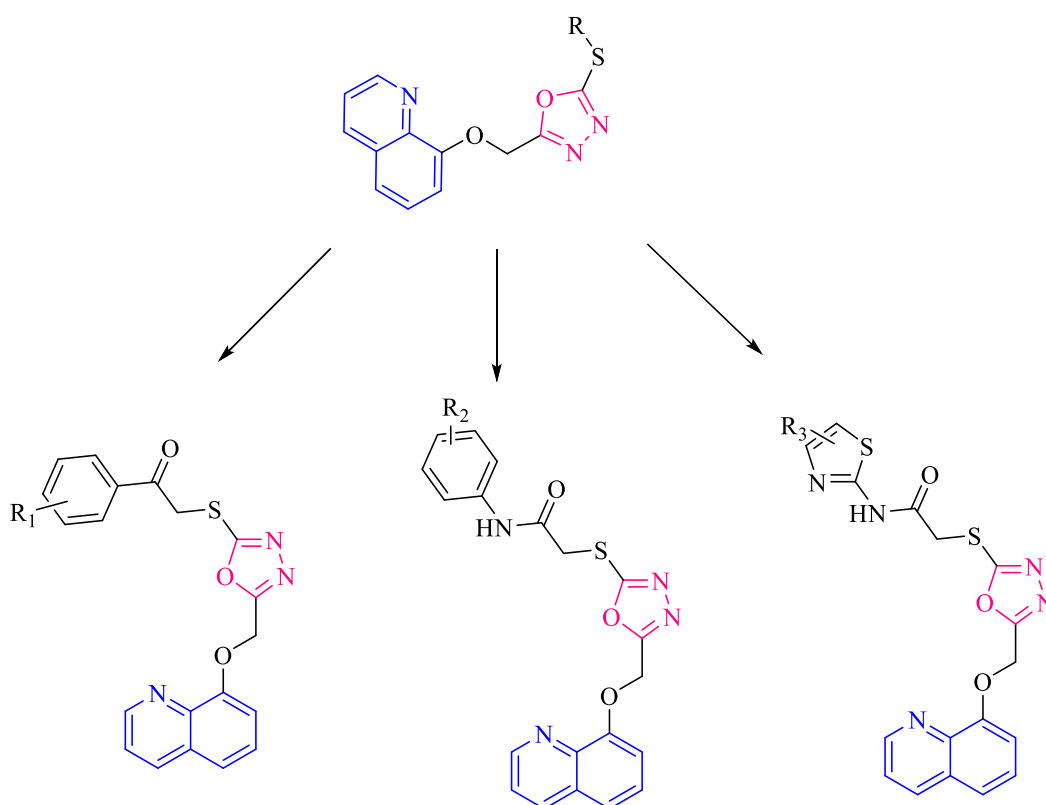
Figure 1.6. *Targeted structures' general representation*

Table 1. *Targeted 2-[(substituted)thio]-5-[(quinolin-8-yloxy)methyl]-1,3,4-oxadiazole products*

	R₁				R₂				R₃	
4a	4b	4c	4d	5a	5b	5c	6a	6b	6c
-H	4-CH₃	4-OCH₃	2,5-di-OCH₃	4-Cl	4-F	4-OCH₃	4,5-di-CH₃	4-CH₃, 5-COOEt	4-phenyl

2. LITERATURE REVIEW

2.1. Oxadiazole Chemistry

Oxadiazoles are heterocycle structures that could be defined in four different isomers according to the positions of nitrogen atoms. These isomers are 1,2,4-oxadiazole (**a**), 1,2,5-oxadiazole (**b**), 1,3,4-oxadiazole (**c**) and 1,2,3-oxadiazole (**d1**) as shown in (**Figure 2.1**). However, 1,2,3-oxadiazole is considered unstable due to ring opening and formation of diazoketone tautomer (**d2**). All these isomers possess the same general formula of $C_2H_2ON_2$ [63].
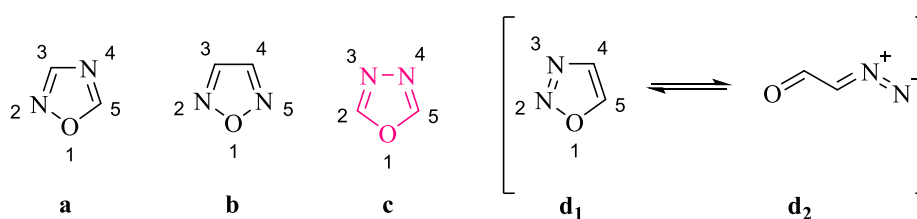
Figure 2.1. *Oxadiazole isomers*

Due to its pharmacological applications versatility, 1,3,4-oxadiazole isoform is considered an auspicious core that offers a wide range of application in the field of medicinal chemistry [64]. One of the most interesting oxadiazole attributes is its aptness to be metabolized by ring cleavage in the body [65].

1,3,4-Oxadiazole tends to act as a weak base because of the inductive effect resulted from the extra heteroatom. The presence of the 1,3,4-oxadiazole ring has an impact on the entire compound's physicochemical and pharmacokinetic properties. In some circumstances, it serves as a flat aromatic linker to retain the structure orientation [66]. Furthermore, oxadiazoles are considered virtuous bio-isosteres for relatively unstable carbonyl-containing groups such as amides, esters, carbamates and hydroxamic esters [67].

In 1965, 1,3,4-oxadiazole was first synthesized and isolated as a liquid having a boiling point of 150° C by Ainsworth starting from ethyl formate (formyl hydrazine) by thermolysis process (**Figure 2.2**) [42].
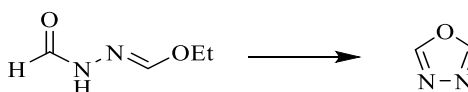
Figure 2.2. *1,3,4-Oxadiazole formation by thermolysis*

A myriad of 1,3,4-oxadiazole synthesis procedures has been reported earlier to afford the 1,3,4-oxadiazole ring [68, 69]. According to the literature, the most prevalent method to synthesize 1,3,4-oxadiazoles is the cyclodehydration of a preformed ring skeleton using dehydrating agents such as phosphorus oxychloride, thionyl chloride, chlorosulphonic acid, phosphorus pentoxide, oleum, phosphoric acid, zinc chloride, etc. The ring might also be closed through condensation reaction by alcohol, carboxylic acid, mercaptans, or hydrogen cyanide elimination (**Figure 2.3**). Some 1,3,4-oxadiazole derivatives are able to be performed through oxidative cyclization using an oxidizing agent. Furthermore, various ring systems such as pyrazoles, hydantoins, and tetrazole have the ability to convert into oxadiazole structures [70].
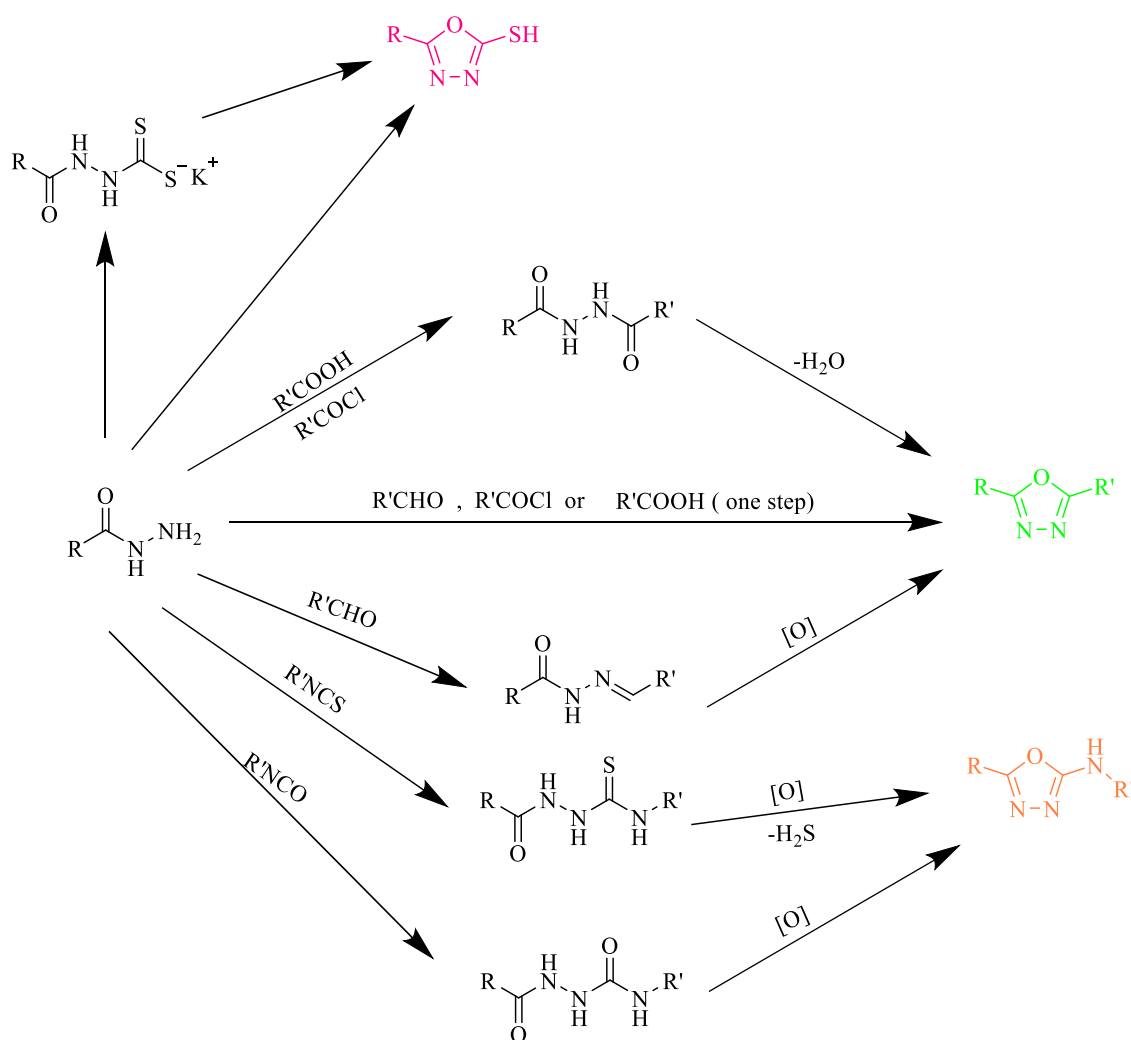
Figure 2.3. *1,3,4-Oxadiazole synthesis pathways*

.

2.1.1. 5-Substituted-1,3,4-oxadiazole-2-thiols synthesis methods

In 1952, Hoggarth proved that 2-phenyl-5- mercapto-1,3,4-oxadiazole could be prepared through methyl 2-benzoyldithiocarbazinate ester and salts cyclization. These esters and salts are produced through acyl hydrazine refluxing with carbon disulfide in pyridine [71].

Later in 1954, Young and Wood prepared a series of 2-substituted-5-mercapto-l,3,4-oxadiazoles by direct refluxing of hydrazides and carbon disulfide mixture in alcoholic potassium hydroxide without acyldithiocarbazic acid esters isolation (**Figure 2.4**) [72].
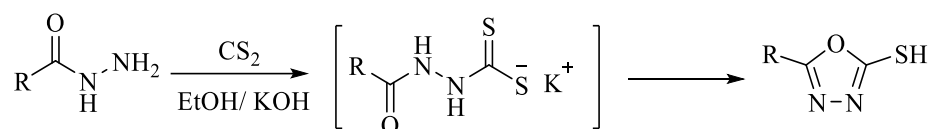
Figure 2.4. *5-Substituted-1,3,4-oxadiazole-2-thiols synthesis using CS$_2$*

In 1960, Sherman synthesized 5-substituted-1,3,4-oxadiazole-2-thiols by reacting hydrazides with thiophosgene in dioxane (**Figure 2.5**) [73].

Figure 2.5. *5-Substituted-1,3,4-oxadiazole-2-thiols synthesis using CSCl$_2$*

5-Substituted-2-mercapto-1,3,4-oxadiazoles have been synthesized from 2-acyldithiocarbazininate salts under microwave irradiation with a satisfactory yield ranged from 69% to 84%. The reaction was performed within 30 seconds when DMF and DMSO were used as solvents, while 120 seconds were needed in the case of pyridine (**Figure 2.6**) [74].
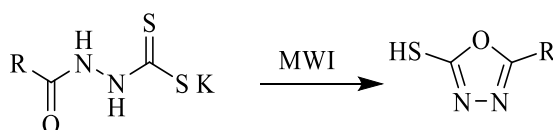
Figure 2.6. *5-Substituted-1,3,4-oxadiazole-2-thiols synthesis under microwave irradiation*

Soleiman-Beigi *et al.* have developed a simple and practical catalyst-free method to synthesize 5-substituted-1,3,4-oxadiazole-2-thiols from hydrazides and carbon disulfide (CS_2) in DMF. The reaction was started by stirring the mixture for 15 min at room temperature then proceeded at 70°C until the ring closure. It was confirmed that thiol tautomer is the only produced product during this reaction (**Figure 2.7**) [75].
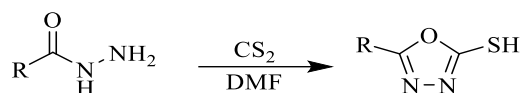
Figure 2.7. *5-Substituted-1,3,4-oxadiazole-2-thiols synthesis using CS_2 in DMF*

Based on the absolute energy values and solvent-solute interactions energy calculations, it has been reported that both thione and thiol tautomers have improved stability in higher polarity solvents. It has also been revealed that the thiol tautomer is generally observed in DMF, whilst the thione form is preferred in acetonitrile [75]. Other studies have emphasized that the thione form is predominant in the solid-state [76].

2.1.2. 5-Substituted-2-amino-1,3,4-oxadiazoles synthesis methods

5-Aryl-2-amino-1,3,4-oxadiazole derivatives have been attained by refluxing acyl-hydrazines and arylsemicarbazide with cyanogen bromide in ethanol or aqueous bicarbonate (**Figure 2.8**). However, 1,2,4-triazolin-5-ones might be generated as by-products under basic conditions [77].
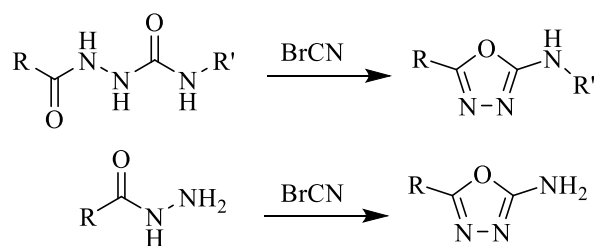
Figure 2.8. *Oxadizole synthesis using BrCN*

Kosmrlj *et al.* described an interesting method to produce 1,3,4-oxadiazoles through acylhydrazines reaction with isocyanates to afford 1,4-disubstituted semicarbazides that oxidizes into stable diazenes. At room temperature, diazenes undergo further oxidation in the presence of triphenylphosphine (Ph_3P) or tributylphosphine (Bu_3P) forming 1,3,4-oxadiazoles (**Figure 2.9**) [78].
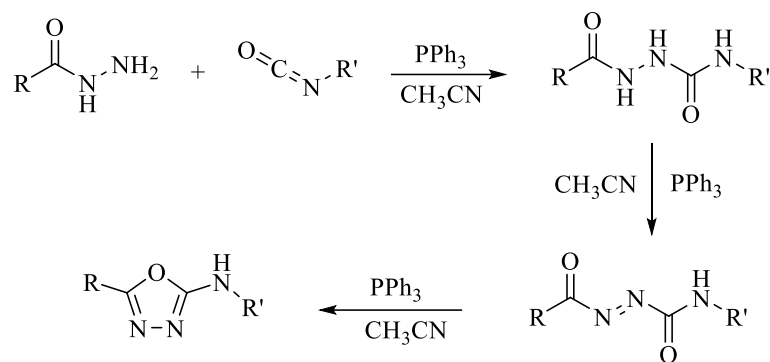
Figure 2.9. *Oxadiazole synthesis using PPh₃*

Hetzheim and Möckel have explained 1,3,4-oxadiazole synthesis using HgO, CuSO₄, and I₂. However, this method produced undesirable by-products and poor yields [70]. Several desulfurizing agents have been reported so far to produce 5-substituted 2-amino-l,3,4-oxadiazole derivatives from *N*- acyl-thiosemicarbazide at various conditions with higher yields (**Figure 2.10**). Among them, 1-ethyl-3-(3-dimethylaminopropyl)carbodiimide (EDC·HCl) in DMSO or *p*-TsCl [79] I₂/KI and NaOH under ultrasound conditions [80], *N,N*-dicyclohexylcarbodiimide (DCC), Burgess reagent, *N,N*-carbonyldiimidazole (CDI) [69], etc.
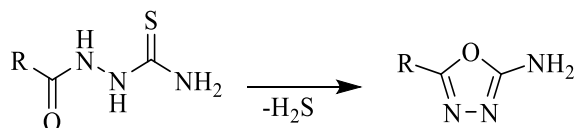
Figure 2.10. *Oxadiazole synthesis from N-acyl-thiosemicarbazide*

Nesynov and Grekov have obtained 5-substituted-2-amino-1,3,4-oxadiazoles from thiosemicarbazides using excess lead monoxide as catalyst and ethanol as solvent (**Figure 2.11**) [81].
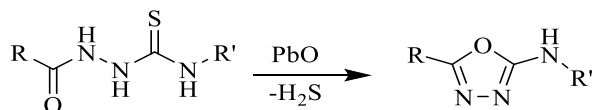
Figure 2.11. *Oxadiazole synthesis using lead monoxide*

Rivera, Balsells and Hansen have attempted to synthesize 5-substituted-2-amino-1,3,4-oxadiazoles from thiosemicarbazides using 1,3-dibromo-5,5-dimethylhydantoin as

an oxidizing agent, NaOH as a base, potassium iodide as catalyst and isopropyl alcohol/acetonitrile as solvent. This procedure is characterized by using a safe and economic oxidant besides the scrapping readiness of dimethylhydantoin byproducts during aqueous workup due to its high-water solubility (**Figure 2.12**) [82].
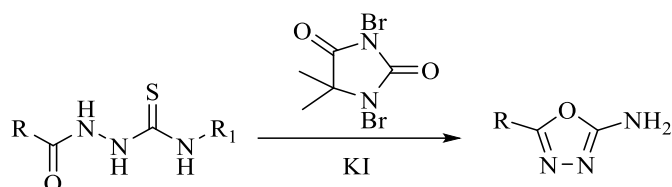
Figure 2.12. *Oxadiazole synthesis using 1,3-dibromo-5,5-dimethylhydantoin*

In 2006, Dolman *et al.* synthesized 5-alkyl- and 5-aryl-2-amino-1,3,4-oxadiazoles by thiosemicarbazide activation toward cyclization using *tosyl*-chloride and pyridine in tetrahydrofuran (THF). This method provides a simple one-pot approach to prepare a wide variety of 5-alkyl- and 5-aryl-2-amino-1,3,4-oxadiazole derivatives with an excellent yield between 78−99% (**Figure 2.13**) [83].
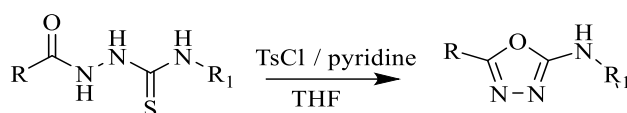
Figure 2.13. *Oxadiazole synthesis using tosyl chloride/pyridine*

In 2012, Guin *et al.* developed a convenient, simple method to produce 2-amino-1,3,4-oxadiazoles from thiosemicarbazide precursors using eco-friendly element iodine and potassium carbonate salt in biphasic medium of ethyl acetate/water (**Figure 2.14**). This method could be introduced to a wide range of functional groups with potential industrial applications due to its high yields [84].
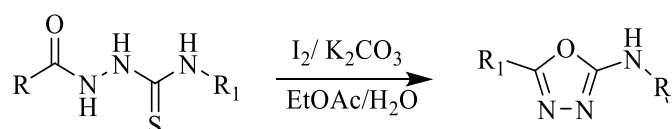
Figure 2.14. *N-acyl-thiosemicarbazide desulfurization*

2.1.3. 2,5-Diaryl(alkyl)-1,3,4-oxadiazole synthesis methods

1,3,4-Oxadiazoles have been obtained by reacting acyl hydrazine with carboxylic acid or ester using a dehydrating agent in a one-step process (**Figure 2.15**). Among them, phosphoric acid, phosphorus pentachloride, phosphorus pentoxide, sulfuric acid, thionyl chloride, Burgess reagent, trifluoroacetic acid, carbodiimide derivatives and *tosyl*-chloride /pyridine [51]. Nevertheless, in the presence of aryl substituents, the dehydrating agent must be selected carefully as these compounds undergo sulfonation by electrophilic attack pathway in the presence of sulfuric acid, oleum, etc., Chlorides of phosphorus and thionyl chloride and phosphorus oxychloride are considered appropriate choices in these cases [85].
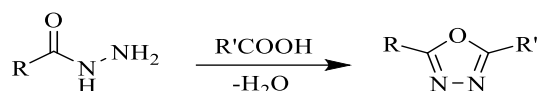
Figure 2.15. *One-step synthesis of 2,5-diaryl-1,3,4-oxadiazole using carboxylic acids*

Moreover, 2,5-diaryl(alkyl)-1,3,4-oxadiazole might be obtained in one-pot procedures starting from acylhydrazine and substituted aldehydes by direct condensation followed by oxidative cyclization under various conditions (**Figure 2.16**), including sodium bisulfite in a mixture of ethanol and water under microwave irradiation, trichloroisocyanuric acid (TCCA) at room temperature and cerium ammonium nitrate (CAN) in dichloromethane [51].

Figure 2.16. *One-step synthesis of 2,5-diaryl-1,3,4-oxadiazole using aldehydes*

Mashraqui *et al.* have proposed a simple, one-pot procedure to attain 2,5-disubstituted-1,3,4-oxadiazoles from hydrazides and acid chlorides in *N*-(2-hydroxypropyl)methacrylamide (HMPA) solvent under the microwave conditions obviating the necessity to use strong acid or any cyclodehydrating agent [86].

14

Figure 2.17. *One-step synthesis of 2,5-diaryl-1,3,4-oxadiazole using acid chlorides*

Another way to produce 1,3,4-oxadiazole was performed by *N*-acylhydrazines reaction with orthoformic esters, imido esters and imido chlorides (**Figure 2.18**). When aromatic hydrazines were reacted with substituted imidochlorides in basic conditions, amine hydrochloride was eliminated [70].
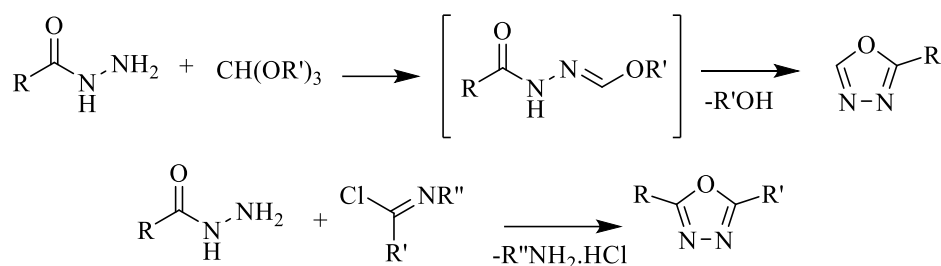
Figure 2.18. *1,3,4-Oxadiazole synthesis using orthoformic ester(up) and imidochloride (down)*

In 1978, Link described a compelling method to produce 1,3,4-oxadiazoles using azirine as a carbon donor in the ring-closing process. Aryl hydrazide was reacted with 3-dimethylamino-2,2-dimethyl-2*H*-azirine to yield 1,3,4-oxadiazole. The reaction proceeded through oxadiazoline formation and dimethylamine elimination in the final step (**Figure 2.19**) [87].
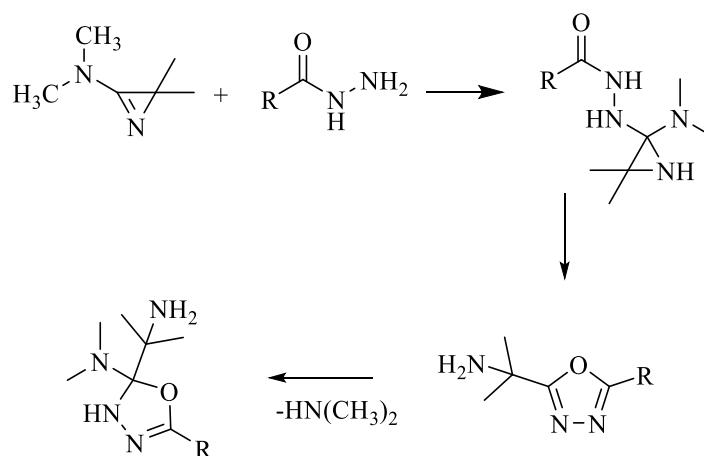
Figure 2.19. *1,3,4-Oxadiazoles by using azirine*

15

In 1988, Rigo *et al.* proposed an efficient method to prepare 1,3,4-oxadiazole derivatives starting from diacyl-hydrazine using hexamethyldisilazane (HMDS) as catalyst triflic acid and acetonitrile (**Figure 2.20**) [88].
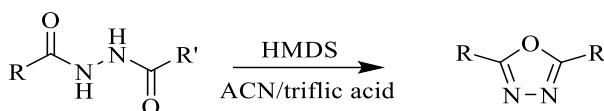
Figure 2.20. *1,3,4-Oxadiazole synthesis using HMDS/ trifilic acid*

In 1993, l,3,4-oxadiazole derivatives were produced through oxidative cyclization of aldehyde hydrazones using phenyl-iodine(III) diacetate (PIDA) as oxidizing agent at room temperature with an acceptable yield [89].
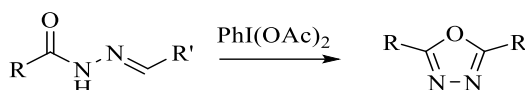
Figure 2.21. *1,3,4-Oxadiazole synthesis using PIDA*

In 1994, Jedlovské and Lesko described a new method to obtain 2,5-disubstituted 1,3,4-oxadiazoles by *N*-acyl-aldehyde hydrazones refluxing with chloramine T (CAT) in ethanol for 1-4 hours with an excellent yield ranged from 95-96% [90].
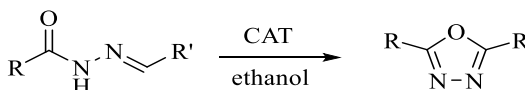
Figure 2.22. *1,3,4-Oxadiazole synthesis using CAT*

In 1995, Oussaid *et al.* prepared 2,5-disubstituted-1,3,4-oxadiazoles under microwave irradiation starting from diacyl-hydrazines in the presence of thionyl chloride with a considerable yield between 78-92% (**Figure 2.23**). The reaction took less time than conventional methods due to microwave acido-basic catalysis [91].
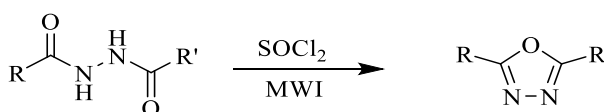
Figure 2.23. *1,3,4-Oxadiazole synthesis under microwave conditions*

In 1999, Isobe and Ishikawa proposed an efficient method to produce 1,3,4-oxadiazoles using 2-chloro-1,3-dimethylimidazolinium chloride (DMC) as a powerful dehydrating agent to cyclize diacylhydrazines in triethylamine (TEA) and dichloromethane with a substantial yield reached to 100% in some cases. The method was also used to prepare 1,3,4-oxadiazole derivatives by direct reaction of acylhydrazine and carboxylic acids (**Figure 2.24**) [92].
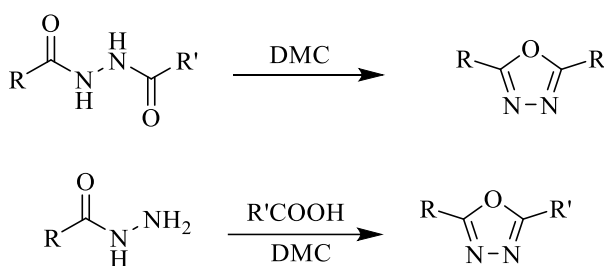
Figure 2.24. *1,3,4-Oxadiazole synthesis using DMC*

In 2001, Tendon and Chhor produced 1,3,4-oxadiazoles in situ by reacting hydrazine hydrate with acid chloride at 0 °C in dry dioxane using BF_3Et_2O as cyclodehydrating agent. The major attribute of this procedure is its simplicity and feasibility with various aromatic and aliphatic substrates [93].
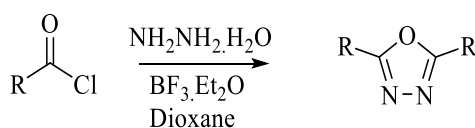
Figure 2.25. *1,3,4-Oxadiazoles synthesis from acid chloride*

Ma *et al.* have developed a novel synthesis method of symmetrical 2,5-disubstituted-1,3,4-oxadiazoles from hydrazides using potassium iodide (KI) in basic methanol media under electrochemical conditions. That approach may be a preferable way to synthesize oxadiazoles because of the mild conditions, cheap oxidant, and environmental friendliness (**Figure 2.26**). However, this method failed to produce the equivalent oxadiazole from aliphatic hydrazides therefore it could be applied only with aromatic hydrazides [94].

Figure 2.26. *1,3,4-Oxadiazole synthesis using KI and MWI*

Yu *et al.* proposed a convenient and transition metal-free oxidative cyclization of acylhydrazones in the presence of potassium carbonate and iodine at 100° C. It has been demonstrated that DMSO was the most effective solvent for this reaction [95].
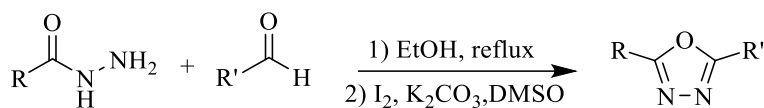
Figure 2.27. *Oxadiazole synthesis using I₂*

In 2011, Pouliot *et al.* prepared 1,3,4-oxadiazole from 1,2-diacylhydrazines using XtalFluor-E ([Et$_2$NSF$_2$]BF$_4$) as a cyclodehydrating agent. XtalFluor-E is a thermally stable compound that enables to perform the reaction at higher temperatures in 1,2-dichloroethane (DCE). They also found that using acetic acid as an additive generally increased yield [96].
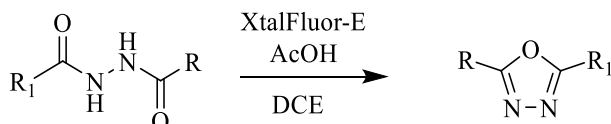
Figure 2.28. *1,3,4-Oxadiazole synthesis using XtalFluor-E*

2.2. 1,3,4-Oxadiazole Derivatives as Anticholinesterases and Monoamine Oxidase Inhibitors

In 1990, Mazouz et *al.* produced a novel 5-aryl-1,3,4-oxadiazol-2(3*H*)-one derivatives and evaluated their *in-vitro* inhibitory properties against monoamine oxidase A and B. Several compounds displayed potent inhibitory activity and selectivity towards the targeted enzymes. However, it was found that 5-(phenyl)-3-(2-cyanoethyl)-1,3,4-oxadiazol2(3*H*)-thione established a selective inhibitory action towards MAO-A enzyme. Extension of the previous structure with an extra phenyl group has inverted the selectivity toward MAO-B enzyme [97].

MAO A: IC$_{50}$=2.1 µM   **MAO A**: IC$_{50}$=22.5 µM
MAO B: IC$_{50}$=37 µM   **MAO B**: IC$_{50}$=0.074 µM
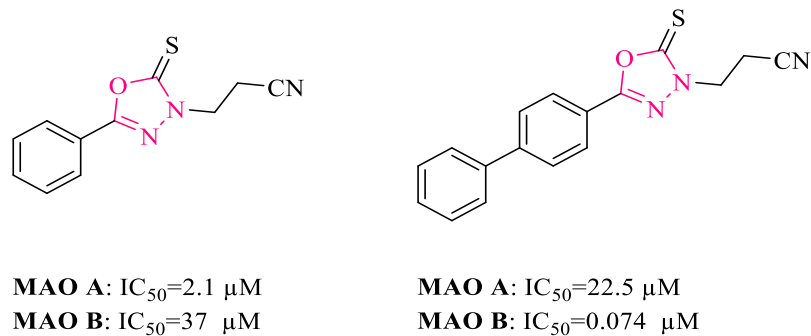
Figure 2.29. *5-Phenyl-3-(2-cyanoethyl)-1,3,4-oxadiazol2(3H)-thione (left) and 5-(4-biphenylyl)-3-(2-cyanoethyl)-1,3,4-oxadiazol2(3H)-thione (right)*

Later in 1993, they developed another 5-[4-(benzyloxy)phenyl]-l,3,4-oxadiazol-2(3*H*)-one series as inhibitors of monoamine oxidase type B. According to the preliminary results, 5- (4-(benzyloxy)phenyl)-3-(2-cyanoethyl)-l,3,4-oxadiazol-2(3*H*)-one) demonstrated a high selectivity towards MAO-B with an IC$_{50}$ in the nanomolar range [98].

MAO B: IC$_{50}$=1.4 nM
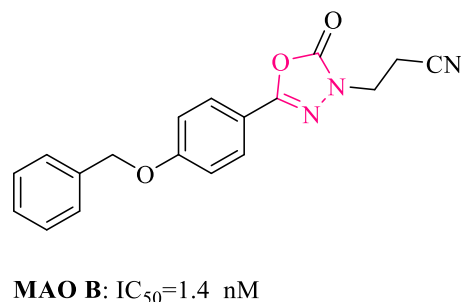
Figure 2.30. *5-(4-(Benzyloxy)phenyl)-l,3,4-oxadiazol-2(3H)-one structure*

In 2013, Rehman *et al*. developed a novel series of (5-substituted-1,3,4-oxadiazole-2yl)-*N*-[(2-methoxy-5-chlorophenyl)-2-sulfanyl]acetamide then evaluated their anticholinesterase activities. Amongst the tested compounds, *o*-methyl and *o*-nitro substituted aromatic ring structures were observed as potent AChE inhibitors (IC$_{50}$ values 34.61 and 40.21 µM), respectively; While the benzyl substituted compound possessed the best BuChE inhibition with an IC$_{50}$ of 33.31 µM [99].

AChE: IC$_{50}$= 34.61µM

AChE: IC$_{50}$= 40.12 µM

BuChE: IC$_{50}$= 33.31 µM
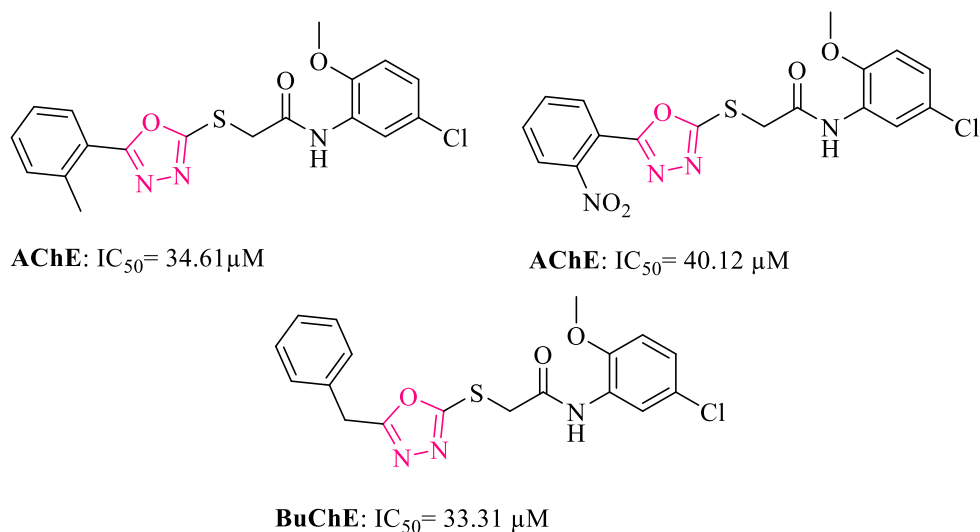
Figure 2.31. *(5-Substituted-1,3,4-oxadiazole-2yl)-N-[(2-methoxy-5-chlorophenyl)-2-sulfanyl]acetamide anticholinesterase potent derivatives*

Siddiqui *et al.* developed a new set of *N*-substituted derivatives of 5-benzyl-1, 3, 4-oxadiazole-2yl-2″-sulfanyl acetamides and screened them against acetylcholinesterase enzyme. The results showed that 2-[(5-benzyl-1,3,4-oxadiazol-2-yl)thio]-N-(2,6-dimethylphenyl)acetamide and 1-[(5-benzyl-1,3,4-oxadiazol-2-yl)thio]-3-phenylpropan-2-one have the potential to inhibit AChE enzyme with IC$_{50}$ values of 17.5 and 24.61 µmoles, respectively [100].

AChE: IC$_{50}$= 17.5 µM

AChE: IC$_{50}$= 24.61 µM
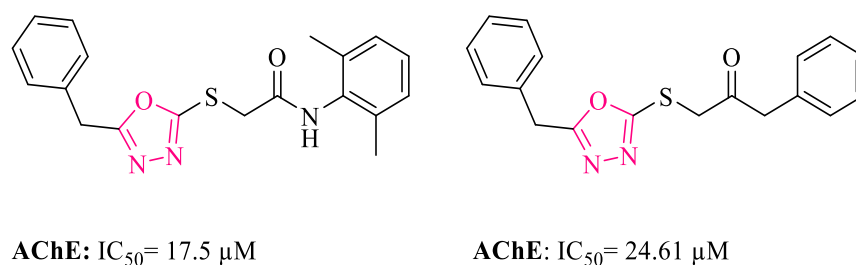
Figure 2.32. *2-[(5-Benzyl-1,3,4-oxadiazol-2-yl)thio]-N-(2,6-dimethylphenyl)acetamide (left), and 1-[(5-benzyl-1,3,4-oxadiazol-2-yl)thio]-3-phenylpropan-2-one (right)*

In 2014, Kamal *et al*. synthesized (*E*)-2-aryl-5-styryl-1,3,4-oxadiazole and (*E*)-2-aryl-5-(2-benzo[d][1,3]dioxol-5-yl)vinyl)-1,3,4-oxadiazole derivatives and studied their biological activity against AChE enzyme. The results revealed that all the synthesized compounds have an acceptable inhibitory activity with IC$_{50}$ values in the range of 13 to

65 µM. Molecular modeling studies proved that the most active compounds perform the same binding manner of donepezil [101].
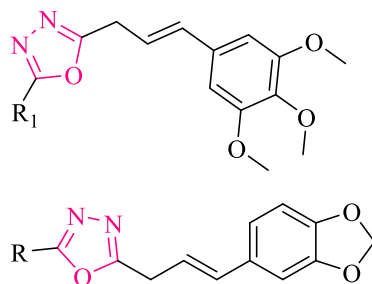
R,R$_1$= (substituted) phenyl, pyridyl, benzofuryl

Figure 2.33. *2-Aryl-5-styryl-1,3,4-oxadiazole(up) and 2-aryl-5-(2-benzo[d][1,3]dioxol-5-yl)vinyl)-1,3,4-oxadiazole (down)*

Rehman *et al.* developed a new series of heterocyclic 3-piperidinyl-1,3,4-oxadiazole derivatives and evaluated their activities against AChE. All the derivatives demonstrated a significant inhibition of acetylcholinesterase enzyme [102].
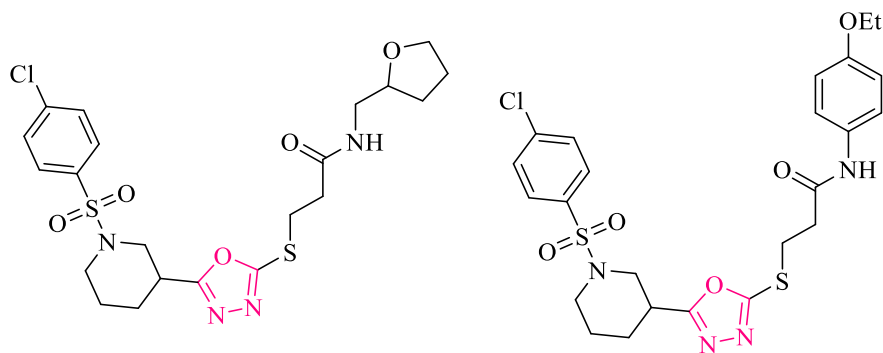
AChE: IC$_{50}$= 3.64 µM   **AChE:** IC$_{50}$= 7.62 µM

Figure 2.34. *3-[(5-(1-[(4-Chlorophenyl)sulfonyl]piperidin-3-yl)-1,3,4-oxadiazol-2-yl) thio]-N-[(tetrahydrofuran-2-yl)methyl]propanamide (left), and 3-[(5-(1-[(4-chlorophenyl)sulfonyl]piperidin-3-yl)-1,3,4-oxadiazol-2-yl)thio]-N-ethoxyphenyl)propanamide (right)*

In 2018, Ibrar *et al.* developed novel coumarin-oxadiazole and coumarin-thiazole hybrids and evaluated their activities against acetylcholinesterase and butyrylcholinesterase with the aim to investigate their potential for the prevention of AD.

Molecular docking studies established that coumarin-oxadiazole derivatives have high inhibitory activity against BuChE [103].
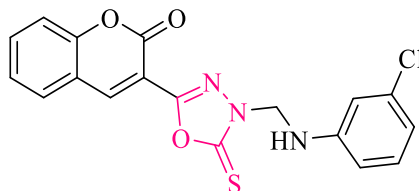
BuChE: $IC_{50}= 0.15\pm0.09\mu M$

Figure 2.35. *3-(4-{[(3-Chlorophenyl)amino]methyl}-5-thioxo-4,5-dihydro-1,3,4-oxadiazol-2-yl)-2H-chromen-2-one*

Abbasi *et al.* synthesized *N*-(5-methyl-1,3-thiazol-2-yl)-2-[5-((un)substituted-phenyl)1,3,4-oxadiazol-2-yl] sulfanyl acetamide derivatives and screened for their potential AChE inhibitory properties. Among all the structures, 2,4-dichloro and 4-amino substituted derivatives showed maximum AChE inhibition with IC_{50} values of 11.49 and 19.35 µM, respectively [104].
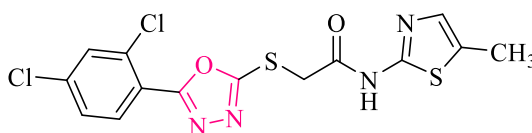
AChE: $IC_{50}= 11.49$ µM
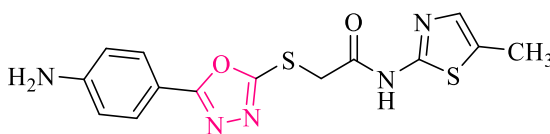
AChE: $IC_{50}= 19.35$ µM

Figure 2.36. *2-[(5-(2,4-Dichlorophenyl)-1,3,4-oxadiazol-2-yl)thio]-N-(5-methylthiazol-2-yl)acetamide (up), and 2-[(5-(4-aminophenyl)-1,3,4-oxadiazol-2-yl)thio]-N-(5-methylthiazol-2-yl)acetamide (down)*

Novel hybrids of 1,3-thiazole and 1,3,4-oxadiazole have been developed and screened for their inhibitory potential against AChE and BuChE enzymes. The results revealed that 3-nitrophenyl group and benzyl group retaining structures emerged with the highest inhibitory effect against AChE with an IC_{50} of 17.25 and 18.36 µM, respectively.

Nevertheless, substitution with 2-nitrophenyl group turned out to BuChE inhibitory action with an IC$_{50}$ value of 56.23 μM [105].
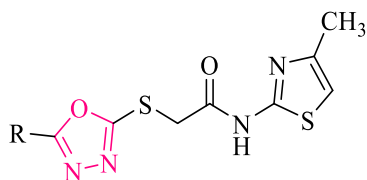
if R= 3-nitrophenyl, benzyl (potent AChEI)
R= 2-nitrophenyl   (potent BuChEI)

Figure 2.37. *1,3-Thiazole-1,3,4-oxadiazole hybrids*

In 2019, Tripathi *et al.* developed new hybrids of 2-aminopyrimidine moiety linked to substituted 1,3,4-oxadiazoles. The study demonstrated AChE inhibitory activity and antioxidant potential of the synthesized 1,3,4-oxadiazole derivatives. 5-(Naphthalen-1-yl)-*N*-(pyrimidin-2-yl)-1,3,4-oxadiazol-2-amine showed a considerable AChE inhibitory activity with a non-competitive enzyme inhibition. Therefore, this compound is expected to be an expedient lead for cognitive dysfunction treatment [106].
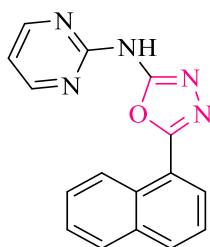
AChE: IC$_{50}$= 6.52 μM

Figure 2.38. *5-(Naphthalen-1-yl)-N-(pyrimidin-2-yl)-1,3,4-oxadiazol-2-amine*

Mishara *et al.* designed and synthesized 5-(substituted) phenyl-*N*-(pyridin-4-yl)-1,3,4-oxadiazol-2-amine derivatives. The resulted products were tested against AChE and BuChE enzymes. According to results, it was apparent that 4-OH substituted derivative has the potential to inhibit AChE-induced Aβ aggregation with an IC$_{50}$ of 1.098 μM in addition to its antioxidant properties [107].
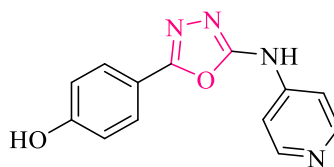
AChE: IC$_{50}$= 1.098 μM

Figure 2.39. *4-(5-(Pyridin-4-ylamino)-1,3,4-oxadiazol-2-yl)phenol*

Bingul *et al*. developed 2-(indol-2-yl)-1,3,4-oxadiazoles and evaluated their acetylcholinesterase and butyrylcholinesterase inhibitory activity. Based on biological assay findings, oxadiazole-containing compounds displayed appreciable AChE and BuChE inhibitory performance [108].
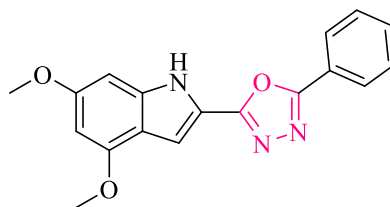
AChE inhibitory =88.22%
BuChE inhibitory =86.87%
comparing to galanthamine

Figure 2.40. *2-(4,6-Dimethoxy-1H-indol-2-yl)-5-phenyl-1,3,4-oxadiazole*

Triazole-oxadiazole conjugates have been synthesized and screened for their inhibitory activity against AChE enzymes. According to behavioral and biochemical results, it was revealed that 2-hydroxyphenyl, 3-hydroxyphenyl and pyridyl substituted moieties possessed noticeable anticholinesterase and antioxidant activities [109].
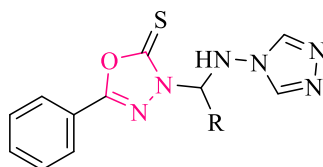
R= (substituted) phenyl, pyridyl

Figure 2.41. *Triazole-oxadiazole conjugates*

In 2020, Tripathi *et al.* designed, synthesized ferulic acid-based 1,3,4-oxadiazole hybrids and evaluated their inhibitory activity against acetylcholinesterase (AChE),

24

butyrylcholinesterase (BuChE) and beta-secretase-1 (BACE-1). The results revealed that 2-methoxy-4-(2-(5-(4-(trifluoromethyl)phenyl)-1,3,4-oxadiazol-2-yl)vinyl)phenol compound had a neuroprotective activity against Aβ-induced oxidative stress showing an inhibitory potential for AChE, BuChE and BACE-1 enzymes with IC_{50}s of 0.068 µM, 0.218 µM and 0.255 µM, respectively [110].
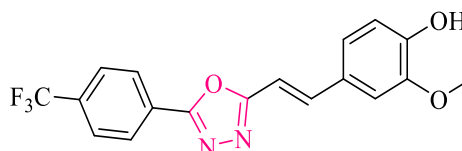
AChE:IC_{50}= 0.068 µM
BuChE: IC_{50}=0.218 µM

Figure 2.42. *2-Methoxy-4-(2-(5-(4-(trifluoromethyl)phenyl)-1,3,4-oxadiazol-2-yl)vinyl)phenol*

In 2021, Mirzazadeh *et al.* synthesized a new set of quinoxalin-1,3,4-oxadiazoles and evaluated their activities against multiple metabolic enzymes including AChE enzyme. According to the results, 3-fluoro substituted derivative showed a twofold higher inhibitory activity against acetylcholinesterase and butyrylcholinesterase in comparison with tacrine [111].
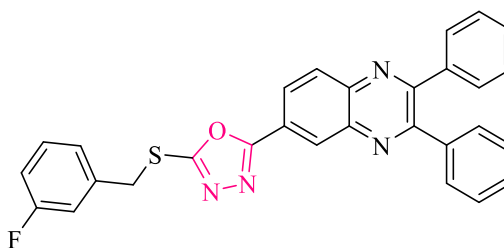
AChE=IC_{50}= 594 nM
BuChE= IC_{50}= 624 nM

Figure 2.43. *2-(2,3-Diphenylquinoxalin-6-yl)-5-[(3-fluorobenzyl)thio]-1,3,4-oxadiazole*

Choubey *et al.* developed novel hybrids bearing *N*-benzylpyrrolidine tethered with substituted 1,3,4-oxadiazole nucleus and screened against AChE, BuChE and BACE-1 enzymes. All compounds showed noticeable AChE inhibitory activities; However, the most promising results against this enzyme

were shown by highly lipophilic and strong electron-withdrawing substitutes, especially CF_3 group containing compounds [112].
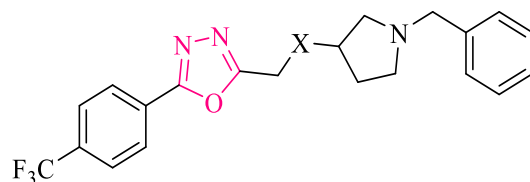
X= NH,   **AChE**:IC_{50}=0.091μM,   **BuChE**: IC_{50}= 0.106 μM
X= NHCH$_2$,   **AChE**:IC_{50}=0.064μM,   **BuChE**: IC_{50}= 0.074 μM

Figure 2.44. *N-Benzylpyrrolidine-oxadiazole hybrids*

A novel series of 5-pyrid-3-yl-1,3,4-oxadiazoles developed and evaluated as potential inhibitors of acetylcholinesterase and butyrylcholinesterase by Elghazawy *et al*. Almost all of the compounds showed considerable inhibition against both cholinesterases with IC_{50} values in the nanomolar range. Amongst the tested compounds, 2-(4-chlorophenyl)-5-(5-phenylpyridin-3-yl)-1,3,4-oxadiazole exhibited the best inhibitory potential against both AChE and BuChE with an IC_{50} of 50.87 nM and 4.77 nM, respectively [50].
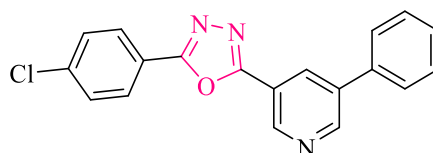
AChE:IC_{50}= 50.87 nM
BuChE: IC_{50}=4.77 nM

Figure 2.45. *2-(4-Chlorophenyl)-5-(5-phenylpyridin-3-yl)-1,3,4-oxadiazole*

George *et al*. developed 1,3,4-oxadiazole-coumarin hybrids and evaluated their anticholinesterase, antioxidant and anti-inflammatory activities. The most potent AChE inhibitors were 7-[(5-(3,4-dihydroxyphenyl)-1,3,4-oxadiazol-2-yl)methoxy]-4-methyl-2*H*-chromen-2-one and 4-methyl-7-[(5-(3,4,5-trihydroxyphenyl)-1,3,4-oxadiazol-2-yl)methox]-2*H*-chromen-2-one with IC_{50} values of 29.56 and 28.68 μM), respectively. While 7-[(5-(3,4-dihydroxyphenyl)-1,3,4-oxadiazol-2-yl)methoxy]-4-methyl-2H-chromen-2-one displayed a notable inhibition of BuChE with IC_{50} value of 23.97 μM [113].

X= CH=CH , (CH$_2$)$_2$
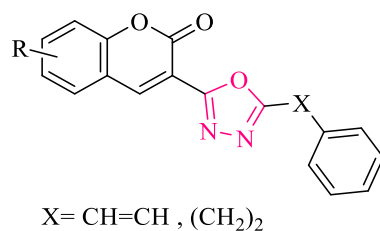
Figure 2.46. *1,3,4-Oxadiazole- coumarin hybrids*

Harfenist *et al.* also developed a series of 5-aryl-2- alkyl-1,3,4-oxadiazole analogues that have been concluded to be potent monoamine oxidase inhibitors [114].
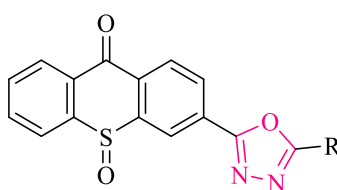
Figure 2.47. *5-Aryl-2-alkyl-1,3,4-oxadiazole analogues*

Later on, a novel set of 1,3,4-oxadiazole-3(2*H*)-carboxamides have been produced and screened for their inhibitory activities toward MAO enzymes. The synthesized compounds demonstrated remarkable inhibitory activity at the concentration of 10^{-5}–10^{-3} M [115].
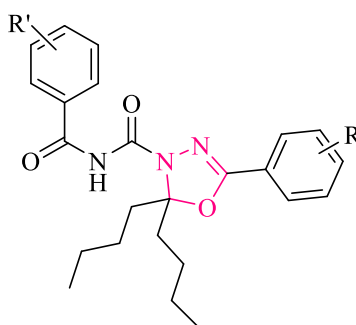
Figure 2.48. *1,3,4-Oxadiazole-3(2H)-carboxamide derivatives*

In 2016, Distinto *et al*. prepared a novel 3-acetyl-2-dichlorophenyl-5-aryl-2,3-dihydro-1,3,4-oxadiazole derivatives and identified their ability to inhibit MAO enzymes. According to preliminary results, various compounds demonstrated preferential inhibitory activity against MAO-B with medium to low nanomolar range IC$_{50}$s [116].

27
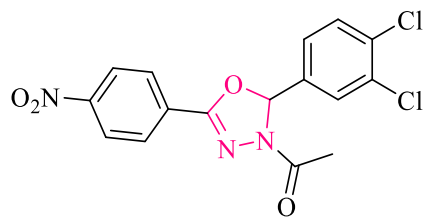
MAO B: IC$_{50}$=7.61 nM

Figure 2.49. *2-(3,4-Dichlorophenyl)-3-acetyl-5-(4-nitrophenyl)-2,3-dihydro-1,3,4-oxadiazole*

Recently, Tok *et al*. developed a new set of 2,5-disubstituted-1,3,4-oxadiazole derivatives and evaluated their potential to inhibit MAO-A and B enzymes. They reported that 1-(4-chlorophenyl)-3-(5-(5-(4-chlorophenyl)-1,3,4-oxadiazol-2-yl)pyridin-2-yl)urea possessed a superior MAO-B inhibitory activity with an IC$_{50}$ value of 0.039 µM [52].
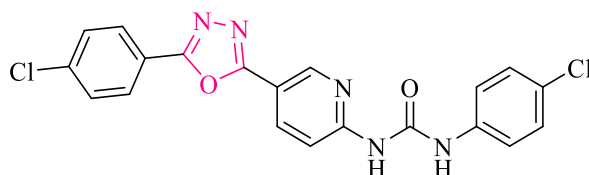
MAO B: IC$_{50}$=0.039 µM

Figure 2.50. *1-(4-Chlorophenyl)-3-(5-(5-(4-chlorophenyl)-1,3,4-oxadiazol-2-yl)pyridin-2-yl)urea*

In 2022, a series of 5-Aryl-1,3,4-oxadiazoles was synthesized and screened for inhibition of AChE and BuChE. All compounds were found as efficient dual inhibitors of both enzymes with IC$_{50}$ range of 12.8–99.2 µM for AChE and from 53.1µM for BuChE.[117].
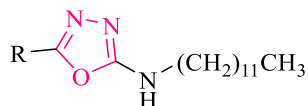
R=aromatic, heteroaromatic rings

Figure 2.51. *5-Aryl-1,3,4-oxadiazoles*

2.3. Quinoline Derivatives as Anticholinesterase and Monoamine Oxidase Inhibitors

Several tacrine analogues was designed, synthesized and screened for their cholinesterases inhibition ability. It was revealed that 6*H*-indeno[2,1-b]quinolin-11-

amine retained higher selectivity toward acetylcholinesterase over butyrylcholinesterase by comparison with tacrine [118] .
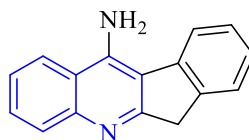
AChE : IC_{50}= 0.35 μM
BuChE : IC_{50}= 3.1 μM

Figure 2.52. *6H-indeno[2,1-b]quinolin-11-amine*

In 1999, Carlier *et al*. developed tacrine-based acetylcholinesterase inhibitors by introducing basic amines bearing different hydrophobic properties along with tacrine structure. The optimal acetylcholine inhibitory activity was provided by 4-aminoquinoline containing heterodimers showing potencies in nanomolar ranges [119].
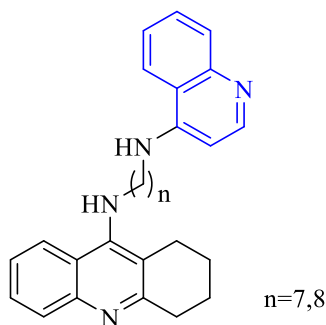
Figure 2.53. *Tacrine-based acetylcholinesterase inhibitors*

In 2009, Camps *et al*. developed two isomeric series of quinoline-chlorotacrine hybrids and evaluated their ability to inhibit AChE, BuChE AChE-induced β-amyloid (Aβ) aggregation. Both series were linked by oligomethylene linker with an amido group at an alterable position. The results showed that the synthesized structures are capable to inhibit AChEs with IC_{50} values in the nanomolar range with a remarkable ability to inhibit the self-induced Aβ aggregation [120].

n= 0, 2   n'= 4-10   R= H, Cl
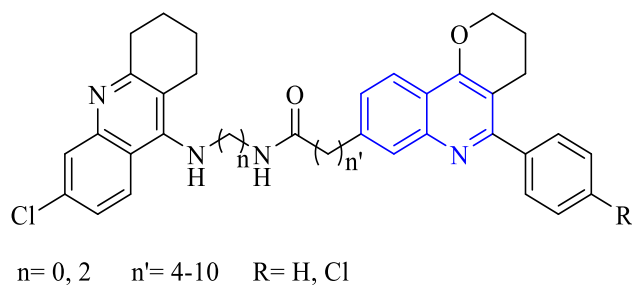
Figure 2.54. *Quinoline-chlorotacrine hybrids*

In 2010, Bachiller *et al.* designed and synthesized novel tacrine-8-hydroxyquinoline hybrids then evaluated their abilities to treat AD. The synthesized compounds showed superior potent inhibitory activity against acetyl- and butyrylcholinesterase enzymes in comparison with tacrine. They also displayed remarkable antioxidant properties and neuroprotective activity [121].
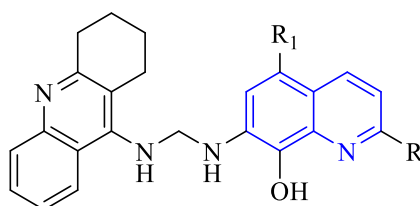
Figure 2.55. *Tacrine-8-hydroxyquinoline hybrids*

A novel series of tacrine analogs were produced and screened for selective inhibitory activities on AChE and BuChE. The obtained results showed that the synthesized structures have a higher affinity and superior activity to that of tacrine towards AChE. Among all synthesized compounds, the preferential acetylcholinesterase inhibitory was shown by the compound having nine-carbons bridge between the nicotinamide moiety and 2,3-dihydro-1*H*-cyclopenta[b]quinolin-9-amine part showing an IC_{50} value of 3.65 nM. Conversely, the highest affinity and inhibition activity toward BuChE was exhibited by ethyl bridge containing structure [122].

X= (CH$_2$)n,
n=2-9
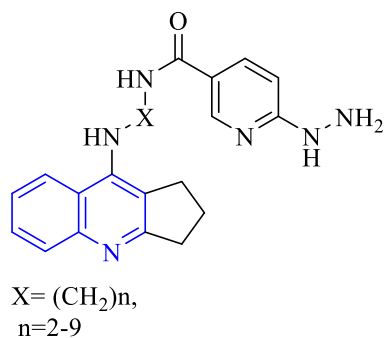
Figure 2.56. *Tacrine analogues*

In 2012, Khorana *et al.* evaluated some β-carboline and quinoline derivatives' ability to inhibit acetylcholinesterase enzyme. The results revealed that 1-benzyl-6-methoxyquinolin-1-ium structure possessed a potent human AChE inhibitory activity with an IC$_{50}$ of 5.29 μM [123].
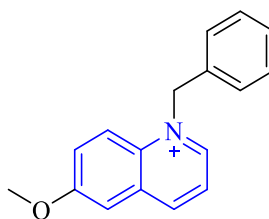
AChE: IC$_{50}$= 2.46 μM

Figure 2.57. *1-Benzyl-6-methoxyquinolin-1-ium*

In 2015, a novel set of 2-arylethenylquinolines were developed and tested for their AChE/BuChE inhibitory potential. The study revealed that the synthesized structures had the potential to act as multifunctional treatments for AD. The most active agent displayed anticholinesterases abilities with IC$_{50}$s of 64 μM and 0.2 μM against AChE and BuChE, respectively. [124].
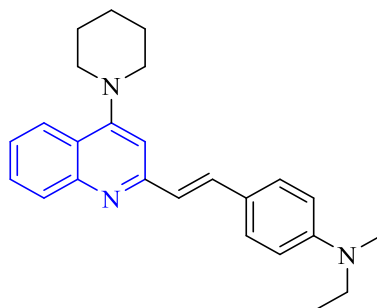
AChE: IC$_{50}$= 64 µM
BuChE: IC$_{50}$= 0.2 µM

Figure 2.58. *(E)-N,N-diethyl-4-(2-(4-(piperidin-1-yl)quinolin-2-yl)vinyl)aniline*

In 2015, Ziab *et al*. synthesized a series of quinolinyl-thienyl chalcones and studied their monoamine oxidases A and B inhibitory activity. Based on biological study results, most structures exhibited potent MAO inhibitory action [125].
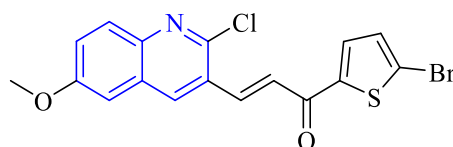
MAO A: IC$_{50}$=0.047 µM
MAO B: IC$_{50}$=0.350 µM
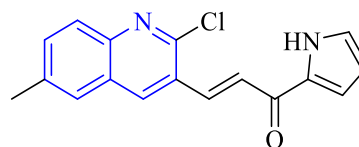
MAO A: IC$_{50}$=0.085 µM
MAO B: IC$_{50}$=0.063 µM

Figure 2.59. *Quinolinyl-thienyl chalcones*

Mantoani *et al*. described the synthesis and biological assessment of new tacrine-donepezil hybrids containing a triazole-quinoline system in the course of inhibition of AChE and BuChE enzymes. Biological assay findings demonstrated that triazole-quinoline hybrids have the potential to bind and inhibit both enzymes with IC$_{50}$s in the micro-molar range [126].
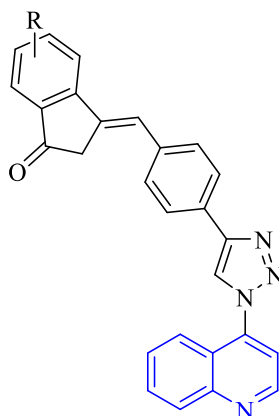
Figure 2.60. *Triazole-quinoline hybrids*

Xia *et al.* synthesized new 2-arylethenyl-*N*-methylquinolinium derivatives and proved their potential to be propitious agents in the treatment of AD. Some of the synthesized compounds displayed significant cholinesterases inhibition potential. 5-(diethylamino)-2-[(E)-2-(1-methylquinolin-1-ium-2-yl)ethenyl]phenol;iodide revealed a remarkable AChE and BuChE inhibitory activity with IC_{50} values of 1.5 and 1.1 µM, respectively. The compound also showed a considerable neuronal cell protection effect against the glutamate-induced cytotoxicity [127].
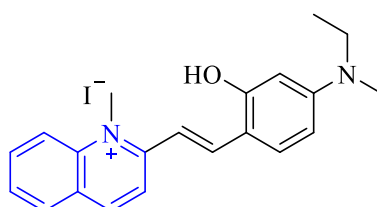
Figure 2.61. *5-(diethylamino)-2-[(E)-2-(1-methylquinolin-1-ium-2-yl)ethenyl]phenol;iodide*

In 2018, two series of quinolinyl chalcones derivatives, 2,6-dimethylquinoline derivatives and 2-methyl-6-methoxyquinoline were designed, synthesized and screened for ChEs inhibition by Shakil shah *et al*. The majority of the synthesized structures were concluded to be effective inhibitors for both BuChE and AChE. The most potent compounds have also demonstrated good oral bioavailability and safety profile [128].

R=CH₃, OCH₃
R'= aromatic rings
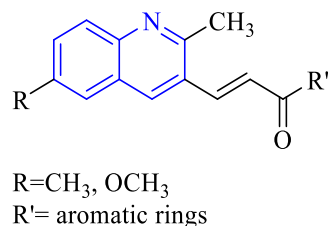
Figure 2.62. *Quinolinyl chalcones derivatives*

Khan *et al.* developed a series of quinoline carboxylic acids and studied their *in-vitro* and *in-silico* inhibitory potential against acetylcholinesterase, butyrylcholinesterase, monoamine oxidase A and B enzymes. The results established that most of the tested compounds retained a significant MAO inhibitory activity with superior selectivity towards MAO-B. Moreover, it was found that introducing di-methoxy moiety at *ortho-* and *para*-position of the aryl ring linked at C_2 of the quinoline construction played a crucial role in AChE inhibitory activity which reached a five-fold higher than the control agent neostigmine [129].

MAO-A: IC_{50}=0.18 µM
MAO-B: IC_{50}=5.39 µM
AChE :IC_{50}= 15.78 µM

MAO-A: IC_{50}=0.51 µM
MAO-B: IC_{50}=0.51 µM
AChE :IC_{50}= 23.70 µM

AChE :IC_{50}= 4.36 µM
MAO-B: IC_{50}=1.19 µM
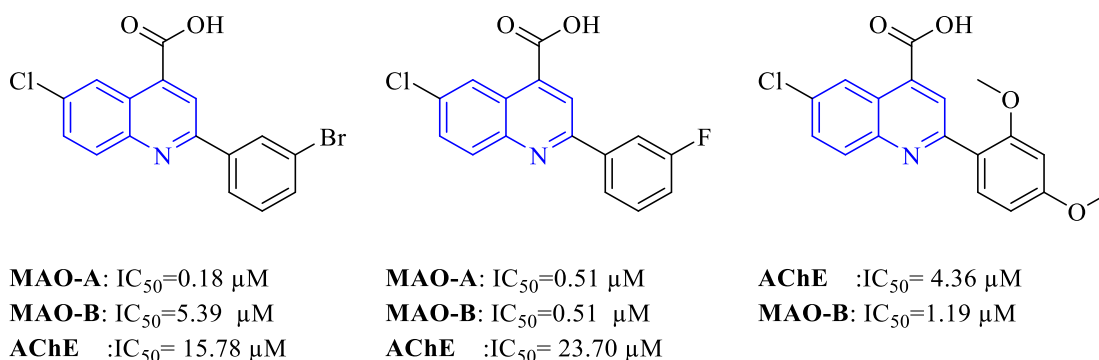
Figure 2.63. *Quinoline carboxylic acid most potent derivatives*

Wu *et al.* developed a novel quinoline-containing series and evaluated their activity against AChE and BuChE enzymes. The synthesized series skeleton also holds tacrine-triazole moieties with an alterable bridge connecting them. Biochemical assay results demonstrated that ethyl piperazine-bridge containing hybrid possessed a noteworthy cholinesterase inhibitory action with IC_{50}s of 4.89 µM and 3.61 µM against AChE and BuChE, respectively [130].
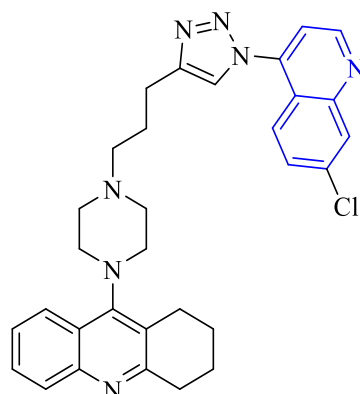
AChE: IC_{50}= 4.89 µM
BuChE: IC_{50}= 3.61 µM

Figure 2.64. *9-(4-(3-(1-(7-Chloroquinolin-4-yl)-1H-1,2,3-triazol-4-yl)propyl)piperazin-1-yl)-1,2,3,4-tetrahydroacridine*

Huang *et al.* developed a multi-target-directed ligand strategy that aims to reduce acetylcholine hydrolysis and inhibit the aggregation of Aβ by integrating AChE inhibitors with a metal chelator functionality. 6-(1-(Dimethylamino)ethyl)quinolin-8-yl ethyl(methyl)carbamate structure showed a promising cognitive improvement in the zebrafish model with a potent AChE inhibitory action reached 1.2 µM which is 7-fold higher than rivastigmine [131].
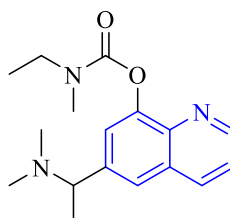
AChE: IC_{50}= 1.2 µM

Figure 2.65. *6-(1-(Dimethylamino)ethyl)quinolin-8-yl ethyl(methyl)carbamate*

Barth *et al.* have conducted a study to investigate the ability of 7-chloro-4-(phenylselanyl)quinoline (4-PSQ) to ameliorate aging-related cognitive impairment in rats. Acetylcholinesterase activity, cholesterol levels and neuroplasticity markers of aged rats were performed throughout the research period. The results revealed that treatment of older rats with 4-PSQ restored short and long term memories by altering synaptic plasticity, modulating the cholinergic system, and modifying cholesterol levels (Barth et

al. 2019). Later on, another study evidenced the ability of 4-PSQ to amend the activity of MAO A and B enzymes and alleviate neuroinflammation [33].
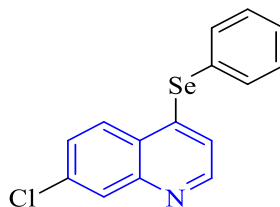
Figure 2.66. *7-Chloro-4-(phenylselanyl) quinoline (4-PSQ)*

Recently, Youdim 2022 rationally designed dual inhibitors of cholinesterase-monoamine oxidase enzymes by incorporating multiple active moieties within a single structure aiming to afford potent and selective agents. The study results demonstrated that 5-[(methyl(prop-2-yn-1-yl)amino)methyl]quinolin-8-ylethyl(methyl)carbamate possessed selective and potent MAO-A inhibitory action, moderate MAO-B inhibition and AChE high selectivity [132].

MAO-A: $IC_{50}=0.0077$ µM
MAO-B: $IC_{50}=7.90$ µM
AChE : $IC_{50}=0.52$ µM
BuChE : $IC_{50}= 44.9$ µM
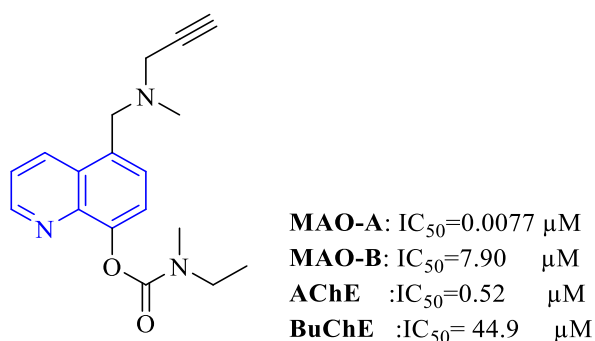
Figure 2.67. *5-[(Methyl(prop-2-yn-1-yl)amino)methyl]quinolin-8-yl ethyl(methyl)carbamate*

3. MATERIALS AND REAGENTS

3.1. Chemicals Reagents

2-Bromo-2',5'-dimethoxyacetophenone	: Sigma-Aldrich, Germany
2-Bromo-3'-chloroacetophenone	: Sigma-Aldrich, Germany
2-Bromo-4'-chloroacetophenone	: Sigma-Aldrich, Germany
2-Bromo-4'-fluroacetophenone	: Sigma-Aldrich, Germany
2-Bromo-4'-methoxyacetophenone	: Sigma-Aldrich, Germany
2-Bromoacetophenone	: Sigma-Aldrich, Germany
4-Cloroaniline	: Sigma-Aldrich, Germany
4-Fluoroaniline	: Sigma-Aldrich, Germany
4-Methoxyaniline	: Sigma-Aldrich, Germany
8-Hydroxyquinoline	: Merck, Germany
Acetone	: Merck, Germany
Acetonitrile	: Sigma-Aldrich, Germany
Acetylcholinesterase (E.C.3.1.1.7)	: Sigma-Aldrich, Germany
Acetylthiocholine iodide (ATC)	: Fluka, Germany
Ampliflu™ Red	: Sigma-Aldrich, Germany
Butyrylcholinesterase (E.C. 3.1.1.8)	: Sigma-Aldrich, Germany
Butyrylthiocholine iodide (BTC)	: Fluka, Germany
Carbon disulfide	: Fluka, Germany
DNP hydrochloride	: Sigma-Aldrich, Germany
DTNB	: Sigma-Aldrich, Germany
Ethanol	: Merck, Germany
Ethyl bromoacetate	: Merck, Germany
H_2O_2	: Sigma-Aldrich, Germany

*h*MAO-A	: Sigma-Aldrich, Germany
*h*MAO-B	: Sigma-Aldrich, Germany
Hydrazine monohydrate	: Sigma-Aldrich, Germany
Hydrochloric acid	: Sigma-Aldrich, Germany
Moclobemide	: Sigma-Aldrich, Germany
Peroxidase from horseradish	: Sigma-Aldrich, Germany
Potassium carbonate	: Sigma-Aldrich, Germany
Potassium hydroxide	: Sigma-Aldrich, Germany
Selegiline	: Sigma-Aldrich, Germany
Tacrine	: Sigma-Aldrich, Germany
THF	: Fisher, UK
Tyramine hydrochloride	: Sigma-Aldrich, Germany

3.2. Instruments and Tools

Electronic analytical balance	: Shimadzu, Libror EB-330 HU, Japan
Mass spectrometer	: Shimadzu, LCMS-IT-TOF, Japan
Melting point detector	: Mettler Toledo-MP90 Melting Point System
Microplate reader	: BioTek-Synergy H1, USA
Nuclear magnetic resonance spectrometer	: Bruker, USA
Robotic pipetting table	: BioTek- Precision XS, USA
Ultraviolet cabinet	: Camag, Cabinet, Switzerland

4. METHODS

4.1. Chemical Synthesis Methods

4.1.1. Ethyl 2-(quinolin-8-yloxy)acetate synthesis 1 (Method A)

8-Hydroxyquinoline (7.25 g, 0.05 mol) was refluxed with ethyl bromoacetate (6.61 mL, 0.06 mol) and potassium carbonate (13.82 g, 0.1 mol) in acetone (100 ml) for 2-3 hours. After TLC analysis, acetone was evaporated and the product was washed and filtered out of water. The product was recrystallized from ethanol [133].
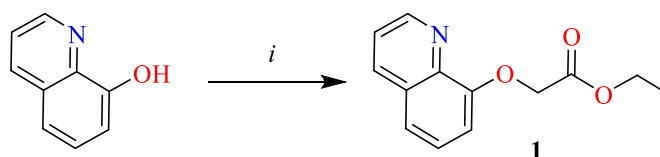
i: ethyl bromoacetate , K_2CO_3, acetone, reflux

Figure 4.1. *Ethyl 2-(quinolin-8-yloxy)acetate synthesis method*

4.1.2. 2-(Quinolin-8-yloxy) acetohydrazide 2 (Method B)

The product of the first step, ethyl 2-(quinolin-8-yloxy)acetate (10.3 g, 0.047 mol) was stirred with hydrazine monohydrate 85% (0.01 mol, 7.3 ml) in ethanol (250 mL) for 1 hour at room temperature to afford 2-(quinolin-8-yloxy)acetohydrazide. The reaction was controlled using TLC, the precipitated product was filtered and recrystallized from ethanol [133].
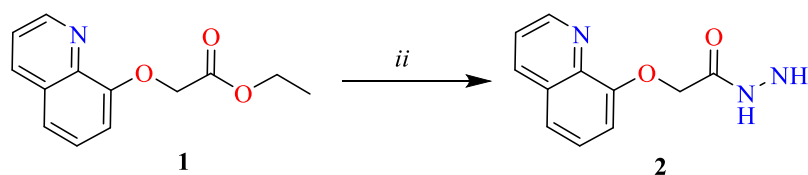
ii: hydrazine monohydrate, ethanol, r.t

Figure 4.2. *2-(Quinolin-8-yloxy)acetohydrazide synthesis method*

4.1.3. 5-[(Quinolin-8-yloxy)methyl]-1,3,4-oxadiazole-2-thiol 3 (Method C)

An ethoxide solution was prepared by dissolving KOH (2.44g, 0.043 mol) in absolute ethanol (100 mL) in 250 mL round-flask. 2-(quinolin-8-yloxy) acetohydrazide (9.27 g, 0.0432 mol) was added to the basic solution then CS_2 (5.1 mL, 0.085 mol) was added dropwise to the reaction solution. The mixture was refluxed for 5-6 hours and

monitored by TLC. Afterward, the resulted mixture was poured onto iced water and acidified using aqueous HCl until pH=5-6. The precipitated product was filtered and dried [134].

iii: 1) CS$_2$, KOH, ethanol, reflux; 2) aq. HCl
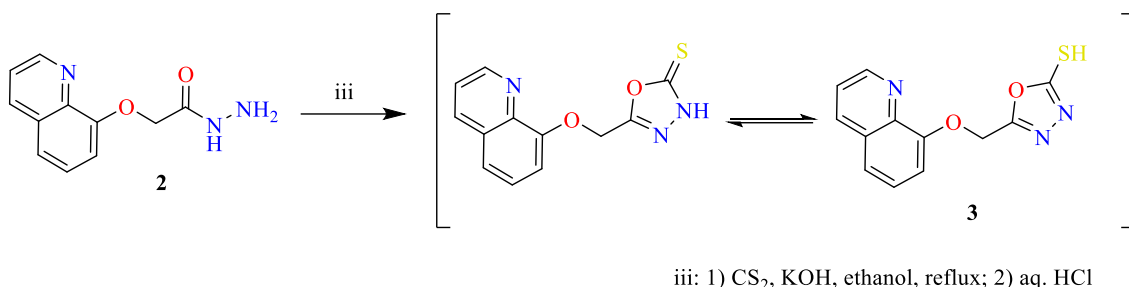
Figure 4.3. *5-[(Quinolin-8-yloxy)methyl]-1,3,4-oxadiazole-2-thiol synthesis method*

4.1.4. 1-(Substituted phenyl)-2-[[5-((quinolin-8-yloxy)methyl)-1,3,4-oxadiazol-2-yl]thio]ethan-1-one (Method D)

5-[(Quinolin-8-yloxy)methyl]-1,3,4-oxadiazole-2-thiol (0.5g, 0.001 mol) was stirred with substituted phenacyl bromide (0.001 mol) in the presence of potassium carbonate and acetone (20 mL) at ambient temperature. The reaction was monitored using TLC, the solvent was evaporated and the product was washed with water, filtered, dried and recrystallized from ethanol [135].

iv: K$_2$CO$_3$, acetone , r.t
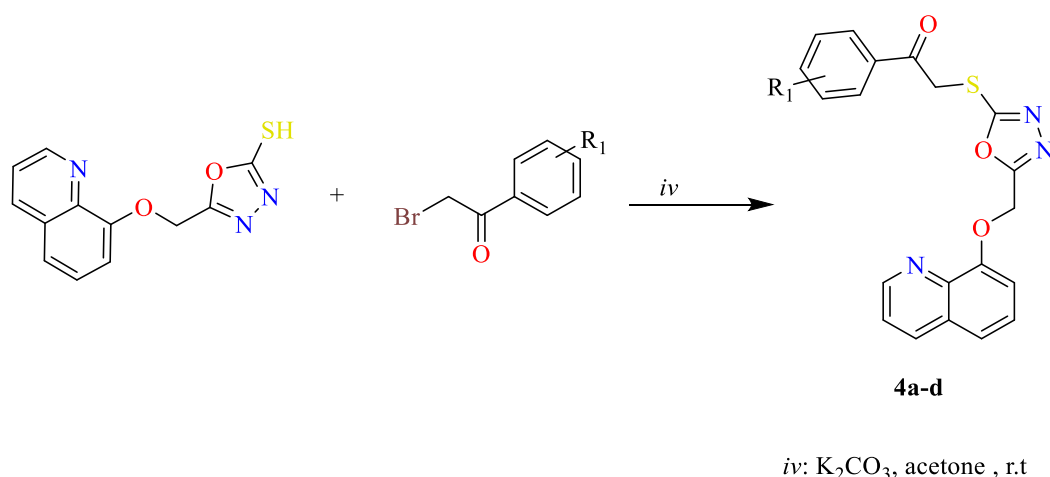
Figure 4.4. *1-(Substituted phenyl)-2-[[5-((quinolin-8-yloxy)methyl)-1,3,4-oxadiazol-2-yl]thio]ethan-1-one synthesis*

4.1.5. 2-Chloro-*N*-(substituted)acetamide (Method E)

2-Chloro-*N*-(thiazol-2-yl/phenyl) acetamide (0.005 mol) was dissolved in tetrahydrofuran THF (20mL) and triethylamine TEA (0.005 mol) at 0-5 °C, then chloroacetylchloride (0.005 mol) was added dropwise to the reaction medium with constant stirring for 1-2 hours. The reaction was controlled using TLC, after THF was evaporated, the products were washed with water, dried and recrystallized from ethanol [136].

vii; THF,TEA at (0-5 ℃)
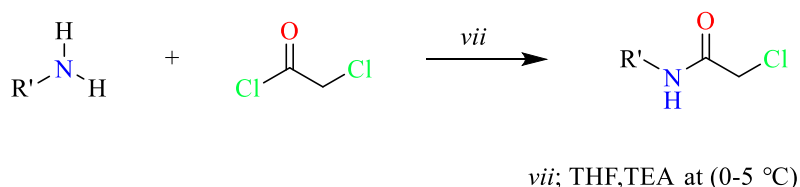
Figure 4.5. *2-Chloro-N-(substituted)acetamide synthesis method*

4.1.6. *N*-(Substituted phenyl∕thiazol-2-yl)-2-[[5-((quinolin-8-yloxy)methyl)-1,3,4-oxadiazol-2-yl]thio]acetamide (Method F)

A solution of 2-chloro-*N*-(substituted)acetamide (0.001 mol) in acetonitrile was added dropwise to a solution of 5-[(quinolin-8-yloxy)methyl]-1,3,4-oxadiazole-2-thiol (0.5g, 0.001 mol) and (0.04 g ,0.001 mol) NaOH in acetonitrile (10 mL). The resulted mixture was refluxed for 10 hours then monitored using TLC. After the solvent was evaporated, the product was washed with brine water and recrystallized from ethanol [137].

R': substituted phenyl/ thiazol-2-yl
viii : NaOH, acetonitrle, reflux
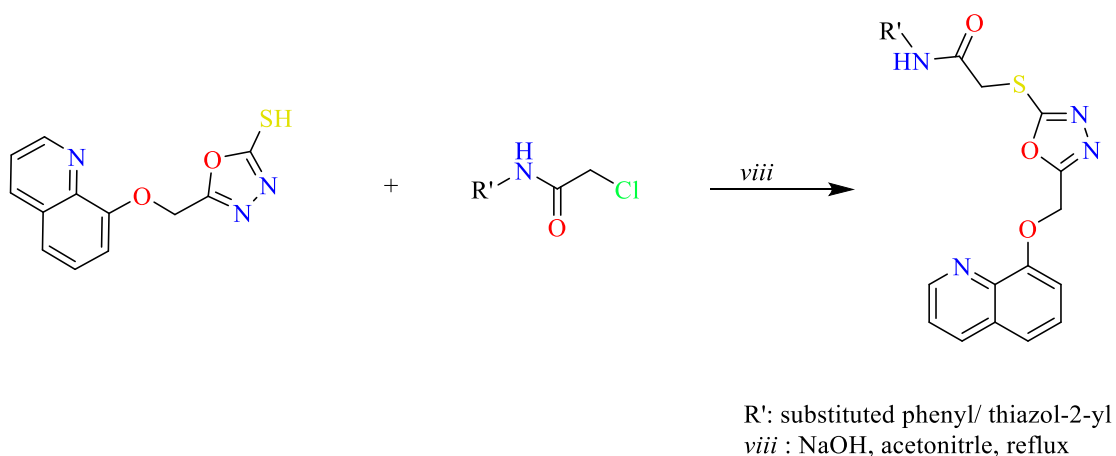
Figure 4.6. *N-(Substituted phenyl/thiazol-2-yl)-2-[[5-((quinolin-8-yloxy)methyl)-1,3,4-oxadiazol-2-yl]thio]acetamide synthesis*

41

4.2. Thin Layer Chromatography (TLC) Studies

In all synthesis procedures, TLC applications have been utilized to control the reactions. Samples of reaction medium were taken, diluted in ethanol then applied onto silica gel 60 F_{254} coated aluminum plates using capillary tubes. The plate was then put in a mobile phase composed of ethyl acetate/ petroleum ether mixtures in different concentrations (9:1, 3:1 and 1:1).

The reaction progression was controlled by comparing the reaction sample spots to starting reactants spots under UV light (254 nm and 366 nm).

4.3. Chemical Analysis

4.3.1. Infra-red (IR) spectrometry

The Shimadzu-IR Affinity-IS equipment was used to obtain the IR spectra of the synthesized compounds. 10 mg of each substance was introduced into the attenuated total reflection (ATR) chamber to obtain the spectrum.

4.3.2. High-resolution mass spectroscopy (HRMS)

Mass spectra of the compounds were detected by LCMS-IT-TOF (Shimadzu, Kyoto, Japan) instrument using electron spray ionization (ESI) technique in negative and positive modes. The samples were prepared by dissolving the synthesized compounds in acetonitrile.

4.3.3. ^{1}H-NMR spectral acquisition

^{1}H-NMR spectra were detected using Bruker 400 MHz. in DMSO-$_{d6}$. The data were expressed as chemical shifts or δ values (ppm) at 400 MHz relative to the internal standard TMS, coupling constants (J) were given in *Hz*.

4.3.4. ^{13}C-NMR spectral acquisition

^{13}C-NMR spectra were detected in DMSO-$_{d6}$ using Bruker at 100 MHz. The results were expressed as chemical shifts or δ values (ppm) relative to the internal standard TMS and coupling constants (J) were given in *Hz*.

4.4. Melting Points Detection

Melting points (M.P) of the synthesized compounds were determined using the Mettler Toledo MP90 Melting Point System. The compounds were placed in close-ended capillary tubes up to 0.5 cm and then located in the designated orifice of the instrument.

After the process was completed, the melting points were determined from the recorded video. Melting points were uncorrected.

4.5. Determination of Anticholinesterase Activity

Acetylcholinesterase and butyrylcholinesterase inhibitory activity of the synthesized compounds were evaluated in 96-well plates using modified Ellman's spectrometric method. A robotic system, Biotek Precision XS (Winooski, VT, USA) has been used to perform the pipetting processes. BioTek-Synergy H1 microplate reader (Winooski, VT, USA) was utilized to measure the inhibition percentage at 412 nm. All solutions were brought 20-25°C prior to the analysis process. Each well contained a mixture of 140 μL phosphate buffer (0.1 M, pH = 8), 20 μL 5,5′-dithiobis-(2-nitrobenzoic acid) DTNB (0.01 M), 20 μL enzyme solution from electric eel AChE or equine serum BuChE in 1% gelatin solution (2.5 U/mL), 20 μL inhibitor solution prepared in 2% aqueous DMSO and 10 μL substrate solution (0.075 M acetylthiocholine iodide (ATC) or butyrylthiocholine iodide (BTC)) producing a final volume of 210 μL. A primary prescreening evaluation for the enzyme inhibitory activities was performed and displayed as percentage at 10^{-3} M and 10^{-4} M concentrations. Donepezil was used as a reference to AChE inhibitory activity while Tacrine was used with BuChE.

The enzyme-inhibitor solutions were prepared by enzyme, inhibitor and the chromogenic reagent DTNB addition to the phosphate buffer and incubation for 15 min at 25 °C. After that, the substrate solution of ATC or BTC was added to the mixture. The absorbance of the produced yellow color was recorded for 5 min at 412 nm. Another inhibitor free enzyme solution was prepared as a control. The readings of the control and inhibitors were corrected with the blank readings. The % inhibition was calculated by applying the following formula **(I)** using the absorbance difference values.

$$\% \; inhibition = \frac{[(A(C)-A(B))-(A(I)-A(B))]}{(A(C)-A(B))} * 100 \qquad \textbf{(I)}$$

Blank (B): inhibitor and substrate free well.
Control (C): inhibitor free well.
A(B): Difference in absorbance measurement for blank.
A(C): Difference in absorbance measurement for control.
A(I): Difference in absorbance measurement for inhibitors.

Compounds with higher than 50% inhibition at 10^{-4}M were screened at lower concentrations (10^{-5}-10^{-9} M). The dose-response curve was obtained using GraphPad 'PRISM' software (version 5.0) by plotting the percentage inhibition versus the log concentration in order to determine the IC_{50} values. [138, 139].

4.6. Determination of Monoamine Oxidase Inhibitory Activity

The synthesized compounds were screened for their potential to inhibit MAO isoenzymes using *in-vitro* fluorometric method. Freshly prepared solutions of inhibitors in 2% DMSO (10^{-3}–10^{-9} M), recombinant *h*MAO-A (0.5 U/mL) and recombinant *h*MAO-B (0.64 U/mL) enzymes in phosphate buffer and a working solution mixture of horseradish peroxidase (200 U/mL, 100 μL), Ampliflu™ Red (20 mM, 200 μL) and tyramine (100 mM, 200 μL) in phosphate buffer have been used. All the volumes were adjusted to 10 mL.

The inhibitor solution (20 μL/well) and *h*MAO-A (100 μL/well) / *h*MAO-B (100 μL/well) were added to 96-well micro test plate then incubated for 30 min at 37 °C. The working solution (100 μL/well) was added and re-incubated for another 30 min. After that, the fluorescence (Ex/Em = 535/587 nm) was measured at 5 min intervals. Another parallel reading was measured using %3 H_2O_2 solution (20 mM 100 μL/well) instead of enzyme solutions to investigate the probable inhibitory effect of the targeted compounds on horseradish peroxidase. Furthermore, the probable non-enzymatic inhibition of the compounds was assessed by mixing inhibitor and working solutions [140, 141]. All experiments were analyzed in quadruplicate then the following equation **(II)** was applied to calculate the inhibition percentage:

$$\%inhibition = \frac{(FC_{t2}-FC_{t1})-(FI_{t2}-FI_{t1})}{FC_{t2}-FC_{t1}} * 100 \quad \textbf{(II)}$$

FC_{t2}: Fluorescence of a control well detected at t_2 time,
FC_{t1}: Fluorescence of a control well detected at t_1 time.
FI_{t2}: Fluorescence of an inhibitor well detected at t_2 time
FI_{t1}: Fluorescence of an inhibitor well detected at t_1 time.

4.7. Prediction of the Pharmacokinetic Profile

SwissADME online tool had been used to predict the pharmacokinetic profile and physicochemical properties of the active structures. The number of hydrogen-bond (H-bond) acceptors and donors, lipophilicity, blood-brain barrier permeability, topological

polar surface area, and drug likeness properties were evaluated in comparison to donepezil [142].

4.8. Molecular Docking

The binding modes of the most potent derivatives were determined using docking simulation targeting the crystal structure of human acetylcholinesterase (PDB ID: *4EY7*) retrieved from protein data bank (PDB) [143]. The crystal structure was optimized by removing the water molecules, heteroatoms and co-factors using the Protein Preparation Wizard protocol of the Schrödinger Suite 2020. The ligands were prepared and optimized by assigning the protonation states, bond orders, atom types using LigPrep module in Schrodinger Maestro. The grid was generated using the Glide module before the docking runs were conducted applying standard precision docking mode [140].

5. RESULTS AND DISCUSSION

5.1. Synthesis of the Targeted Compounds

5.1.1. Ethyl 2-(quinolin-8-yloxy)acetate 1
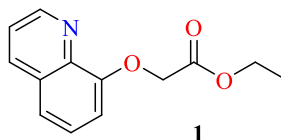
Figure 5.1. *Compound 1 structure*

Ethyl 2-(quinolin-8-yloxy)acetate **1** was synthesized according to method A. Brown crystals, compound **1** yield: 95%, measured M.P.=56 °C, literature melting point= 60 °C [144].
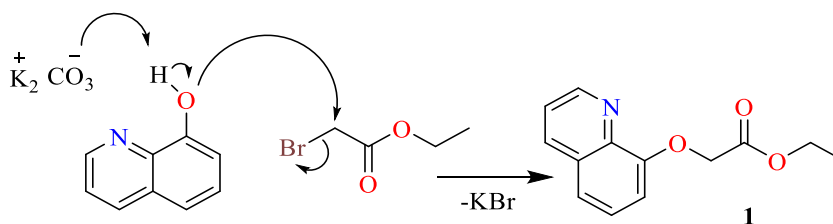
Figure 5.2. *Schematic representation of method A mechanism*

5.1.2. 2-(Quinolin-8-yloxy)acetohydrazide 2
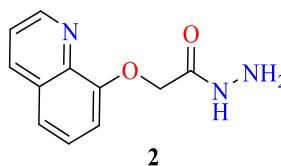
Figure 5.3. *Compound 2 structure*

2-(Quinolin-8-yloxy)acetohydrazide **2** was synthesized according to method B. Compound **2** yield: 90%, measured M.P. =144 , literature melting point = 140 °C [144].
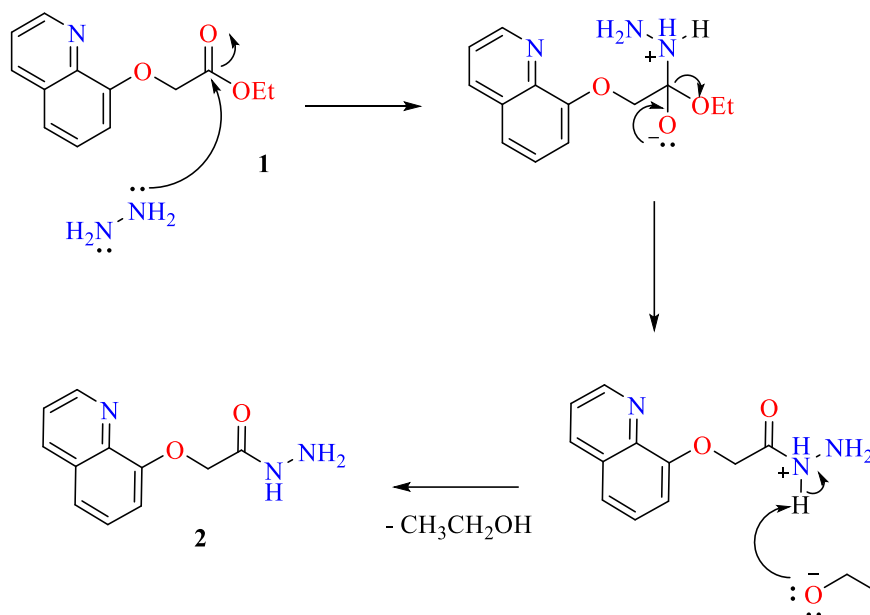
Figure 5.4. *Schematic representation of method B mechanism*

5.1.3. 5-[(Quinolin-8-yloxy)methyl]-1,3,4-oxadiazole-2-thiol 3
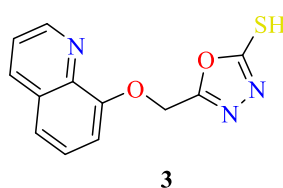
Figure 5.5. *Compound 3 structure*

5-[(Quinolin-8-yloxy)methyl]-1,3,4-oxadiazole-2-thiol **3** was synthesized according to method C. Compound **3** yield: 60%, measured M.P. =222 °C , literature melting point= 224 °C [145].

Figure 5.6. *Schematic representation of method C mechanism*

5.1.4. 1-(Substituted phenyl)-2-[[5-((quinolin-8-yloxy)methyl)-1,3,4-oxadiazol-2-yl]thio]ethan-1-one (4a-d)

1-(Substituted phenyl)-2-[[5-((quinolin-8-yloxy)methyl)-1,3,4-oxadiazol-2-yl]thio]ethan-1-one derivatives (**4a-d**) were synthesized according to method D and F.

4a-d

Figure 5.7. *Compounds **4a-d** general structure*

Figure 5.8. *Schematic representation of method D mechanism*

5.1.4.1. 1-Phenyl-2-[[5-((quinolin-8-yloxy)methyl)-1,3,4-oxadiazol-2-yl]thio]ethan-1-one (4a)
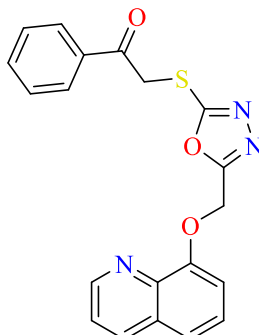
Figure 5.9. *Chemical structure of compound 4a*

Compound **4a** was synthesized according to method D. Yield 73%, M.P. =110-111 °C.

FTIR (ATR, cm^{-1}): 3053 (aromatic C-H stretching), 2920-2960 (aliphatic C-H stretching), 1676 (C=O), 1500-1600 (N=C, C=C stretching), 1261 (aromatic C-O stretching, oxadiazole), 1172 (aliphatic C-O stretching), 1118 (monosubstituted benzene).

^{1}H-NMR: (400 MHz, DMSO-d_6, ppm) *δ:* 5.16 (2H, s, CO-CH$_2$), 5.60 (2H, s, O-CH$_2$), 7.36 (1H, dd , J_1= 7.74 , J_2=1.06 *Hz*, quinoline C$_7$-H),7.52 (1H,t, *J*= 8.04 *Hz,* phenyl C$_4$-H) ,7.55-7.63 (4H, m, aromatic-H), 7.71 (1H, t, *J*=7.42 *Hz,* phenyl C$_4$-H), 8.02 (2H, d, *J*=7.12 *Hz,* phenyl C$_{2,5}$-H), 8.35 (1H, dd , J_1= 8.30 , J_2=1.70 Hz, quinoline C$_4$-H), , 8.87 (1H, dd , J_1= 4.13 , J_2 =1.74 Hz, quinoline C$_2$-H).

^{13}C-NMR: (100 MHz, DMSO-d_6, ppm) *δ :* 41.10(S-CH$_2$), 60.89(O-CH$_2$), 111.94, 121.94, 122.53, 127.03, 128.91, 129.36, 129.61, 134.46, 135.45, 136.45, 140.135, 140.91, 153.35, 164.14, 165.05, 192.71(C=O).

HRMS (*m/z*): [M+H]$^+$ calculated for C$_{20}$H$_{15}$N$_3$O$_3$S: 378.0907; found: 378.0910.

DOPNALAB

Item	Value
Acquired Date&Time	7.06.2022 09:23:06
Acquired by	System Administrator
Filename	C:\Users\dopnalab\Desktop\MASAÜSTÜ\LEYLA YURTDAŞ\MEN\MENA-11.ispd
Spectrum name	MENA-11
Sample name	MENA-1
Sample ID	
Option	
Comment	
No. of Scans	15
Resolution	4 [cm-1]
Apodization	Happ-Genzel
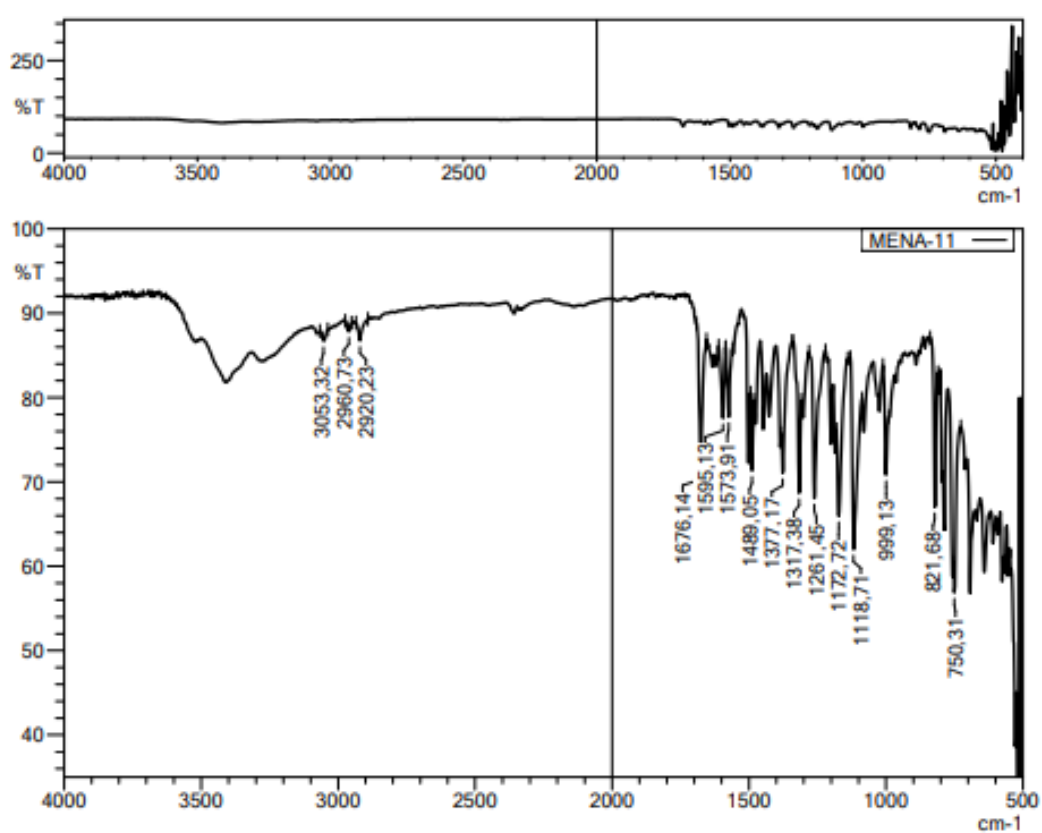
Figure 5.10. *IR spectrum of compound 4a*

51

5.16
5.61
7.36
7.36
7.38
7.38
7.50
7.52
7.54
7.56
7.56
7.57
7.58
7.58
7.59
7.60
7.61
7.61
7.63
7.63
7.69
7.71
7.73
8.04
8.05
8.35
8.35
8.37
8.37
8.87
8.88
8.88
8.89

2.00
1.99
1.15
1.39
4.35
1.08
1.94
1.07
1.11
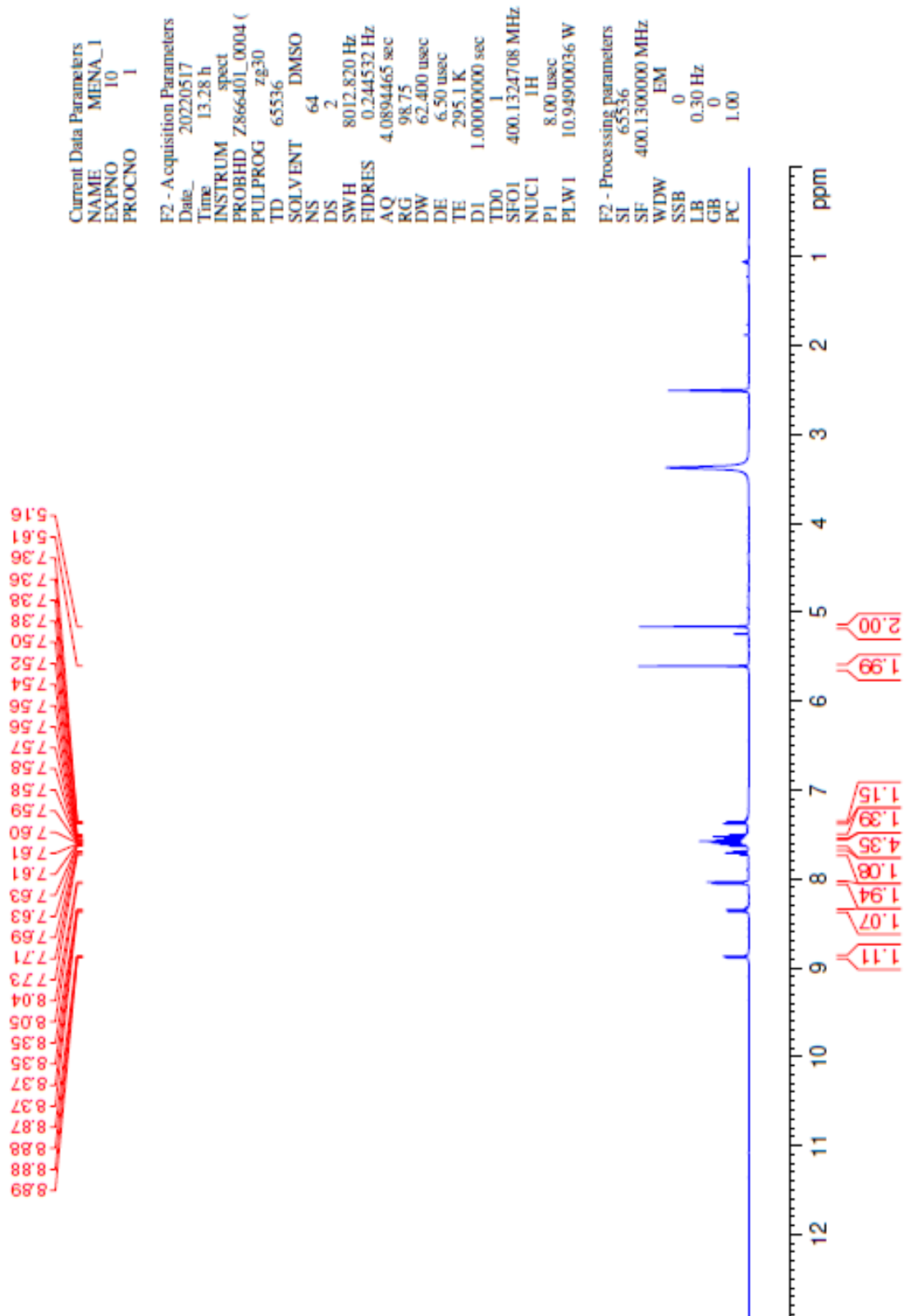
Figure 5.11. *¹H-NMR spectrum of compound* *4a*
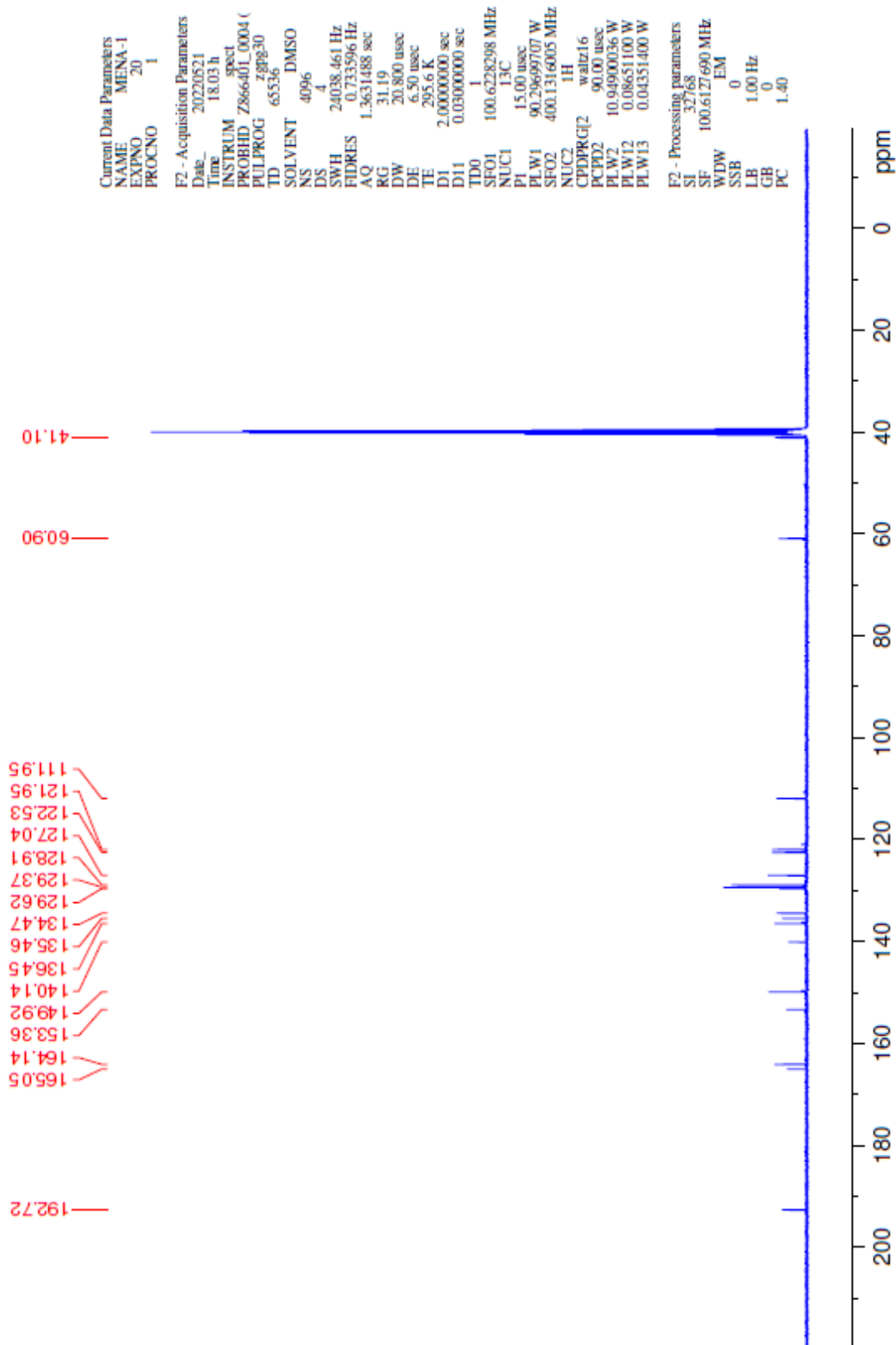
Figure 5.12. *¹³C-NMR spectrum of compound **4a***
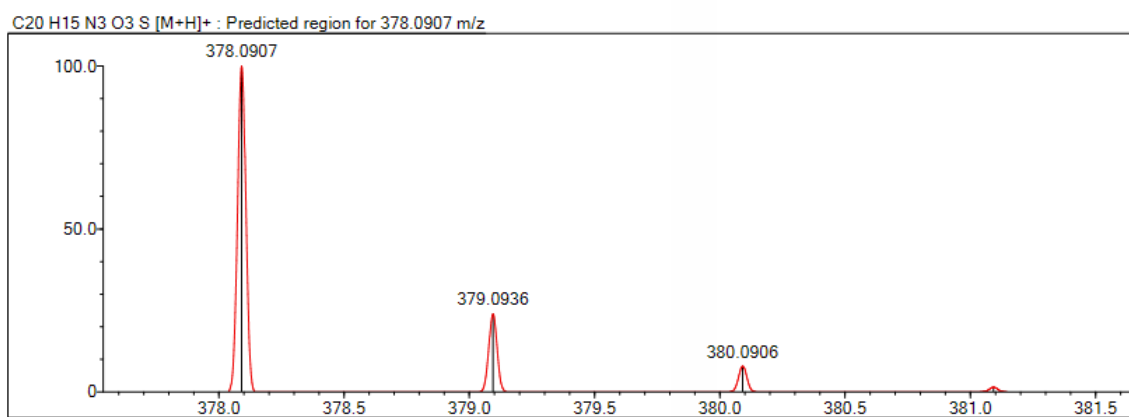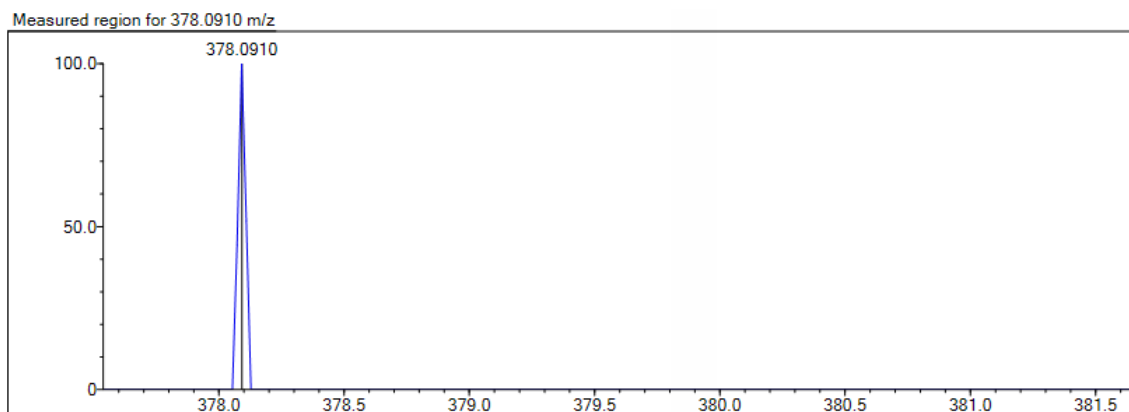
Rank	Score	Formula (M)	Ion	Meas. m/z	Pred. m/z	Df. (mDa)	Df. (ppm)	Iso	DBE
1	0.00	C20 H15 N3 O3 S	[M+H]+	378.0910	378.0907	0.3	0.79	0.00	15.0

Figure 5.13. *Mass spectrum of compound **4a***

5.1.4.2. 2-[[5-((Quinolin-8-yloxy)methyl)-1,3,4-oxadiazol-2-yl]thio]-1-(p-tolyl)ethan-1-one (4b)

Figure 5.14. *Chemical structure of compound 4b*

Compound **4b** was synthesized according to method D. Yield 64%, M.P. = 148-149°C.

FTIR (ATR, cm^{-1}): 3053 (aromatic C-H stretching), 2848-2954 (aliphatic C-H stretching), 1674 (C=O stretching), 1602-1490 (C=N ,C=C stretching), 1261 (C-O stretching, oxadiazole), 1165 (C-O stretching, ether), 1118 (1,4 disubstituted benzene).

^{1}HNMR: (400 MHz, DMSO-d_6, ppm) δ: 2.40 (3H, s, phenyl-CH$_3$), 5.11 (2H, s, CO-CH$_2$), 5.60 (2H, s, O-CH$_2$), 7.36 (1H, d, J=1.76 Hz, quinoline C$_7$-H), 7.52(1H, t, J= 7.95 Hz, phenyl-H) 7.56-7.63 (3H, m, aromatic-H), 7.93 (2H, d, J=8.2 Hz, aromatic-H), 8.36 (1H, dd, J_1= 8.3, J_2=1.67 Hz, quinoline C$_4$-H), 8.95 (1H, dd, J_1= 4.12, J_2=1.7 Hz, quinoline C$_2$-H).

^{13}C-NMR: (100 MHz, DMSO-d_6, ppm) δ: 21.69 (CH$_3$), 41.10 (S-CH$_2$), 60.88 (O-CH$_2$), 111.97, 121.94, 122.53, 127.07, 129.02, 129.62, 129.89, 132.96, 136.55, 140.02, 145.05, 149.86, 153.30, 164.10, 165.09, 192.19(C=O).

HRMS (*m/z*): [M+H]$^+$ calculated for C$_{21}$H$_{17}$N$_3$O$_3$S: 392.1063; found: 392.1049.

Item	Value
Acquired Date&Time	7.06.2022 09:28:31
Acquired by	System Administrator
Filename	C:\Users\dopnalab\Desktop\MASAÜSTÜ\LEYLA YURTDAŞ\MEN\MENA-8.1.ispd
Spectrum name	MENA-8.1
Sample name	MENA-8
Sample ID	
Option	
Comment	
No. of Scans	15
Resolution	4 [cm-1]
Apodization	Happ-Genzel
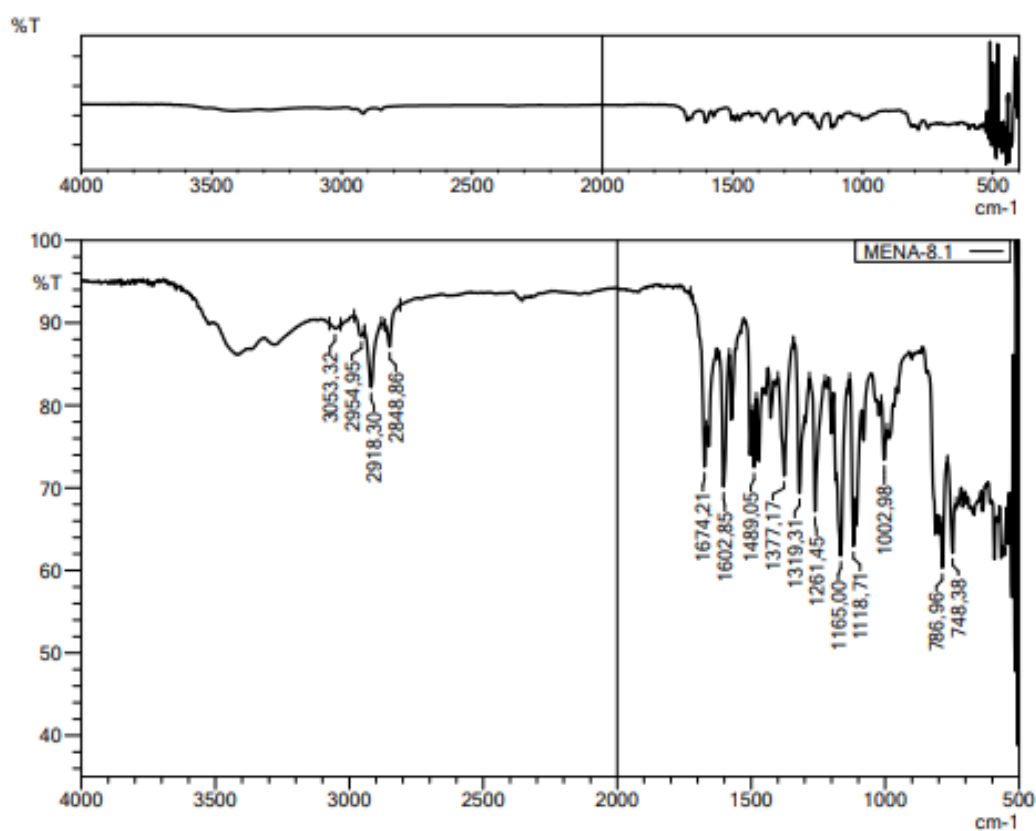
Figure 5.15. *IR spectrum of compound **4b***
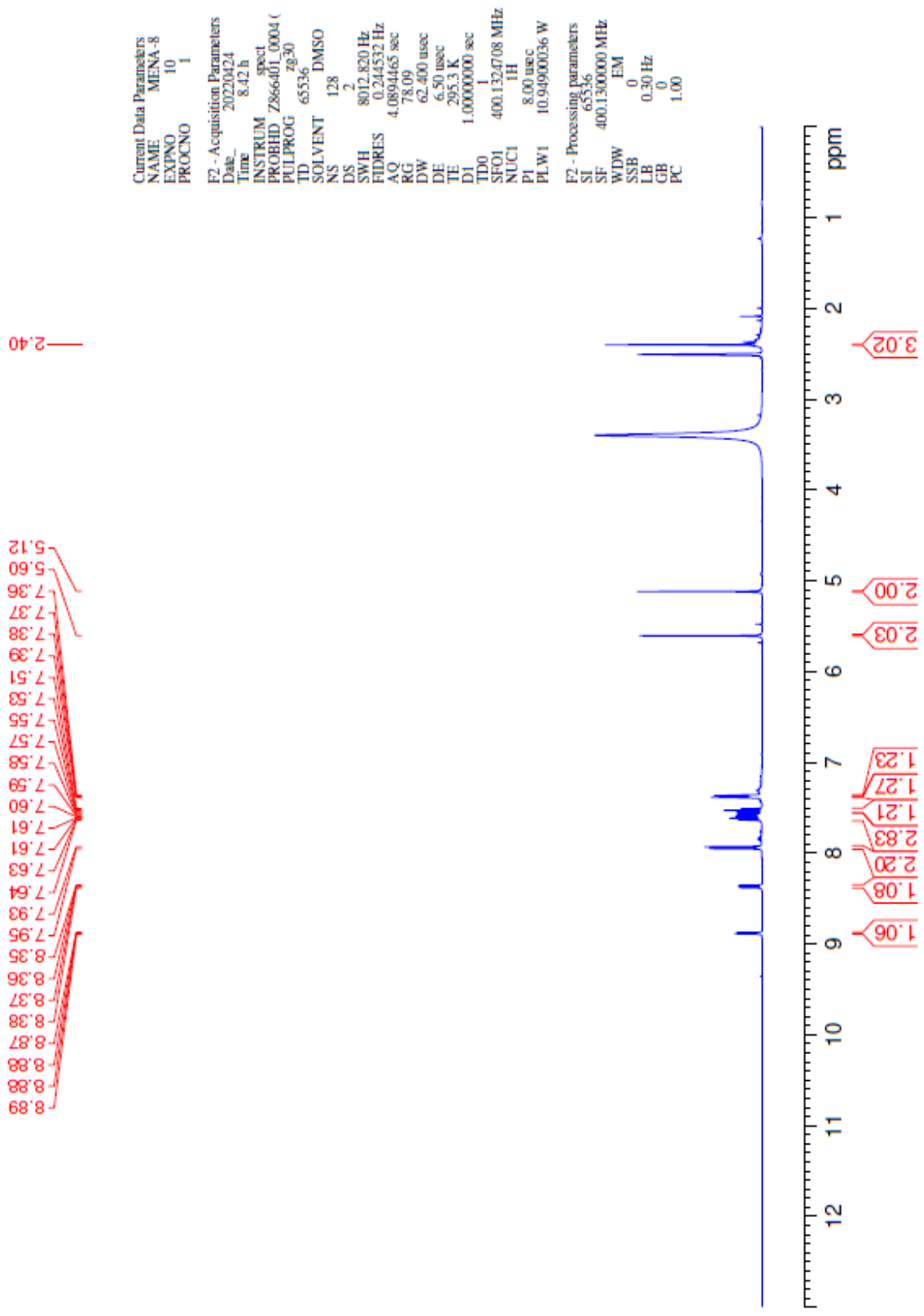
Figure 5.16. *¹H-NMR spectrum of compound **4b***
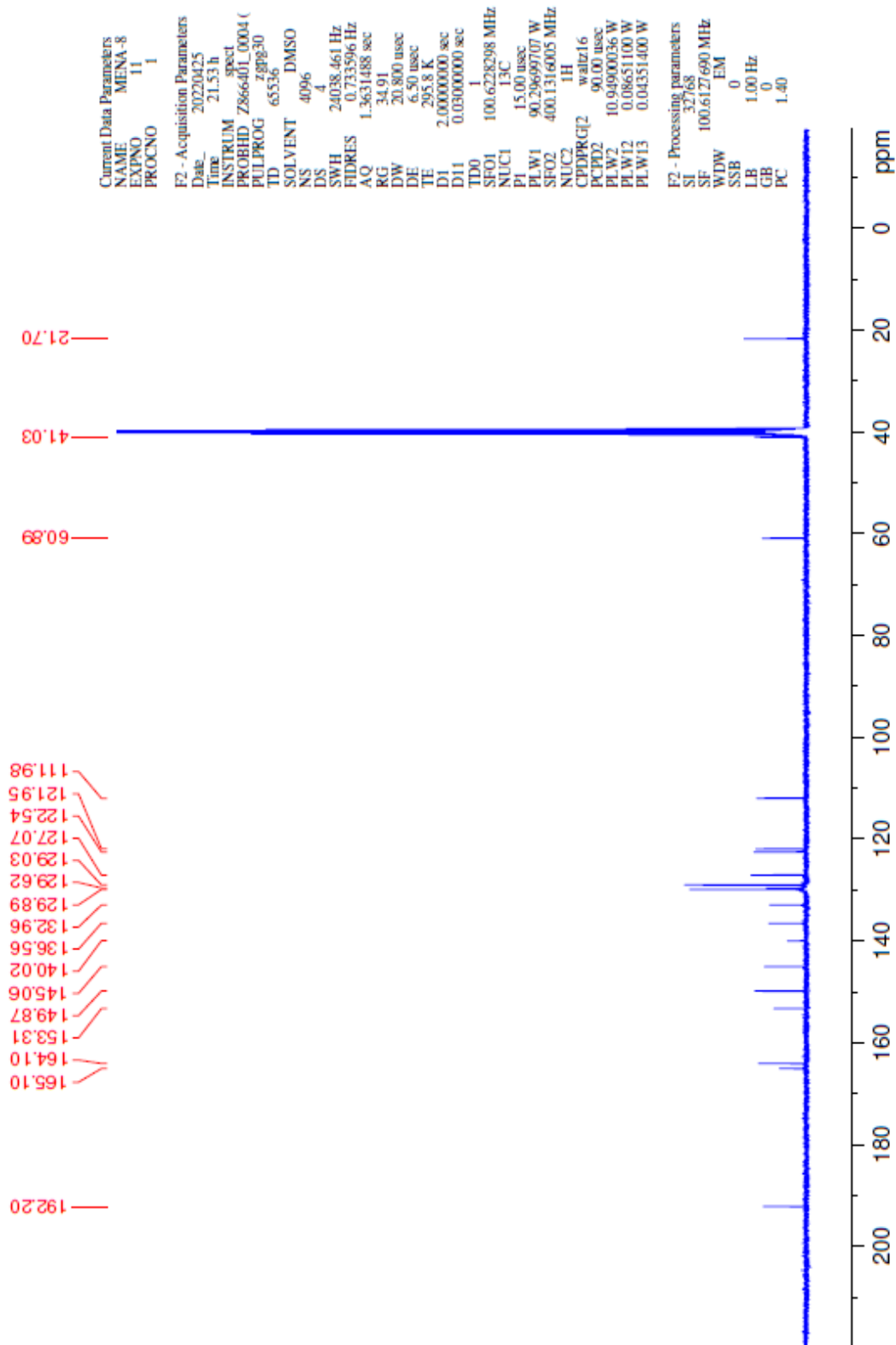
Figure 5.17. .*¹³C-NMR spectrum of compound* **4b**

Figure 5.18. *Mass spectrum of compound **4b***

5.1.4.3. 1-(4-Methoxyphenyl)-2-[[5-[(quinolin-8-yloxy)methyl)-1,3,4-oxadiazol-2-yl]thio]ethan-1-one (4c)
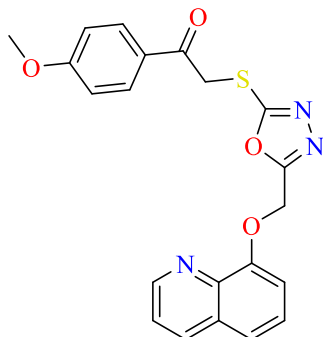
Figure 5.19. *Chemical structure of compound 4c*

Compound **4c** was synthesized according to method D. Yield 71%, M.P. =170-171 °C.

FTIR (ATR, cm^{-1}): 3010-3057 (aromatic C-H stretching), 2918-2848 (aliphatic C-H stretching), 1668 (C=O stretching), 1500-1595 (C=N , C=C stretching), 1257 (C-O stretching, oxadiazole), 1165 (C-O stretching, ether), 1107 (1,4 disubstituted benzene).

^{1}HNMR: (400 MHz, DMSO-d_6, ppm) δ: 3.86 (3H, s, O-CH$_3$), 5.09 (2H, s, CO-CH$_2$), 5.61 (2H, s, O-CH$_2$), 7.08 (2H, d , *J*=1.76 Hz, phenyl-H), 7.37 (1H, d , *J*= 6.93 Hz, quinoline C$_7$-H), 7.52-7.63 (3H, m, quinoline-H), 8.02 (2H, d, *J*=8.9 Hz, phenyl-H), 8.36 (1H, dd , *J$_1$*= 8.29 , *J$_2$*=1.50 Hz, quinoline C$_4$-H), 8.88 (1H, dd , *J$_1$*= 4.09 , *J$_2$*=1.58 Hz, quinoline C$_2$-H).

^{13}C-NMR: (100 MHz, DMSO-d_6, ppm) δ :40.91 (S-CH$_2$), 56.12 (O-CH$_3$), 60.91 (O-CH$_2$), 112.01, 114.57, 121.94, 122.53, 127.08, 128.30, 129.62, 131.34, 136.62, 139.96, 149.83, 153.28, 164.07, 164.21, 165.17, 190.98 (C=O).

HRMS (*m/z*): [M+H]$^+$ calculated for C$_{21}$H$_{17}$N$_3$O$_4$S:408.1013; found:408.1019.

DOPNALAB

Item	Value
Acquired Date&Time	7.06.2022 09:33:49
Acquired by	System Administrator
Filename	C:\Users\dopnalab\Desktop\MASAÜSTÜ\LEYLA YURTDAŞ\MEN\MENA-9.1.ispd
Spectrum name	MENA-9.1
Sample name	MENA-9
Sample ID	
Option	
Comment	
No. of Scans	15
Resolution	4 [cm-1]
Apodization	Happ-Genzel
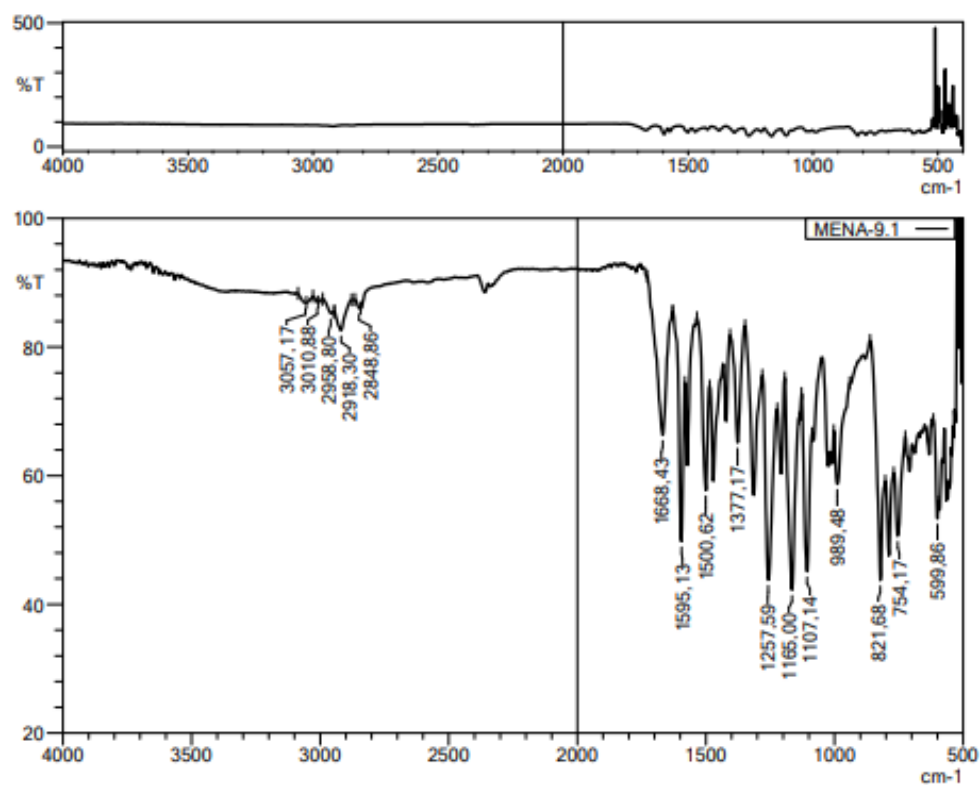
Figure 5.20. *IR spectrum of compound 4c*

61
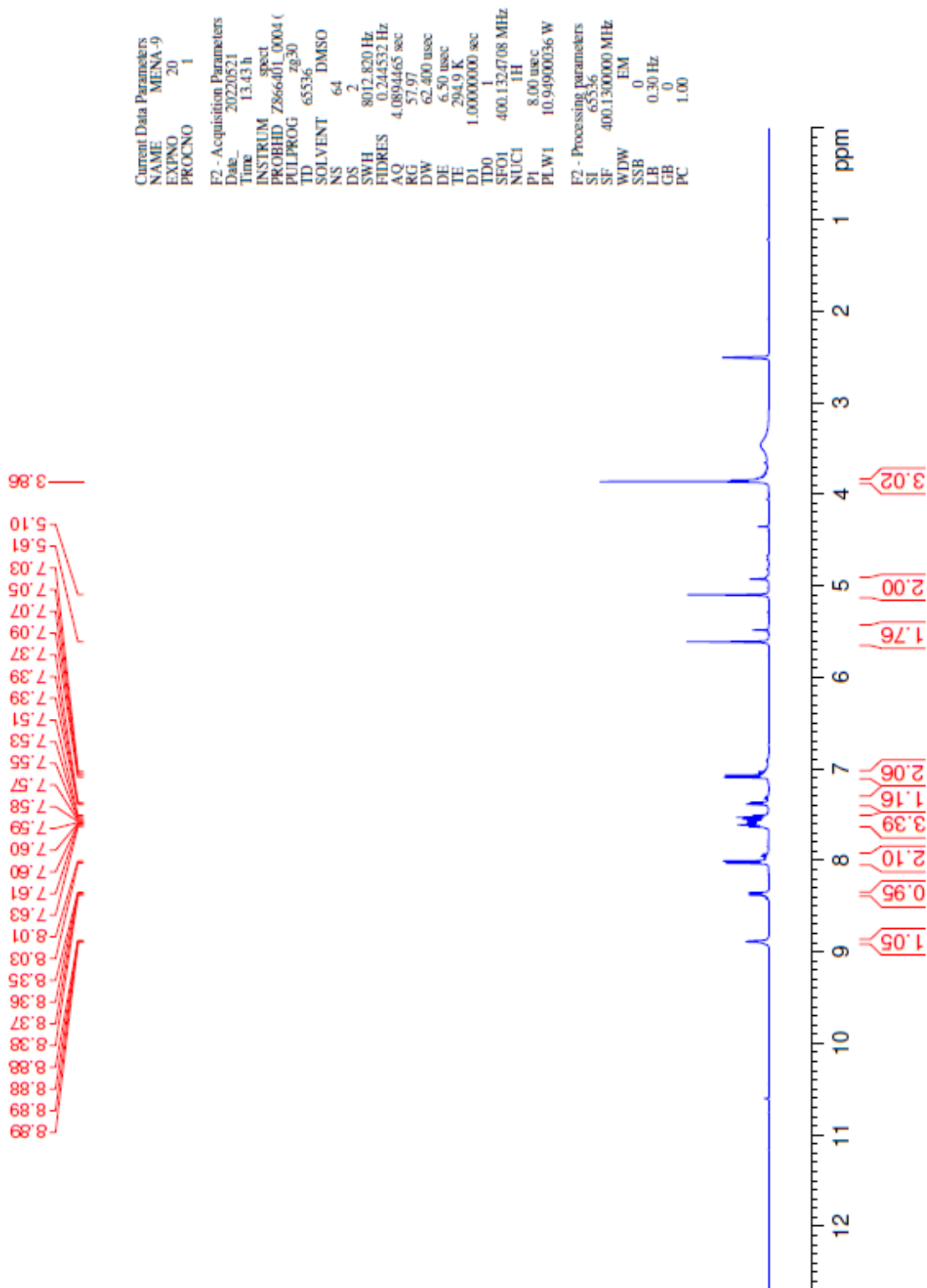
Figure 5.21. *¹H-NMR spectrum of compound **4c***

Current Data Parameters
NAME   MENA-9
EXPNO   30
PROCNO   1

F2 - Acquisition Parameters
Date_   20220525
Time   16.18 h
INSTRUM   spect
PROBHD   Z866401_0004 (
PULPROG   zgpg30
TD   65536
SOLVENT   DMSO
NS   1024
DS   4
SWH   24038.461 Hz
FIDRES   0.733596 Hz
AQ   1.3631488 sec
RG   31.19
DW   20.800 usec
DE   6.50 usec
TE   296.4 K
D1   2.00000000 sec
D11   0.03000000 sec
TD0   1
SFO1   100.6228298 MHz
NUC1   13C
P1   15.00 usec
PLW1   90.29699707 W
SFO2   400.1316005 MHz
NUC2   1H
CPDPRG[2   waltz16
PCPD2   90.00 usec
PLW2   10.94900036 W
PLW12   0.08651100 W
PLW13   0.04351400 W

F2 - Processing parameters
SI   32768
SF   100.6127690 MHz
WDW   EM
SSB   0
LB   1.00 Hz
GB   0
PC   1.40

Figure 5.22. *¹³C-NMR spectrum of compound **4c***
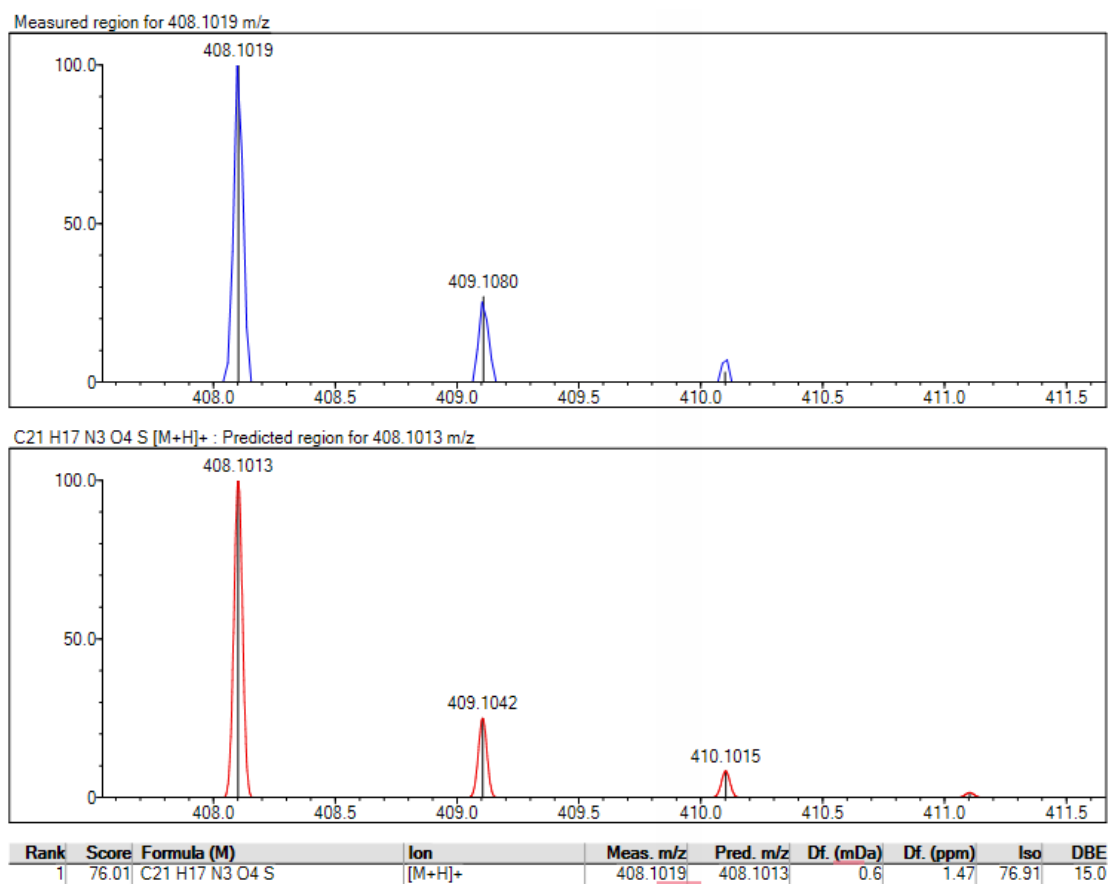
Figure 5.23. *Mass spectrum of compound **4c***

5.1.4.4. 1-(2,5-Dimethoxyphenyl)-2-[[5-((quinolin-8-yloxy)methyl)-1,3,4-oxadiazol-2-yl]thio]ethan-1-one (4d)
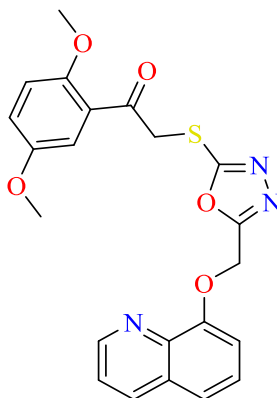
Figure 5.24. *Chemical structure of compound 4d*

Compound **4d** was synthesized according to method F. Yield 69%, M.P. = 124-125°C.

FTIR (ATR, cm^{-1}): 3000-3050 (aromatic C-H stretching), 2835-2937 (aliphatic C-H stretching), 1643 (C=O stretching), 1608 (C=N stretching), 1494 (C=C stretching), 1263 (C-O stretching, oxadiazole), 1157 (C-O stretching, ether).

^{1}HNMR: (400 MHz, DMSO-d_6, ppm) δ: 3.37 (3H, s, O-CH$_3$), 3.89 (3H, s, O-CH$_3$), 4.92 (2H, s, CO-CH$_2$), 5.60 (2H, s, O-CH$_2$), 7.19 -7.22 (2H, m, aromatic-H), 7.37 (1H, d, J_1= 7.7, J_2=1.02 Hz, quinoline C$_7$-H), 7.50-7.63 (4H, m, aromatic-H), 8.34 (1H, dd, J_1= 8.33, J_2=1.72 Hz, quinoline C$_4$-H), 8.87 (1H, dd , J_1= 4.14 , J_2=1.71 Hz, quinoline C$_2$-H).

^{13}C-NMR: (100 MHz, DMSO-d_6, ppm) δ:45.01 (S-CH$_2$), 56.04 (O-CH$_3$), 56.95 (O-CH$_3$), 60.91 (O-CH$_2$), 111.94, 114.15, 114.80, 121.81, 121.93, 122.51, 125.48, 127.01, 129.61, 136.44, 140.13, 149.89, 153.37, 153.47, 153.88, 164.06, 165.27, 192.64 (C=O).

HRMS (*m/z*): [M+H]$^+$ calculated for C$_{22}$H$_{19}$N$_3$O$_5$S:438.1118; found: 438.1119.

DOPNALAB

Item	Value
Acquired Date&Time	7.06.2022 09:42:30
Acquired by	System Administrator
Filename	C:\Users\dopnalab\Desktop\MASAÜSTÜ\LEYLA YURTDAŞ\MEN\MENA-12.1.ispd
Spectrum name	MENA-12.1
Sample name	MENA-12
Sample ID	
Option	
Comment	
No. of Scans	15
Resolution	4 [cm-1]
Apodization	Happ-Genzel
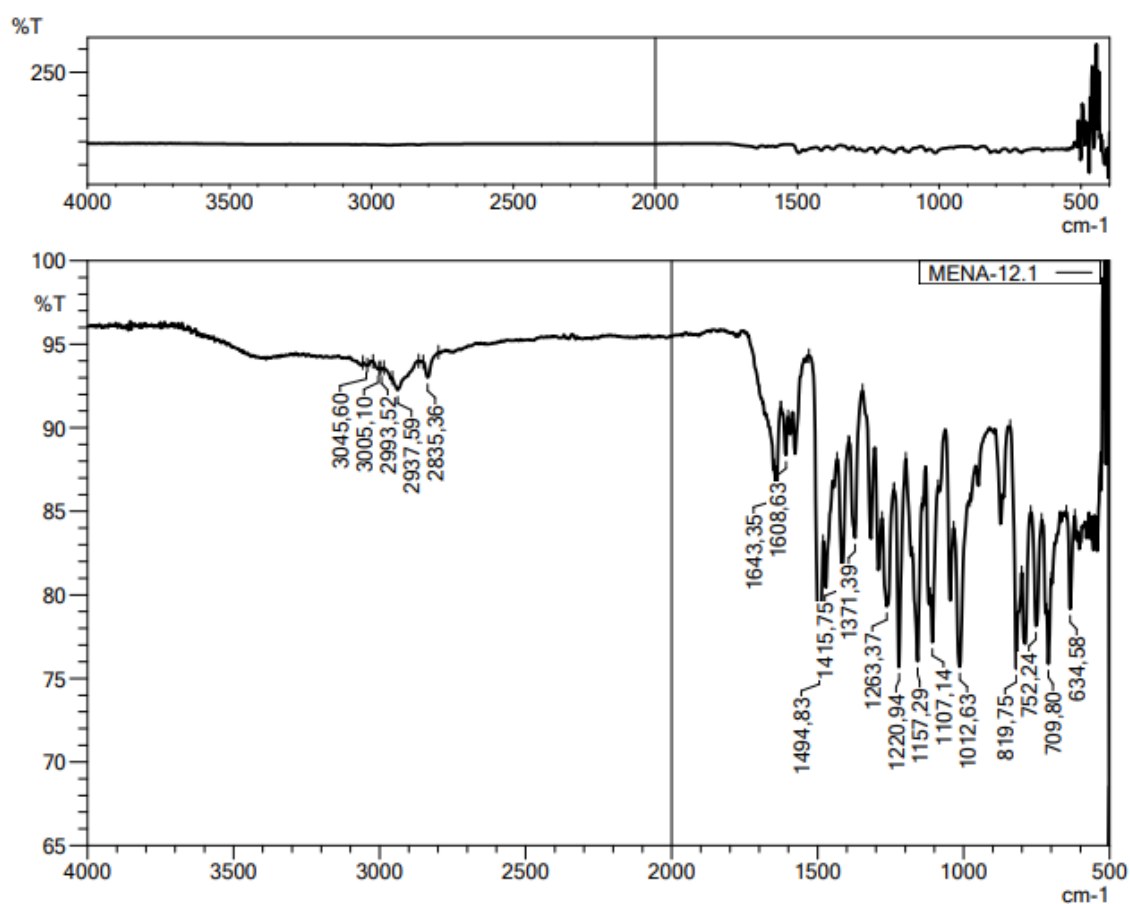
Figure 5.25. *IR spectrum of compound* **4d**
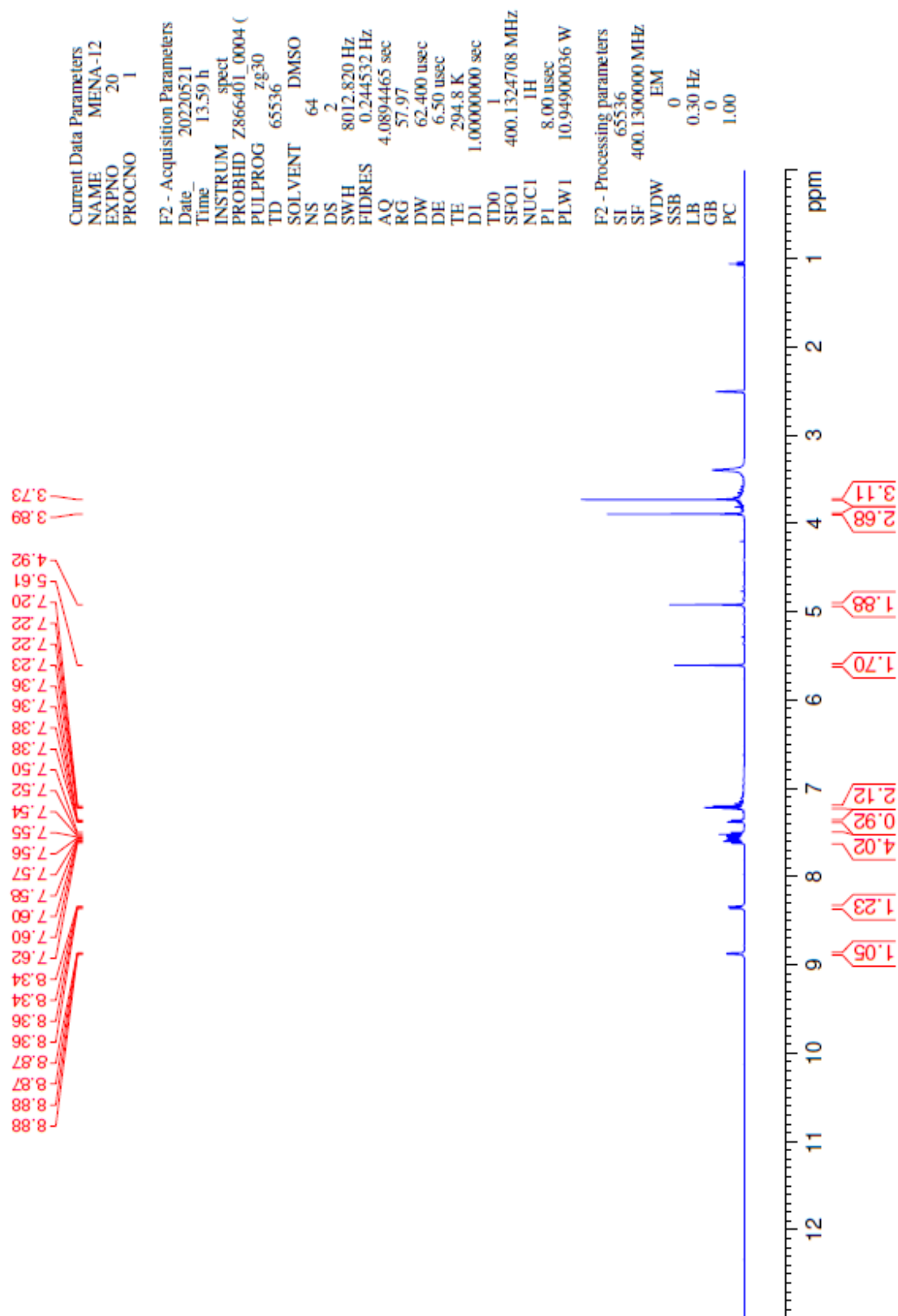
Figure 5.26. *¹H-NMR spectrum of compound* **4d**

192.64

165.28
164.06
153.88
153.47
153.37
149.89
140.14
136.44
129.62
127.02
125.49
122.51
121.94
121.81
114.81
114.15
111.94

60.91
56.95
56.04

45.02

200 180 160 140 120 100 80 60 40 20 ppm
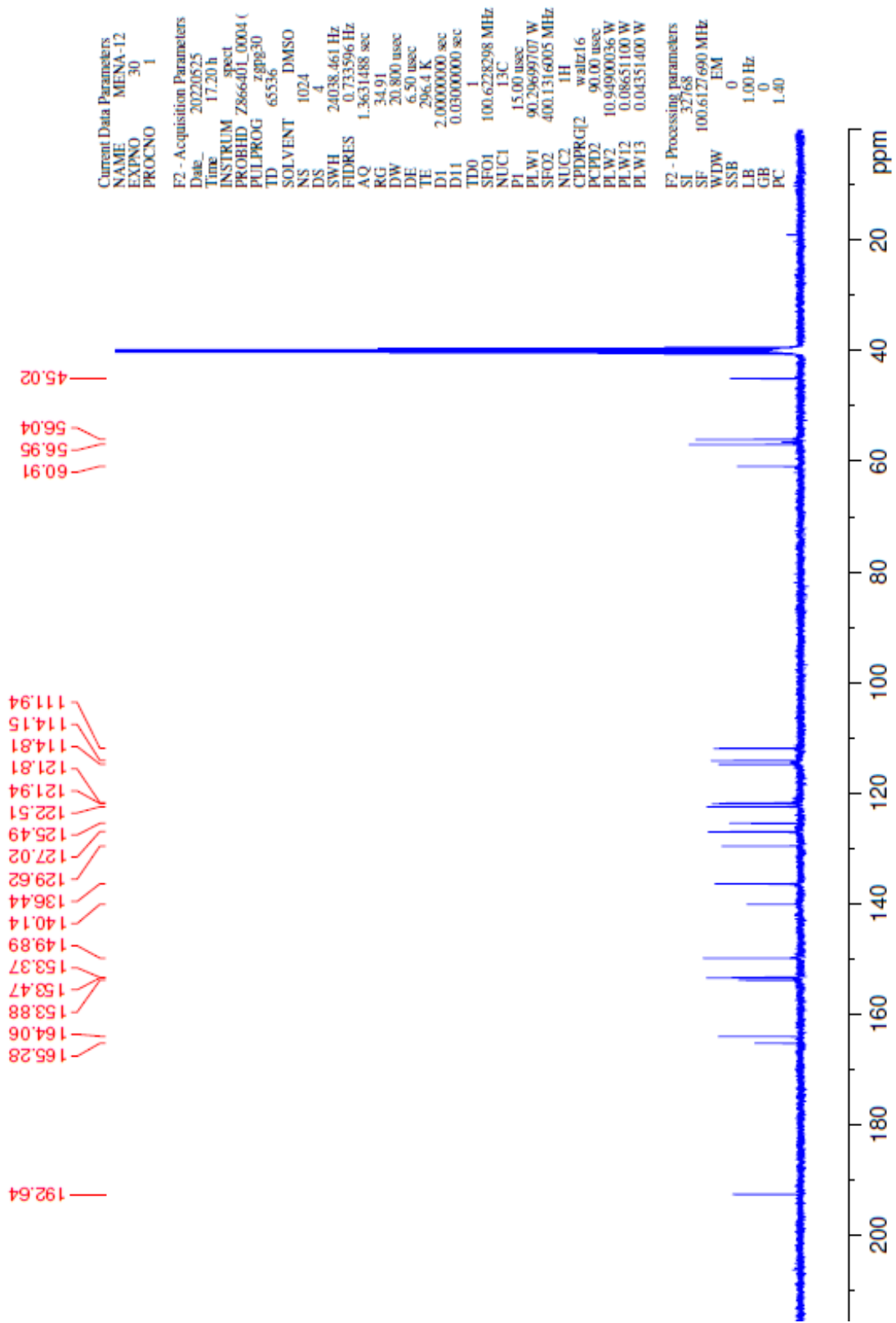
Figure 5.27.^{13}*C-NMR spectrum of compound* **4d**

C22 H19 N3 O5 S [M+H]+ : Predicted region for 438.1118 m/z

Rank	Score	Formula (M)	Ion	Meas. m/z	Pred. m/z	Df. (mDa)	Df. (ppm)	Iso	DBE
1	84.58	C22 H19 N3 O5 S	[M+H]+	438.1119	438.1118	0.1	0.23	84.58	15.0
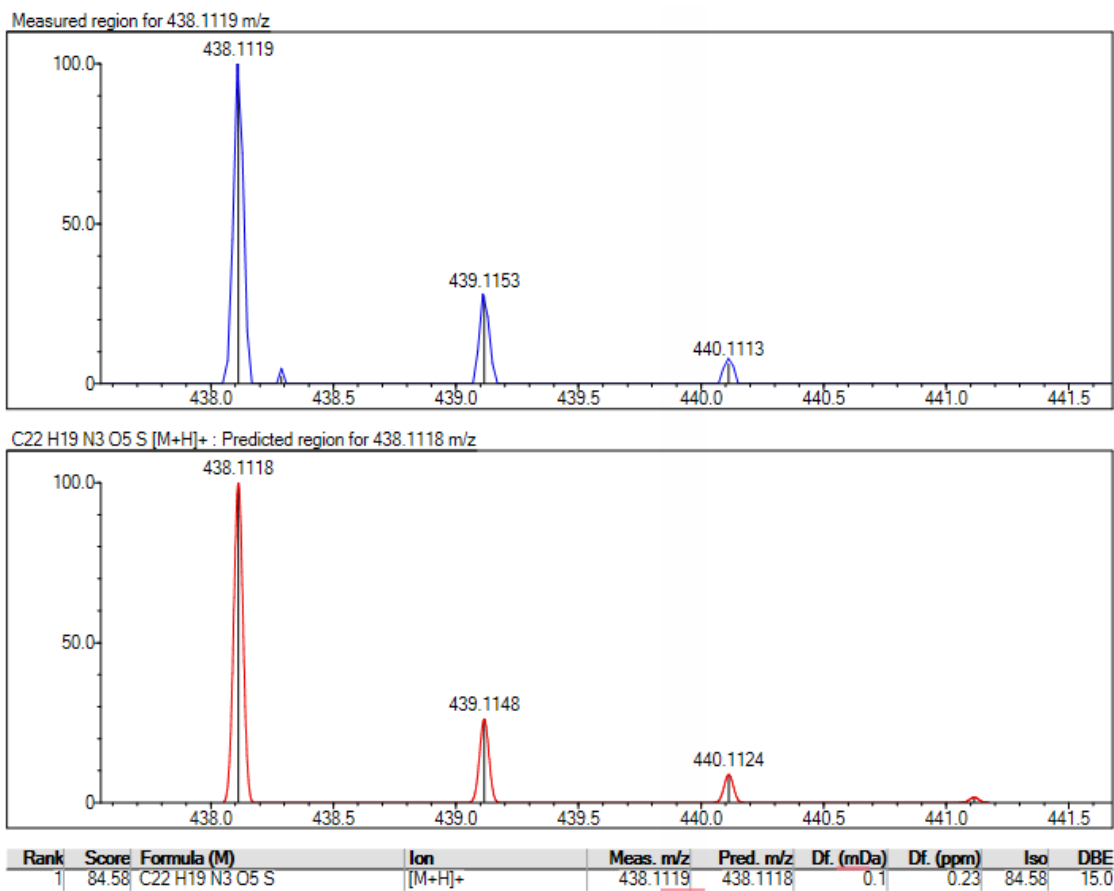
Figure 5.28. *Mass spectrum of compound **4d***

5.1.5. *N*-(4-Substituted phenyl)-2-[[5-((quinolin-8-yloxy)methyl)-1,3,4-oxadiazol-2-yl]thio]acetamide (5a-c)
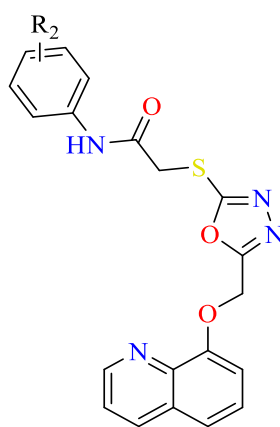
5a-c

Figure 5.29. *Compounds **5a-c** general structure*

N-(4-substituted phenyl)-2-[[5-((quinolin-8-yloxy)methyl)-1,3,4-oxadiazol-2-yl]thio]acetamide derivatives were synthesized according to method E and F.
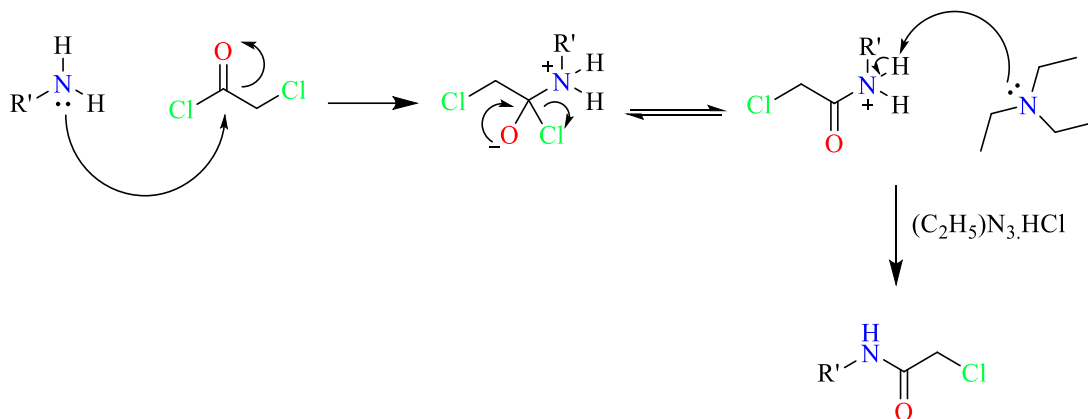
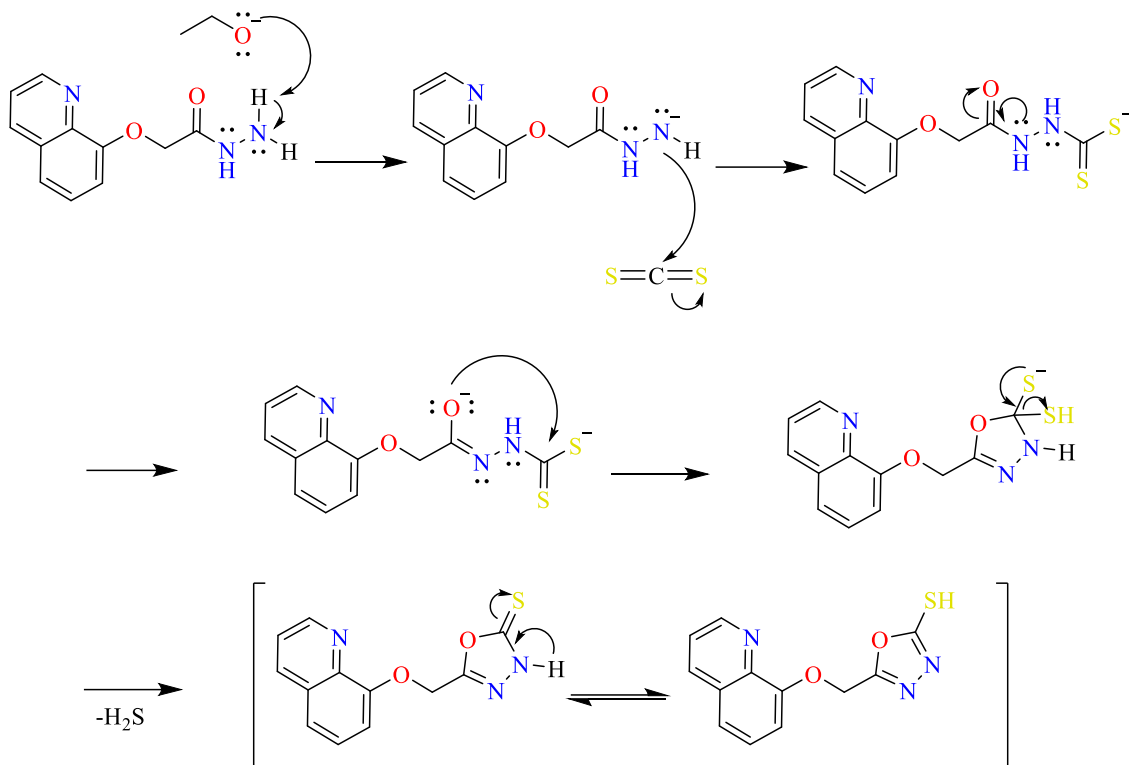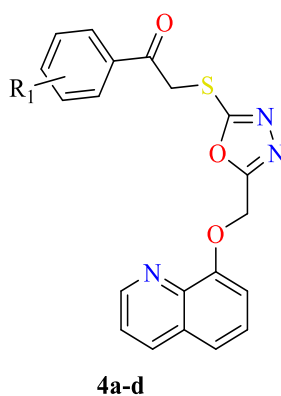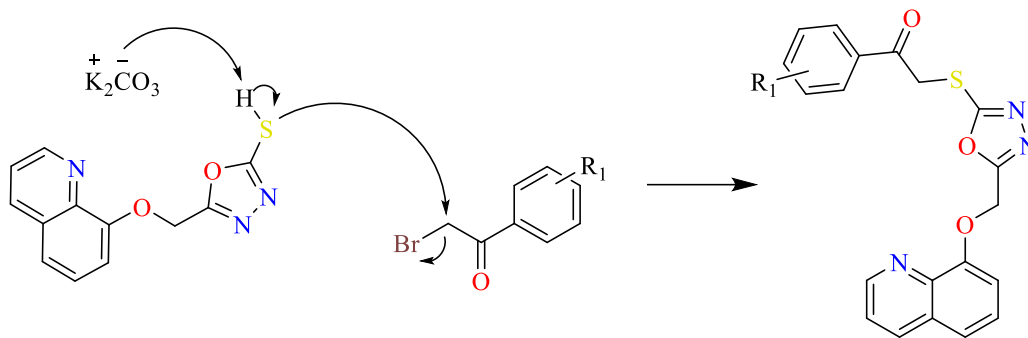**Figure 5.30.** *Schematic representation of method E mechanism*
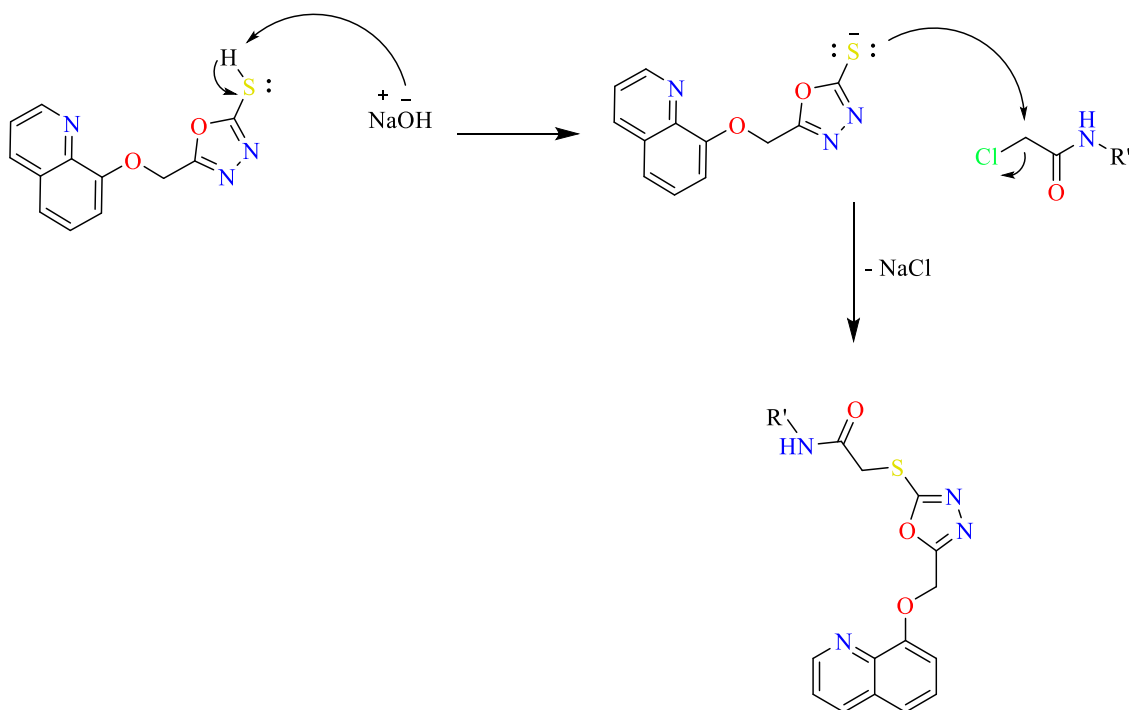
Figure 5.31. *Schematic representation of method F mechanism*

*5.1.5.1. N-(4-Chlorophenyl)-2-[[5-((quinolin-8-yloxy)methyl)-1,3,4-oxadiazol-2-yl]thio]acetamide (5a)*
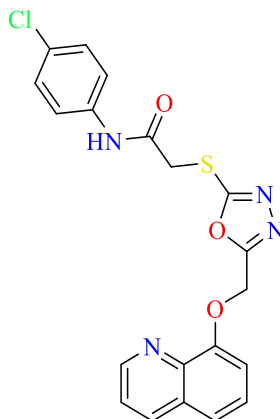
Figure 5.32. *Chemical structure of compound 5a*

Compound **5a** was synthesized according to method E and F. Yield= 79%, M.P. =182-183 °C.

FTIR (ATR, cm^{-1}): 3172-3207 (N-H stretching), 3051-3061 (aromatic C-H stretching), 2920-2978 (aliphatic C-H stretching), 1730 (C=O stretching),1662 (C=N stretching), 1490-1570 (C=C stretching), 1240 (C-O stretching, oxadiazole), 1087(C-O stretching, ether), 1116 (1,4 disubstituted benzene).

^{1}H-NMR: (400 MHz, DMSO-d_6, ppm) δ: 4.10 (2H, s, CO-CH$_2$), 4.75 (2H, s, O-CH$_2$), 7.30 (1H, d, J=7.67 Hz, aromatic-H), 7.36 (1H, d, J=8.86 Hz, quinoline C$_7$-H), 7.50-7.60 (6H, m, aromatic-H), 8.34-8.37 (1H, m, quinoline-H), 8.80-8.89 (1H, m, quinoline-H), 10.52 (1H, s, NH).

^{13}C-NMR: (100 MHz, DMSO-d_6, ppm) δ: 37.22 (S-CH$_2$), 56.49 (S-CH$_2$), 111.98, 121.20, 121.96, 122.51, 127.04, 127.69, 129.21, 136.44, 138.05, 140.14, 149.90, 153.37, 164.19, 165.07, 165.27 (C=O).

HRMS (*m/z*): [M+H]$^+$ calculated for C$_{20}$H$_{15}$N$_4$O$_3$ClS:427.0626; found: 427.0609.

DOPNALAB

Item	Value
Acquired Date&Time	21.07.2022 15:44:38
Acquired by	System Administrator
Filename	C:\Users\dopnalab\Desktop\MASAÜSTÜ\LEYLA YURTDAŞ\MEN\MENC2.1.ispd
Spectrum name	MENC2.1
Sample name	MENC2
Sample ID	
Option	
Comment	
No. of Scans	15
Resolution	4 [cm-1]
Apodization	Happ-Genzel
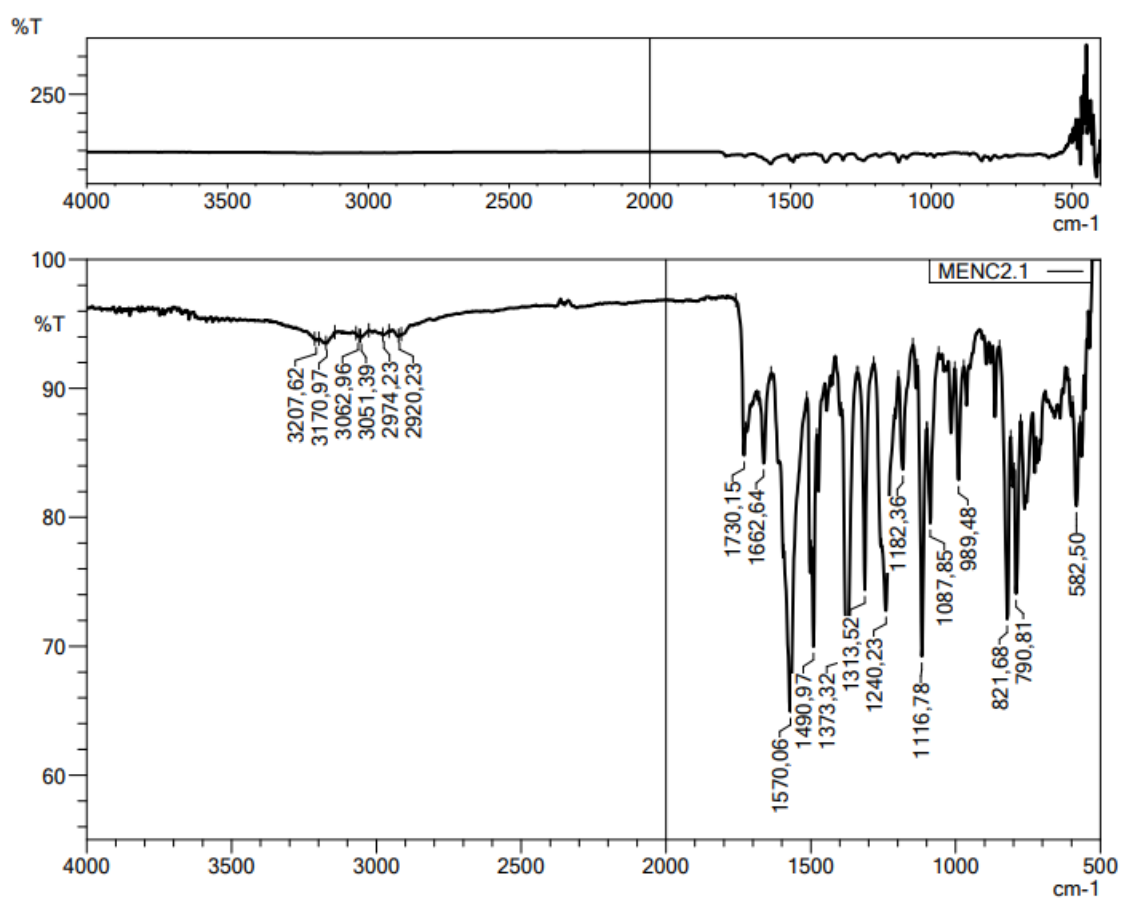
Figure 5.33. *IR spectrum of compound* **5a**
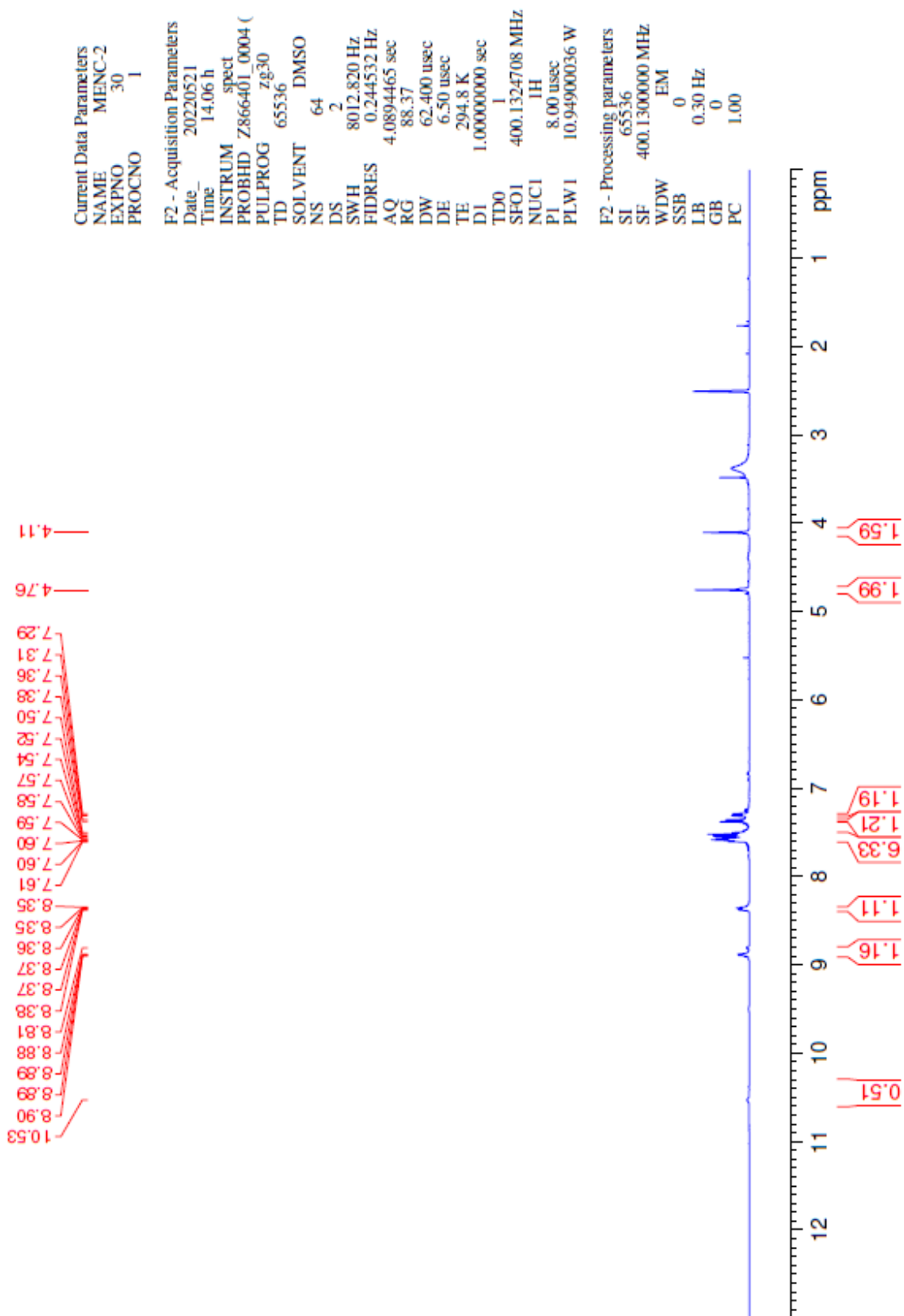
Figure 5.34. *¹H-NMR spectrum of compound **5a***
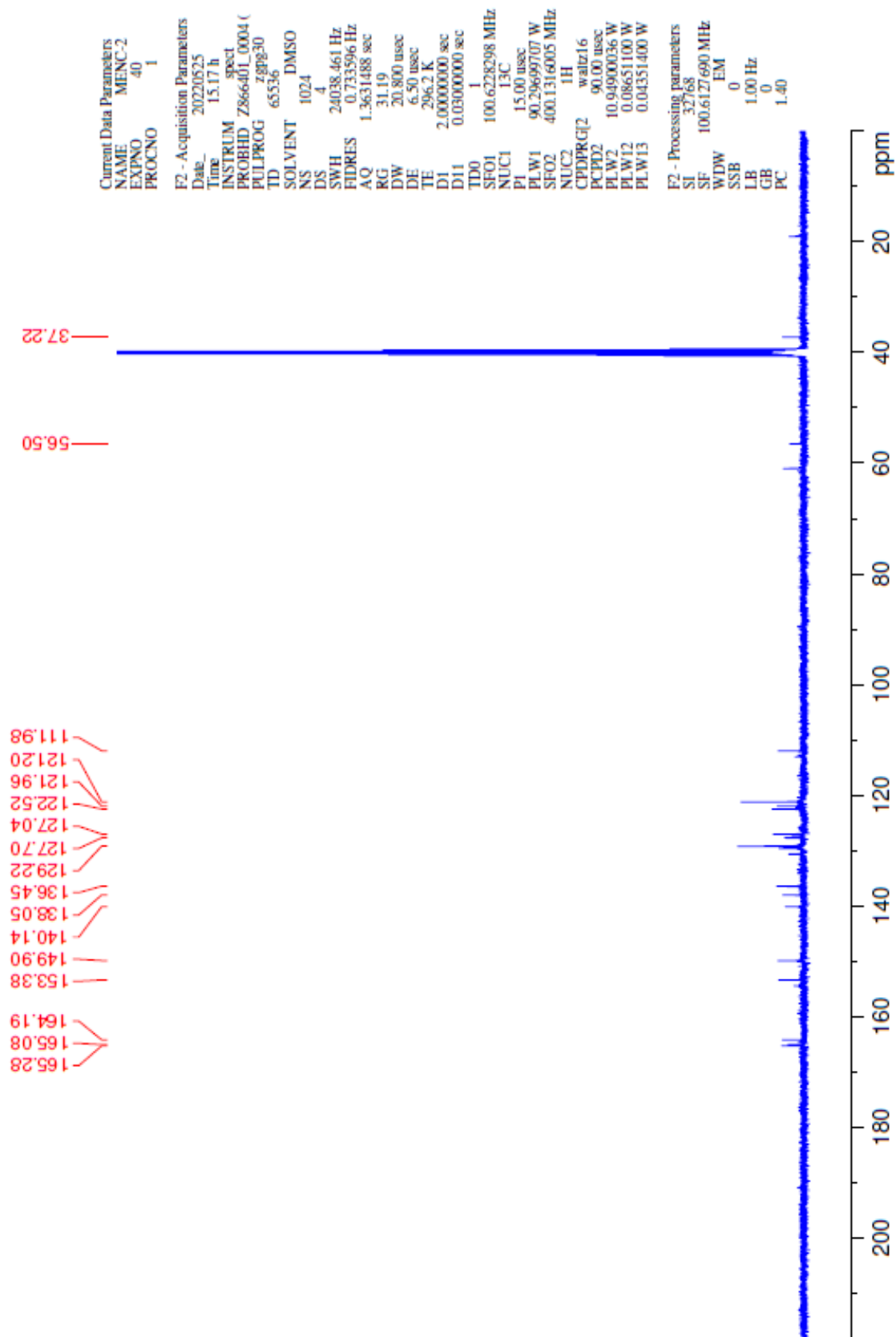
Figure 5.35. *¹³C-NMR spectrum of compound **5a***

74
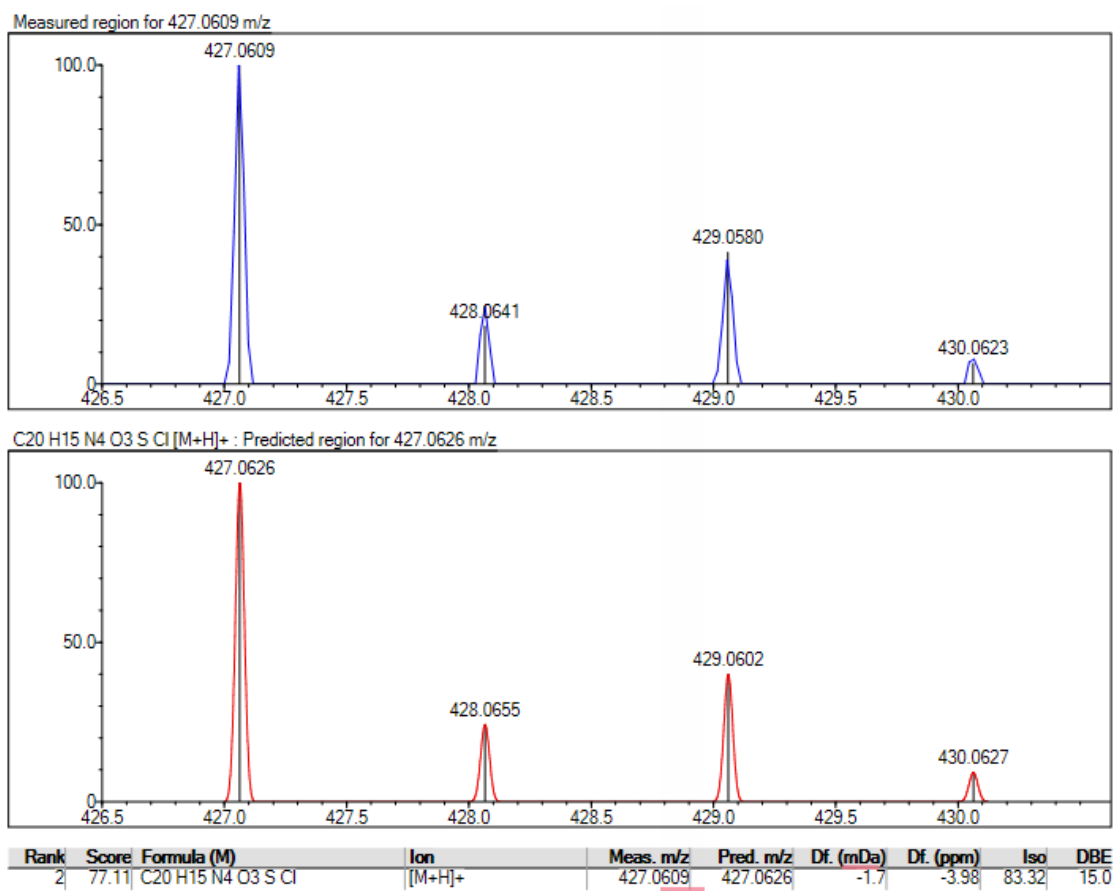
Figure 5.36. *Mass spectrum of compound* **5a**
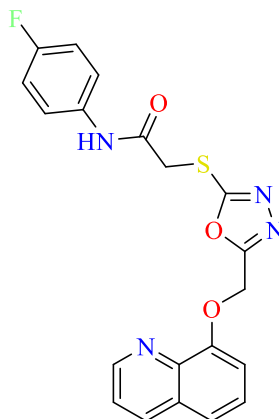
Figure 5.37. *Chemical structure of compound 5b*

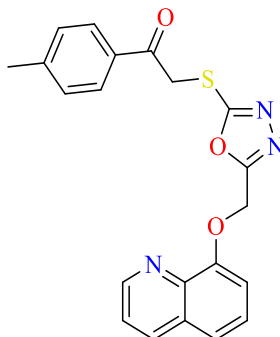Compound **5b** was synthesized according to method E and F. Yield= 87%, M.P. =182-183 °C.

FTIR (ATR, cm^{-1}): 3292-3122 (N-H stretching), 3066 (aromatic C-H stretching), 2976-2841 (aliphatic C-H stretching), 1707 (C=O stretching), 1618 (C=N stretching), 1544 (C=C stretching), 1228 (C-O stretching, oxadiazole), 1116 (1,4 disubstituted benzene).

^{1}H-NMR: (400 MHz, DMSO-d_6, ppm) δ: 3.92 (2H, s, CO-CH$_2$), 4.55 (2H, s, O-CH$_2$), 7.28-7.37 (4H, m, aromatic-H), 7.51-7.58 (4H, m, aromatic-H), 8.36 (1H, d, J=6.17 Hz, quinoline C$_4$-H), 8.77-8.80 (1H, m, quinoline C$_4$-H).

^{13}C-NMR: (100 MHz, DMSO-d_6, ppm) δ: 32.49 (S-CH$_2$), 51.04 (S-CH$_2$), 116.07, 116.29, 120.31, 122.45, 127.60, 129.19, 130.85, 132.53, 136.84, 139.80, 149.65, 172.05 (C=O).

HRMS (*m/z*): [M+H]$^+$ calculated for C$_{20}$H$_{15}$N$_4$O$_3$FS: 411.0922 ; found: 411.0916 .

Item	Value
Acquired Date&Time	7.06.2022 09:54:44
Acquired by	System Administrator
Filename	C:\Users\dopnalab\Desktop\MASAÜSTÜ\LEYLA YURTDAŞ\MEN\MENC-3.1.ispd
Spectrum name	MENC-3.1
Sample name	MENC-3
Sample ID	
Option	
Comment	
No. of Scans	15
Resolution	4 [cm-1]
Apodization	Happ-Genzel

Figure 5.38. *IR spectrum of compound* **5b**

Figure 5.39. *¹H-NMR spectrum of compound **5b***

Figure 5.40. *¹³C-NMR spectrum of compound **5b***

Measured region for 411.0916 m/z

C20 H15 N4 O3 F S [M+H]+ : Predicted region for 411.0922 m/z

Rank	Score	Formula (M)	Ion	Meas. m/z	Pred. m/z	Df. (mDa)	Df. (ppm)	Iso	DBE
1	75.02	C20 H15 N4 O3 F S	[M+H]+	411.0916	411.0922	-0.6	-1.46	75.90	15.0

Figure 5.41. *Mass spectrum of compound 5b*

5.1.5.3. N-(4-Methoxyphenyl)-2-[[5-((quinolin-8-yloxy)methyl)-1,3,4-oxadiazol-2-yl]thio]acetamide (5c)

Figure 5.42. *Chemical structure of compound 5c*

Compound **5c** was synthesized according to method E and F. Yield= 74%, M.P. = 206-207°C.

FTIR (ATR, cm^{-1}): 3251-3196 (N-H stretching), 3053 (aromatic C-H stretching), 2954-2848 (aliphatic C-H stretching), 1674 (C=O stretching), 1620 (C=N stretching), 1556 (C=C stretching), 1244 (C-O stretching, oxadiazole), 1170 (C-O stretching, ether), 1029 (1,4 disubstituted benzene).

^{1}H-NMR: (400 MHz, DMSO-$_{d6}$, ppm) δ: 3.79 (3H, s , O-CH$_3$), 4.20 (2H, s, CO-CH$_2$), 4.85 (2H, s, O-CH$_2$), 7.03 (2H, d, *J*=8.9 Hz, phenyl C$_{3,5}$-H), 7.23 (2H, d, *J*=8.9 Hz, phenylC$_{2,6}$-H), 7.29 (1H, d , *J*=7.44 Hz, quinoline C$_7$-H), 7.50-7.63 (3H, m, aromatic-H), 8.38 (1H, dd , *J$_1$*= 8.28 , *J$_2$*=1.5 Hz, quinoline C$_4$-H), 8.95 (1H, dd , *J$_1$*= 4.12 , *J$_2$*=1.5 Hz, quinoline C$_2$-H), 10.79 (1H, s, NH).

^{13}C-NMR: (100 MHz, DMSO-d_6, ppm) δ: 33.44 (S-CH$_2$), 55.84 (O-CH$_3$), 69.28 (O-CH$_2$), 113.00, 114.74, 121.20, 121.75, 122.54, 127.27, 127.82, 129.82, 136.64, 140.35, 150.01, 154.40, 159.58, 159.68, 164,59, 171.77(C=O).

HRMS (*m/z*): [M+H]$^+$ calculated for C$_{21}$H$_{18}$N$_4$O$_4$S: 423.1122 ; found: 423.1122 .

DOPNALAB

Item	Value
Acquired Date&Time	7.06.2022 09:47:04
Acquired by	System Administrator
Filename	C:\Users\dopnalab\Desktop\MASAÜSTÜ\LEYLA YURTDAŞ\MEN\MENC-5.1.ispd
Spectrum name	MENC-5.1
Sample name	MENC-5
Sample ID	
Option	
Comment	
No. of Scans	15
Resolution	4 [cm-1]
Apodization	Happ-Genzel
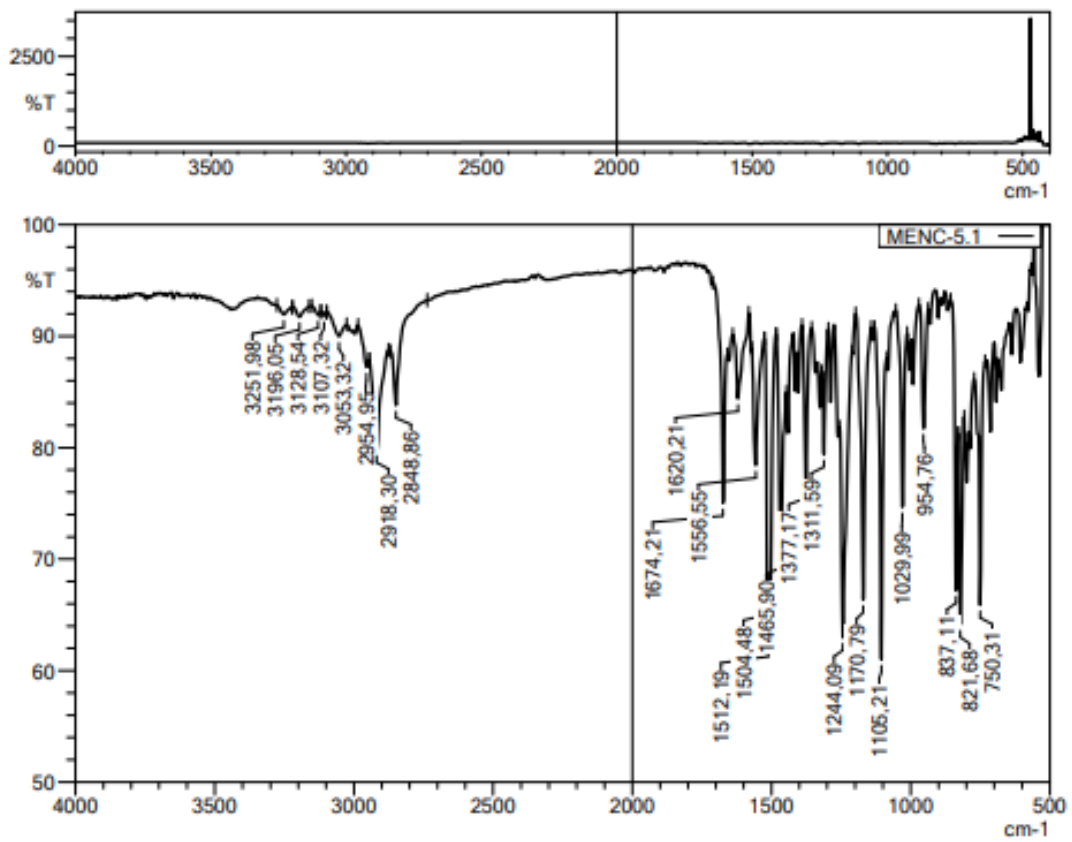
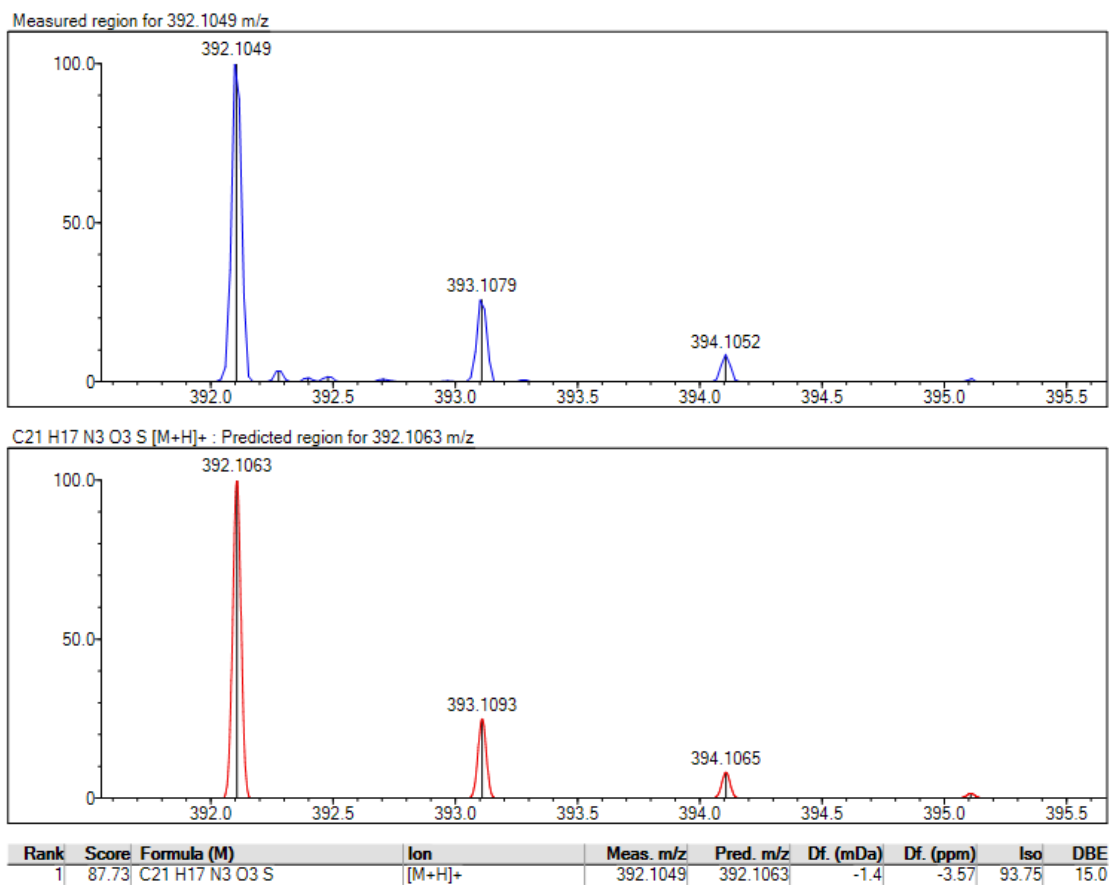**Figure 5.43. IR spectrum of compound 5c**

82
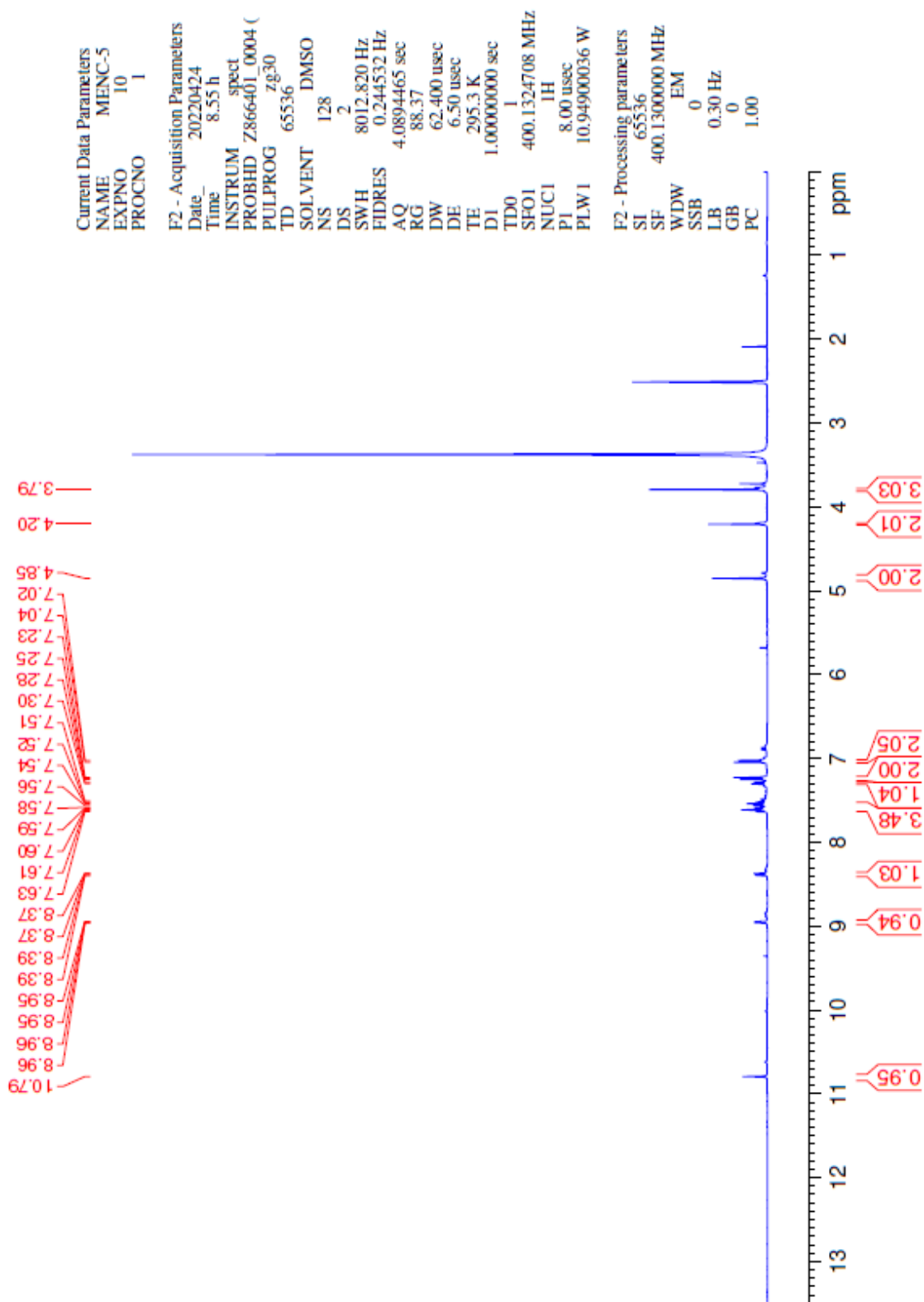
Figure 5.44. *¹H-NMR spectrum of compound **5c***
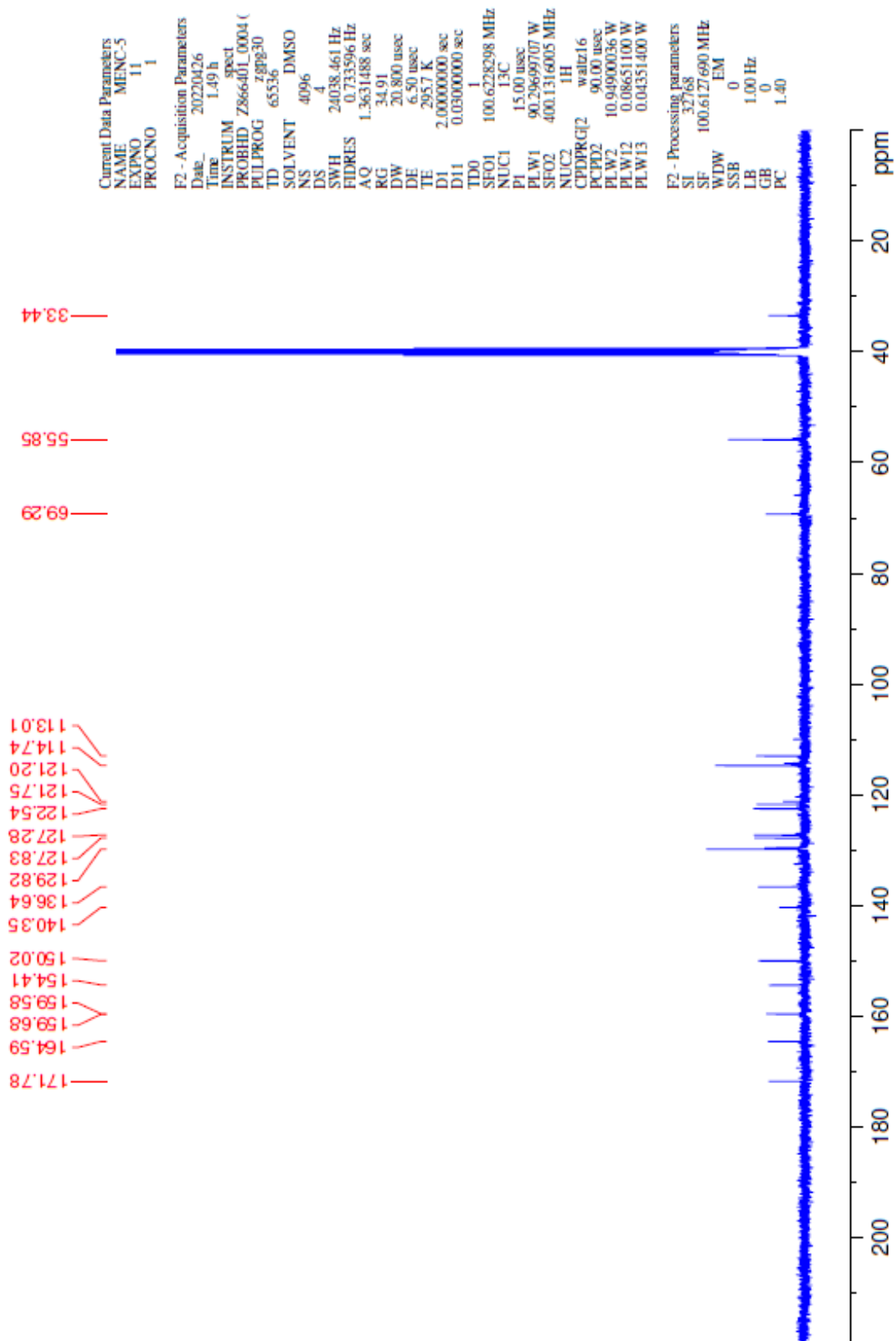
Figure 5.45. *¹³C-NMR spectrum of compound **5c***
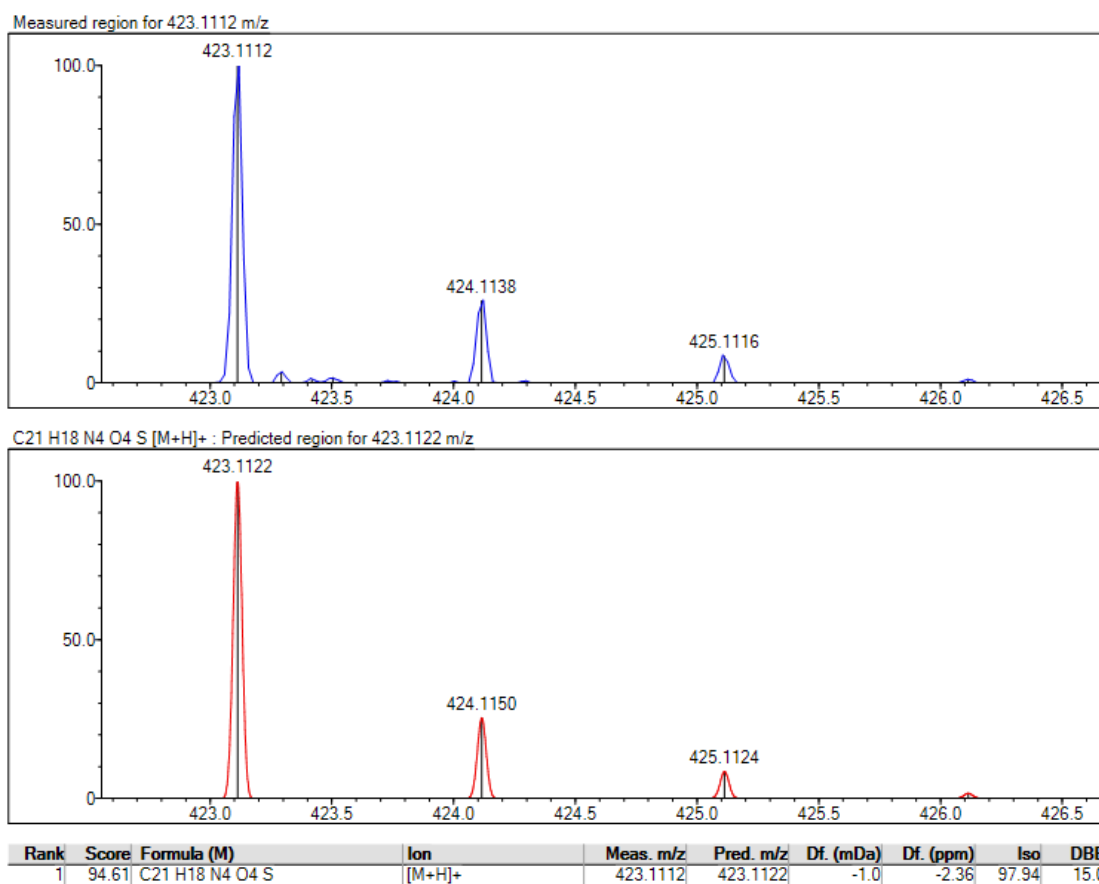
Figure 5.46. *Mass spectrum of compound 5c*

5.1.6. *N*-(Substituted thiazol-2-yl)-2-[[5-((quinolin-8-yloxy)methyl)-1,3,4-oxadiazol-2-yl]thio]acetamide (6a-c)

N-(Substituted thiazol-2-yl)-2-[[5-((quinolin-8-yloxy)methyl)-1,3,4-oxadiazol-2-yl]thio]acetamide derivatives were also synthesized according to method E and F.

6a-c
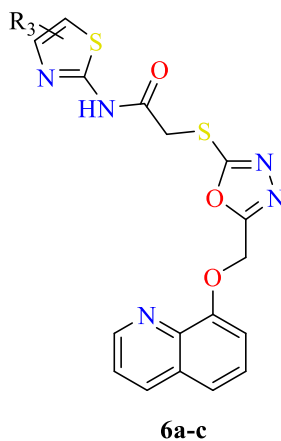
Figure 5.47. *Compounds 6a-c general structure*

5.1.6.1. N-(4,5-Dimethylthiazol-2-yl)-2-[[5-((quinolin-8-yloxy)methyl)-1,3,4-oxadiazol-2-yl]thio]acetamide (6a)
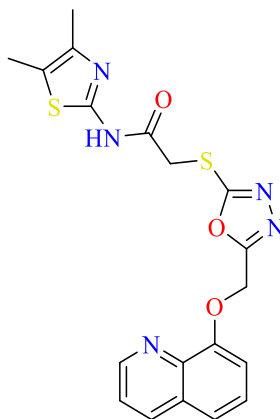
Figure 5.48. *Chemical structure of compound **6a***

Compound **6a** was synthesized according to method E and F. Yield= 83 %, M.P. = 175-176 °C.

FTIR (ATR, cm^{-1}): 3153 (N-H stretching), 3045 (aromatic C-H stretching), 2918 (aliphatic C-H stretching), 1670 (C=O stretching), 1618-1500 (C=N ,C=C stretching), 1253 (C-O stretching, oxadiazole), 1163 (C-O stretching, ether).

^{1}H-NMR: (400 MHz, DMSO-d_6, ppm) δ: 2.15 (3H, s, thiazole CH$_3$), 2.23 (3H, s, thiazole CH$_3$), 4.36 (2H, s, CO-CH$_2$), 5.60 (2H, s, O-CH$_2$), 7.36 (1H, d, J= 7.45 Hz, quinoline C$_7$-H), 7.50-7.63 (3H, m, aromatic-H), 8.35 (1H, d, J= 8.16 Hz, quinoline C$_4$-H), 8.87 (1H, d, J= 2.56 Hz, quinoline C$_2$-H), 12.27 (1H, s, NH).

^{13}C-NMR: (100 MHz, DMSO-d_6, ppm) δ: 10.81 (-CH$_3$), 14.68 (-CH$_3$), 35.93 (S-CH$_2$), 60.97 (O-CH$_2$), 112.02, 121.97, 122.49, 127.02, 129.61, 136.41, 140.15, 149.90, 153.37, 164.28, 164.82 (C=O).

HRMS (*m/z*): [M+H]$^+$ calculated for C$_{19}$H$_{17}$N$_5$O$_3$S$_2$:428.0846; found 428.0851.

DOPNALAB

Item	Value
Acquired Date&Time	7.06.2022 10:00:04
Acquired by	System Administrator
Filename	C:\Users\dopnalab\Desktop\MASAÜSTÜ\LEYLA YURTDAŞ\MEN\MENF-2.1.ispd
Spectrum name	MENF-2.1
Sample name	MENF-2
Sample ID	
Option	
Comment	
No. of Scans	15
Resolution	4 [cm-1]
Apodization	Happ-Genzel
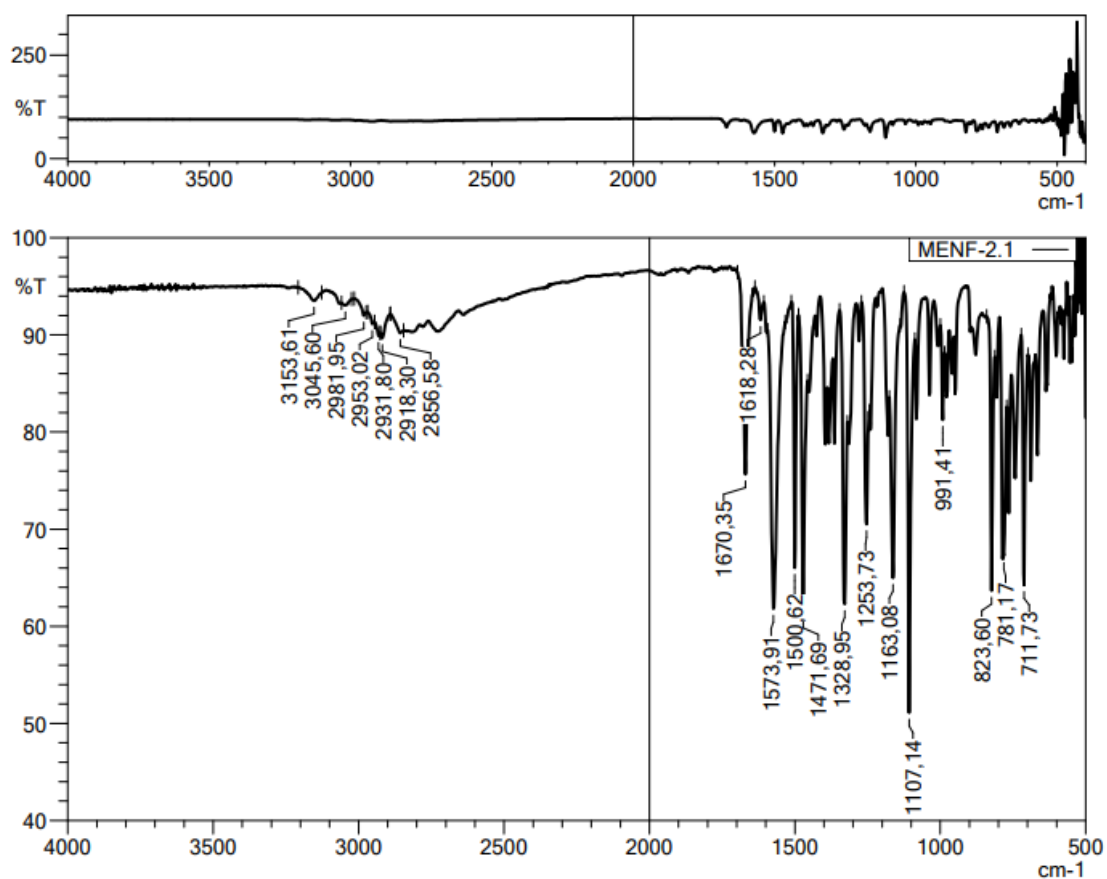
Figure 5.49. *IR spectrum of compound* **6a**

88
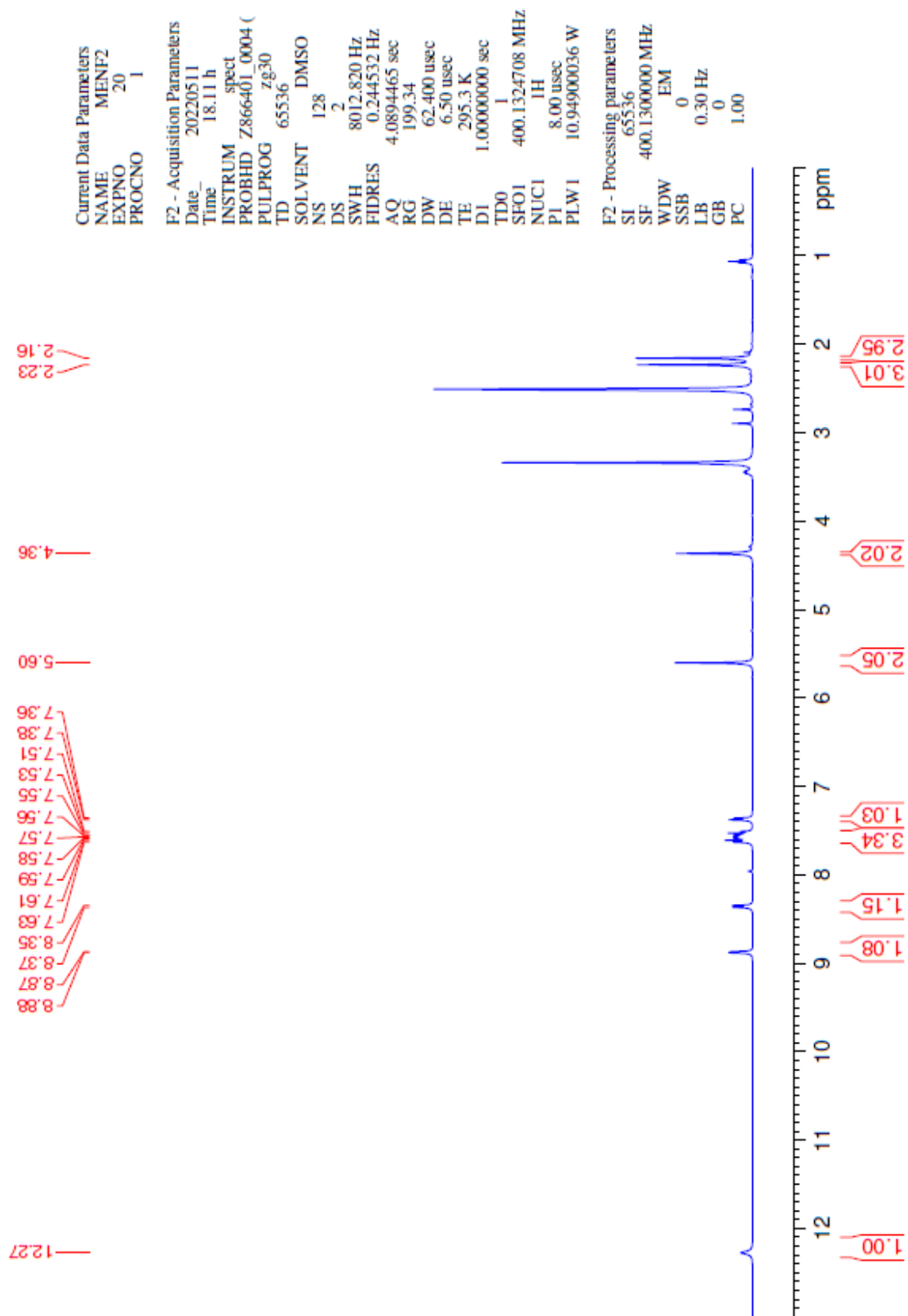
Figure 5.50. *¹H-NMR spectrum of compound 6a*
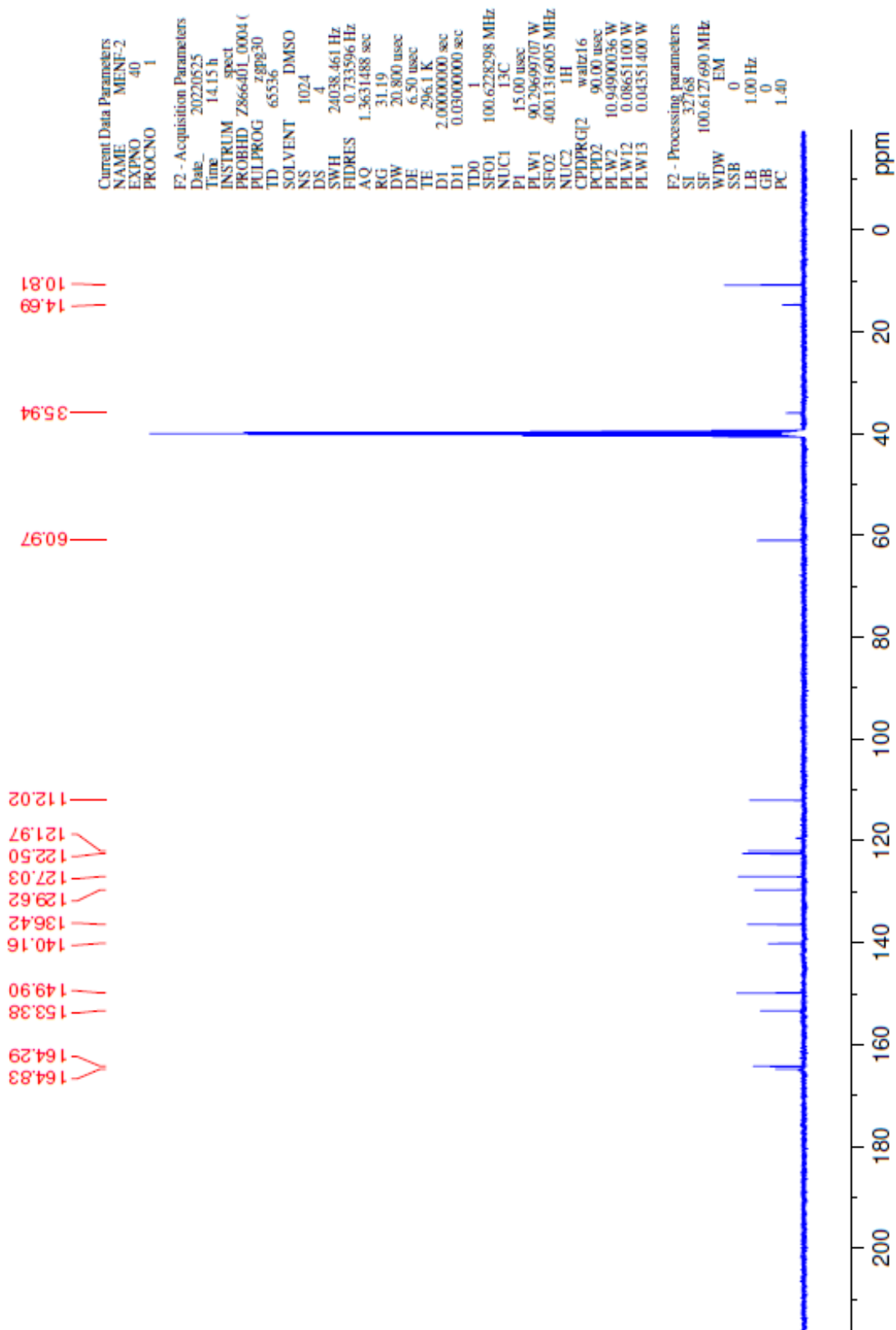
Figure 5.51. *¹³C-NMR spectrum of compound **6a***
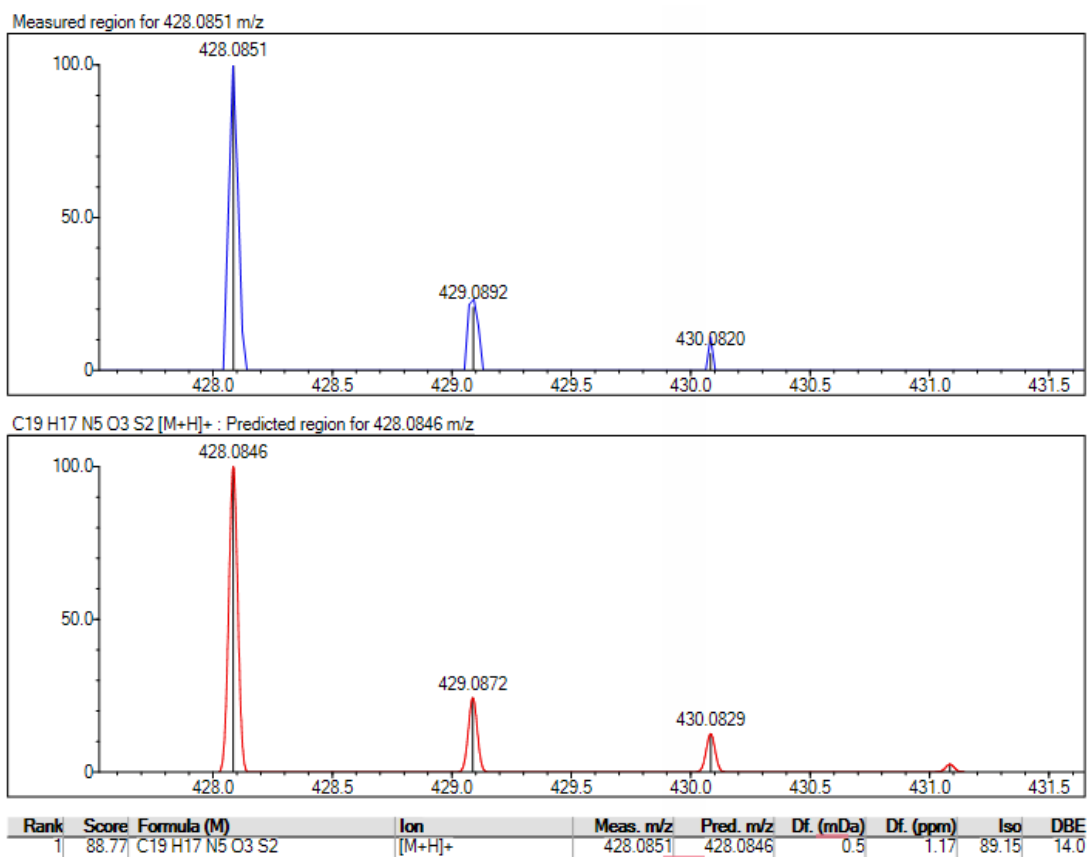
Figure 5.52. *Mass spectrum of compound 6a*

5.1.6.2. Ethyl 4-methyl-2-[2-[(5-((quinolin-8-yloxy)methyl)-1,3,4-oxadiazol-2-yl)thio]acetamido]thiazole-5-carboxylate (6b)
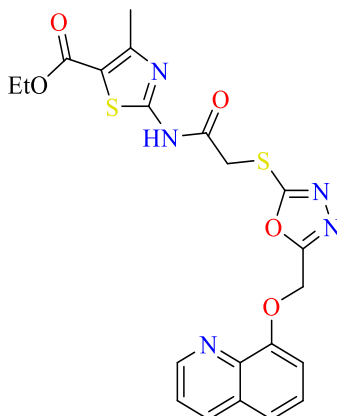
Figure 5.53. *Chemical structure of compound 6b*

Compound **6b** was synthesized according to method E and F. Yield 88%, M.P. = 208-209 °C.

FTIR (ATR, cm⁻¹): 3145 (N-H stretching), 3062 (aromatic C-H stretching), 2985-2873 (aliphatic C-H stretching), 1693 (C=O stretching), 1622-1500 (C=N , C=C stretching), 1284 (C-O stretching, oxadiazole), 1166 (C-O stretching, ether).

¹H-NMR: (400 MHz, DMSO-d_6, ppm) δ: 1.27 (3H, t , J = 7.1 Hz, CH$_3$-CH$_2$), 2.54 (3H, s, thiazole-CH3), 3.34 (2H, q, J=7.1, CH$_3$-CH$_2$), 4.43 (2H, s, CO-CH$_2$), 5.60 (2H, s, O-CH$_2$), 7.36 (1H, dd , J_1= 7.7, J_2=1.03 Hz, quinoline C$_7$-H), 7.50-7.61 (3H, m, aromatic-H) , 8.34 (1H, dd , $J1$= 8.33 , $J2$=1.68 Hz, quinoline C$_4$-H), 8.86 (1H, dd , J_1= 4.12 , J_2=1.71 Hz, quinoline C$_2$-H), 12.91 (1H, s, NH).

¹³C-NMR: (100 MHz, DMSO-d_6, ppm) δ: 14.63(CH$_3$-CH$_2$), 17.44 (thiazole-CH$_3$), 35.89 (S-CH$_2$), 60.93 (CH$_3$-CH$_2$), 61.04 (O-CH$_2$), 111.96, 114.87, 121.95, 122.47, 127.00, 129.60, 136.40, 140.13, 149.87, 153.36, 162.42, 164.35, 166.60 (C=O).

HRMS (*m/z*): [M+H]⁺ calculated for C$_{21}$H$_{19}$N$_5$O$_5$S$_2$: 486.0900 ; found: 486.0908.

DOPNALAB

Item	Value
Acquired Date&Time	7.06.2022 10:12:15
Acquired by	System Administrator
Filename	C:\Users\dopnalab\Desktop\MASAÜSTÜ\LEYLA YURTDAŞ\MEN\MENF-4.1.ispd
Spectrum name	MENF-4.1
Sample name	MENF-4
Sample ID	
Option	
Comment	
No. of Scans	15
Resolution	4 [cm-1]
Apodization	Happ-Genzel
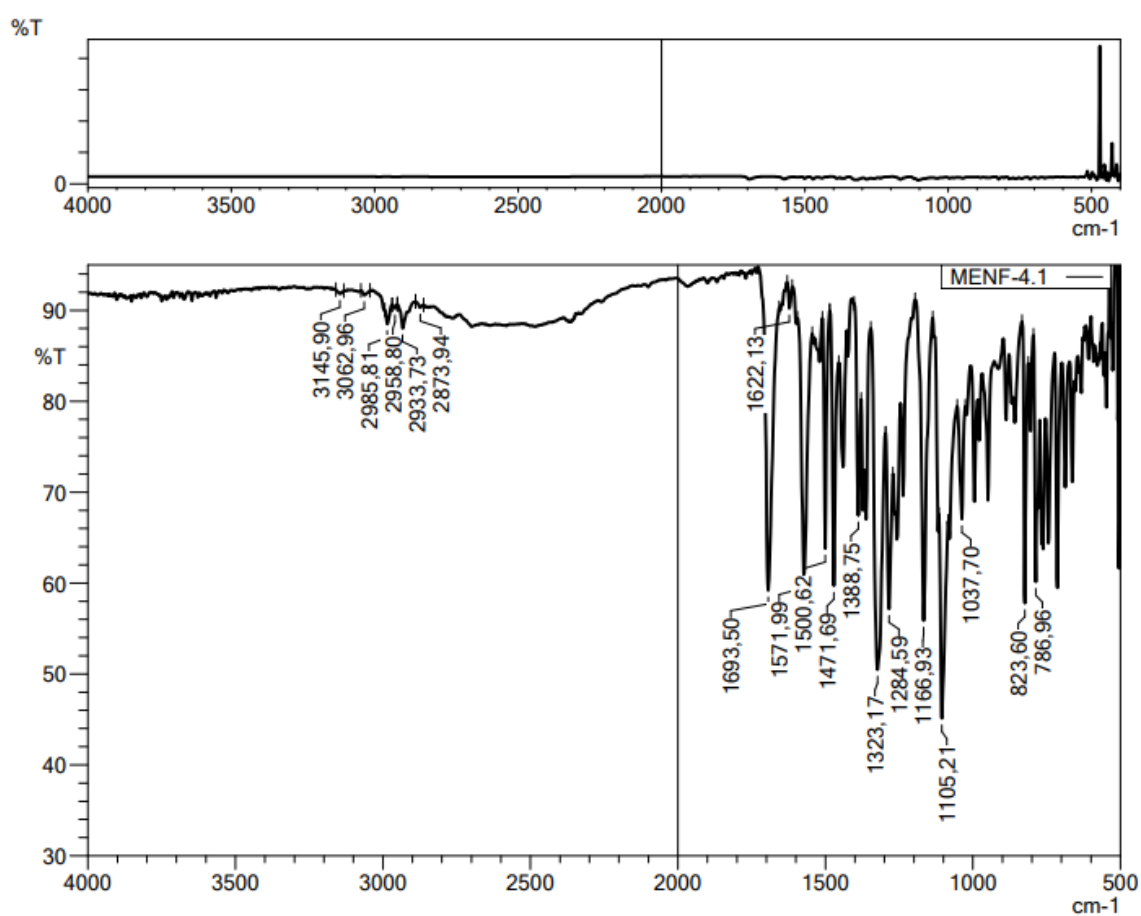
Figure 5.54. *IR spectrum of compound* *6b*

93
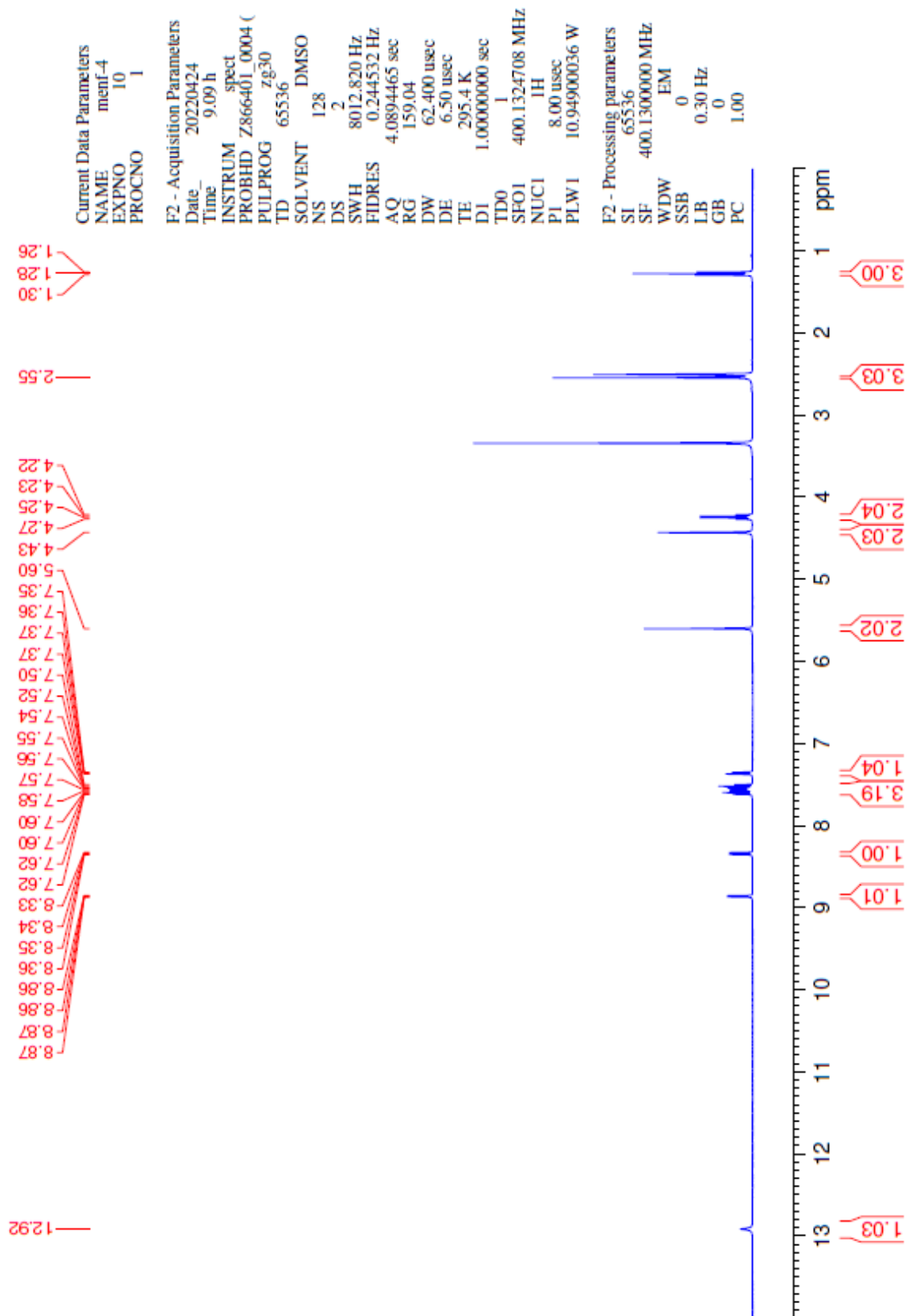
Figure 5.55. *¹H-NMR spectrum of compound **6b***

14.64
17.45
35.89
60.94
61.05
111.96
114.88
121.95
122.48
127.01
129.60
136.40
140.14
149.88
153.37
162.43
164.36
164.67
166.60
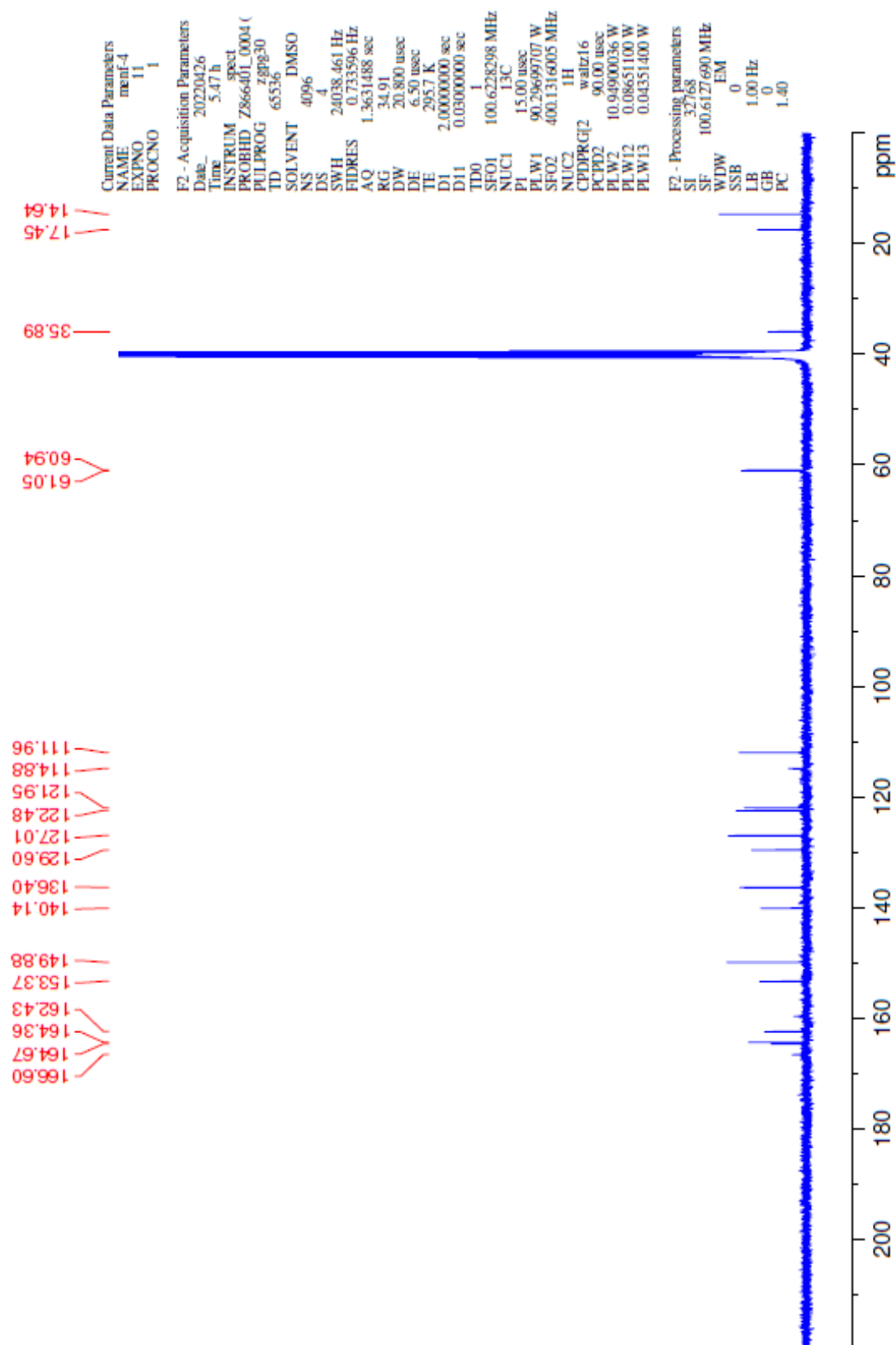
Figure 5.56. *¹³C-NMR spectrum of compound **6b***

95
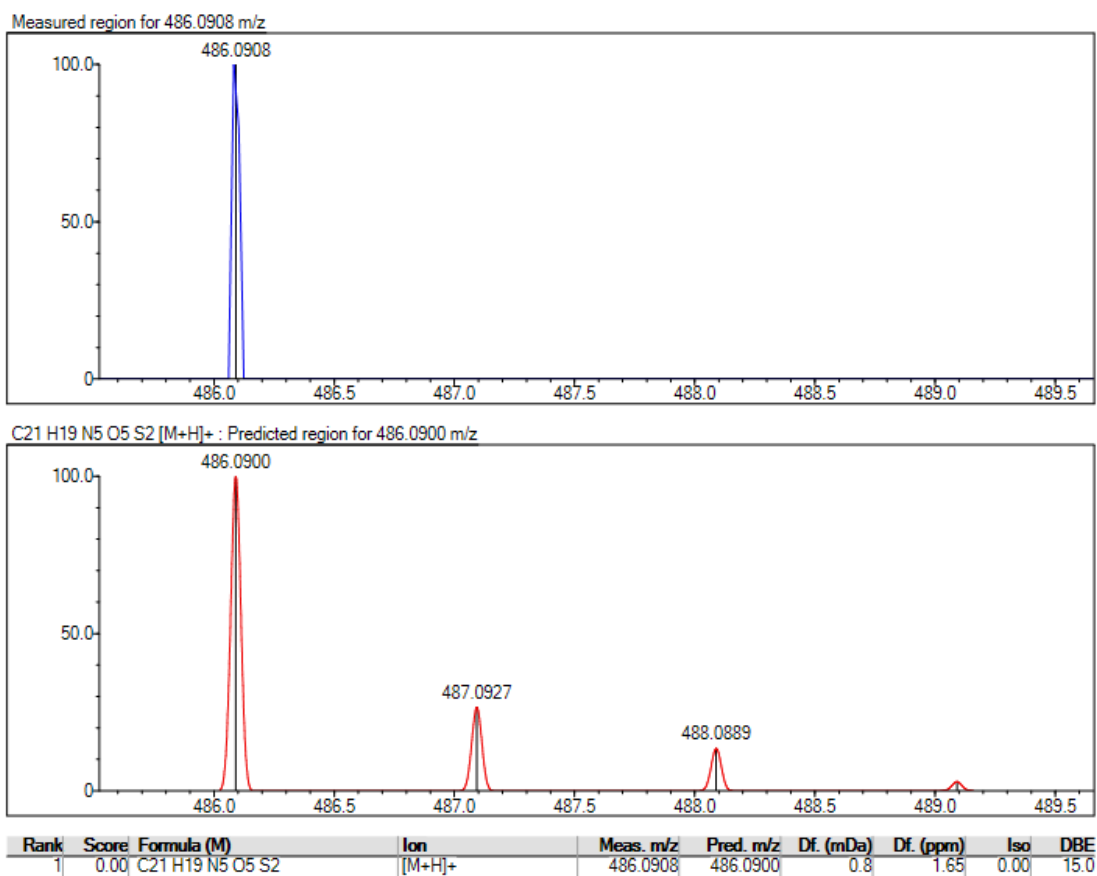
Figure 5.57. *Mass spectrum of compound **6b***

5.1.6.3. N-(4-Phenylthiazol-2-yl)-2-[[5-((quinolin-8-yloxy)methyl)-1,3,4-oxadiazol-2-yl]thio]acetamide (6c)
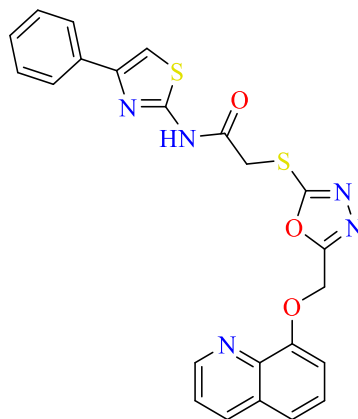
Figure 5.58. *Chemical structure of compound 6c*

Compound **6c** was synthesized according to method E and F Yield 86%, M.P. = 188-189°C.

FTIR (ATR, cm-1): 3128 (N-H stretching), 3062-3026 (aromatic C-H stretching), 2991-2848 (aliphatic C-H stretching), 1678 (C=O stretching), 1698-1562 (C=N, C=C stretching), 1236 (C-O stretching, oxadiazole), 1163 (C-O stretching, ether).

^{1}H-NMR: (400 MHz, DMSO-d_6, ppm) δ: 4.46 (2H, s, CO-CH$_2$), 5.61 (2H, s, O-CH$_2$), 7.33 (1H, t, J= 7.28 Hz, aromatic-H), 7.37 (1H, d, J=7.64 Hz, quinoline C$_7$-H), 7.44 (2H, t, J= 7.48 Hz, aromatic-H), 7.50-7.62 (3H, m, aromatic-H), 7.67 (1H, s, thiazole-H), 7.9 (2H, d, J= 7.98, aromatic-H), 8.35 (1H, d, J=8.15 Hz, quinoline C$_4$-H), 8.87 (1H, d, J=3.97 Hz, Quinoline C$_2$-H), 12.75 (1H, s, NH).

^{13}C-NMR: (100 MHz, DMSO-d_6, ppm) δ: 35.89, 61.02, 108.91, 112.13, 121.99, 122.50, 126.15, 127.06, 128.33, 129.22, 129.62, 134.62, 136.55, 140.04, 149.45, 149.86, 149.86, 153.31, 158.03, 164.33, 164.80, 164.87 (C=O).

HRMS (*m/z*): [M+H]$^+$ calculated for C$_{23}$H$_{17}$N$_5$O$_3$S$_2$: 476.0846; found: 476.0805.

DOPNALAB

Item	Value
Acquired Date&Time	7.06.2022 10:04:26
Acquired by	System Administrator
Filename	C:\Users\dopnalab\Desktop\MASAÜSTÜ\LEYLA YURTDAŞ\MEN\MENF-5.1.ispd
Spectrum name	MENF-5.1
Sample name	MENF-5
Sample ID	
Option	
Comment	
No. of Scans	15
Resolution	4 [cm-1]
Apodization	Happ-Genzel
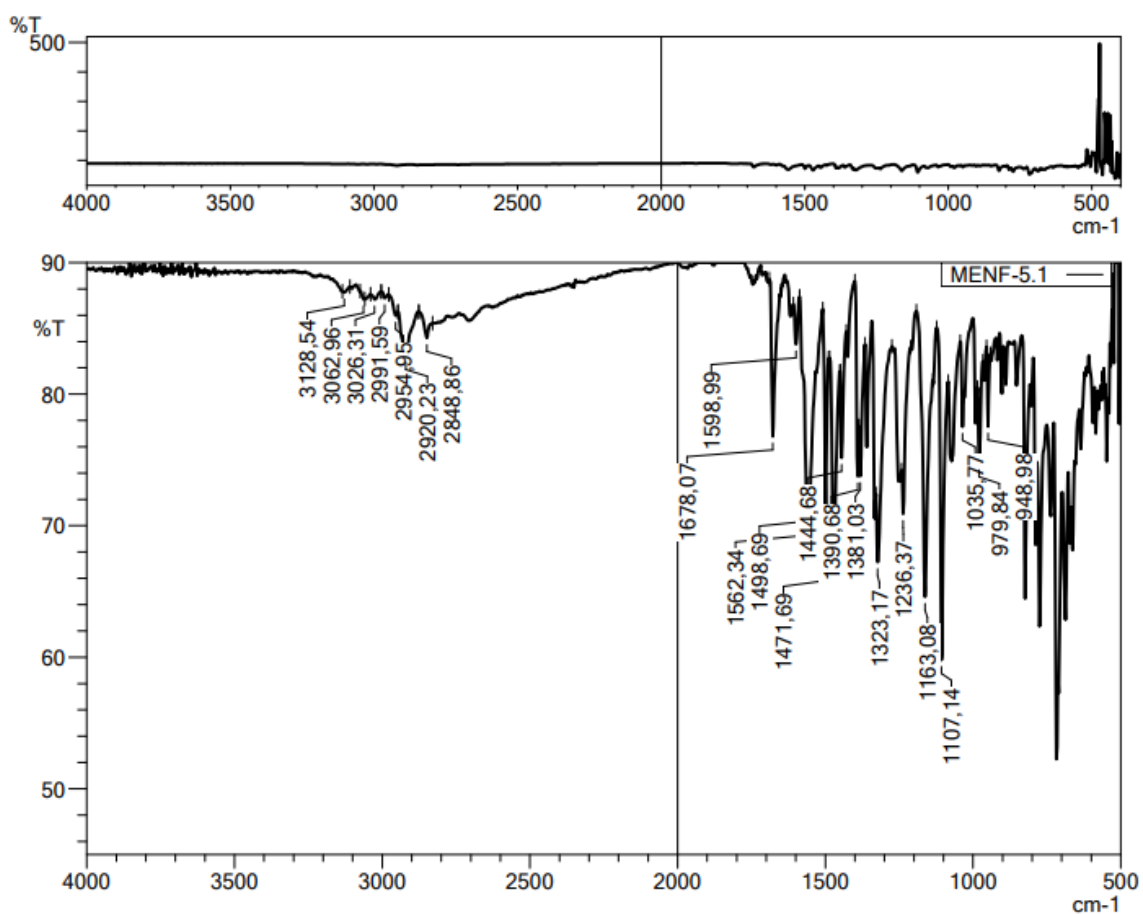
Figure 5.59. *IR spectrum of compound 6c*
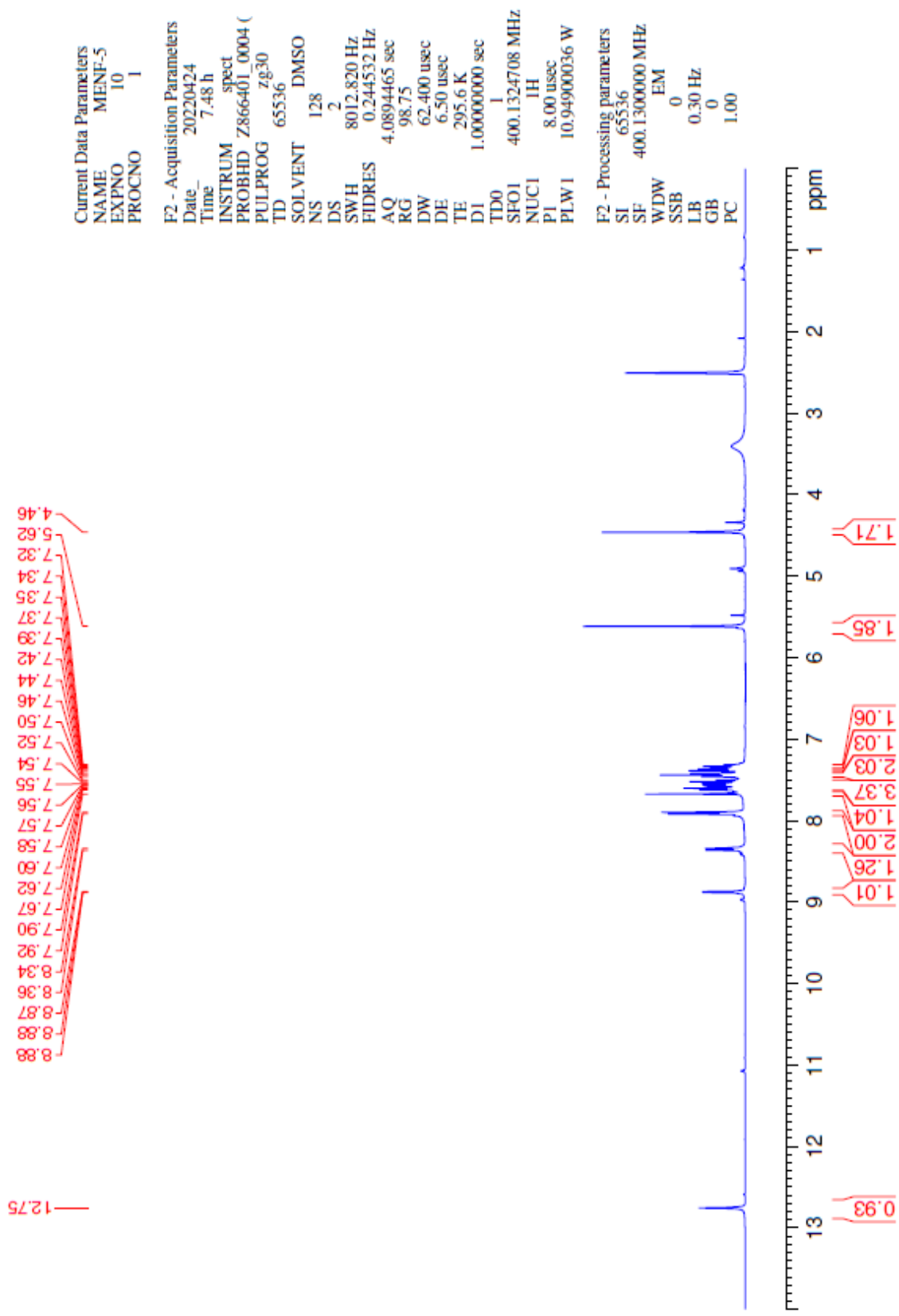
Figure 5.60. *¹H-NMR spectrum of compound* **6c**
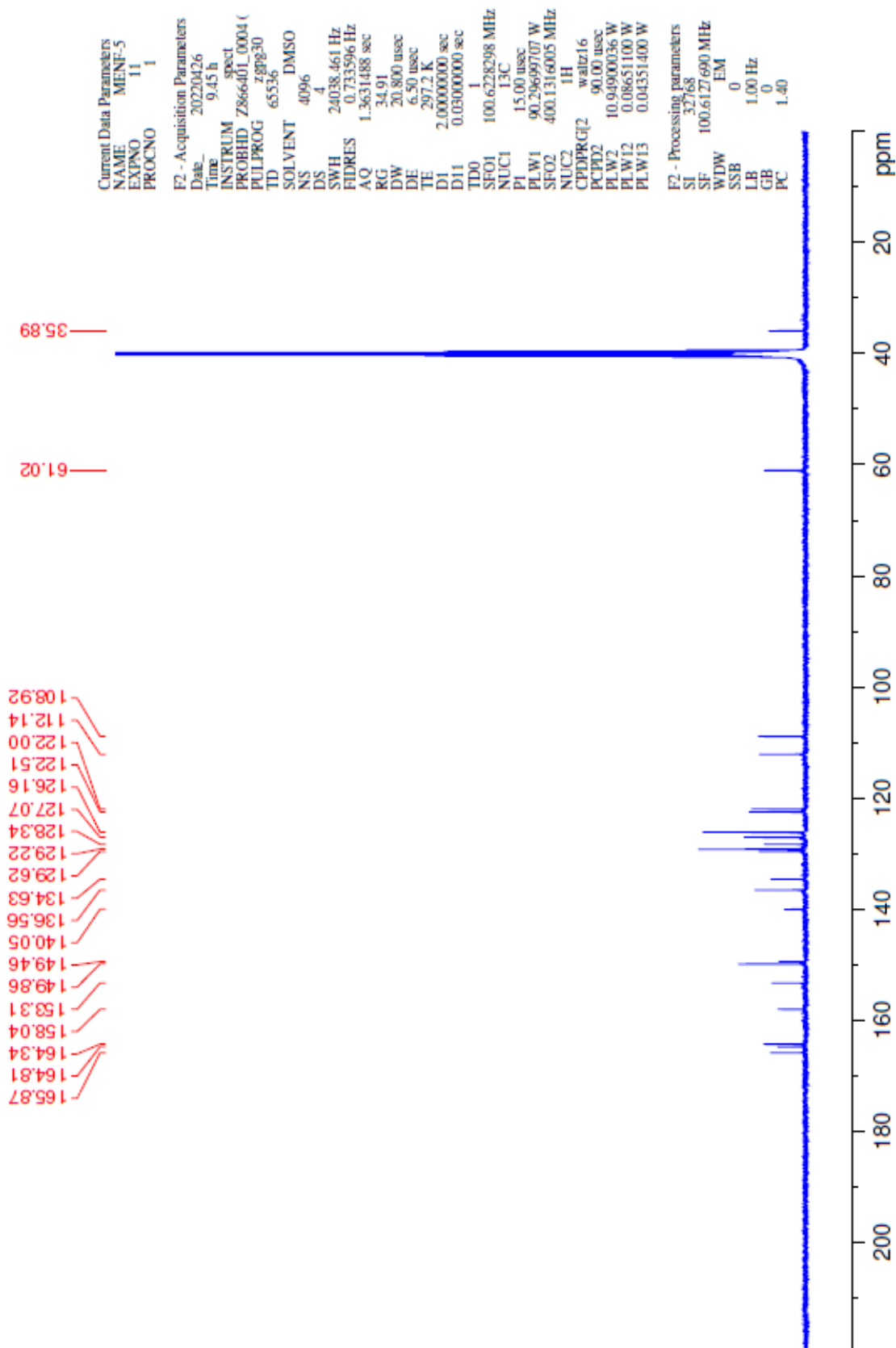
Figure 5.61. *¹³C-NMR spectrum of compound* **6c**
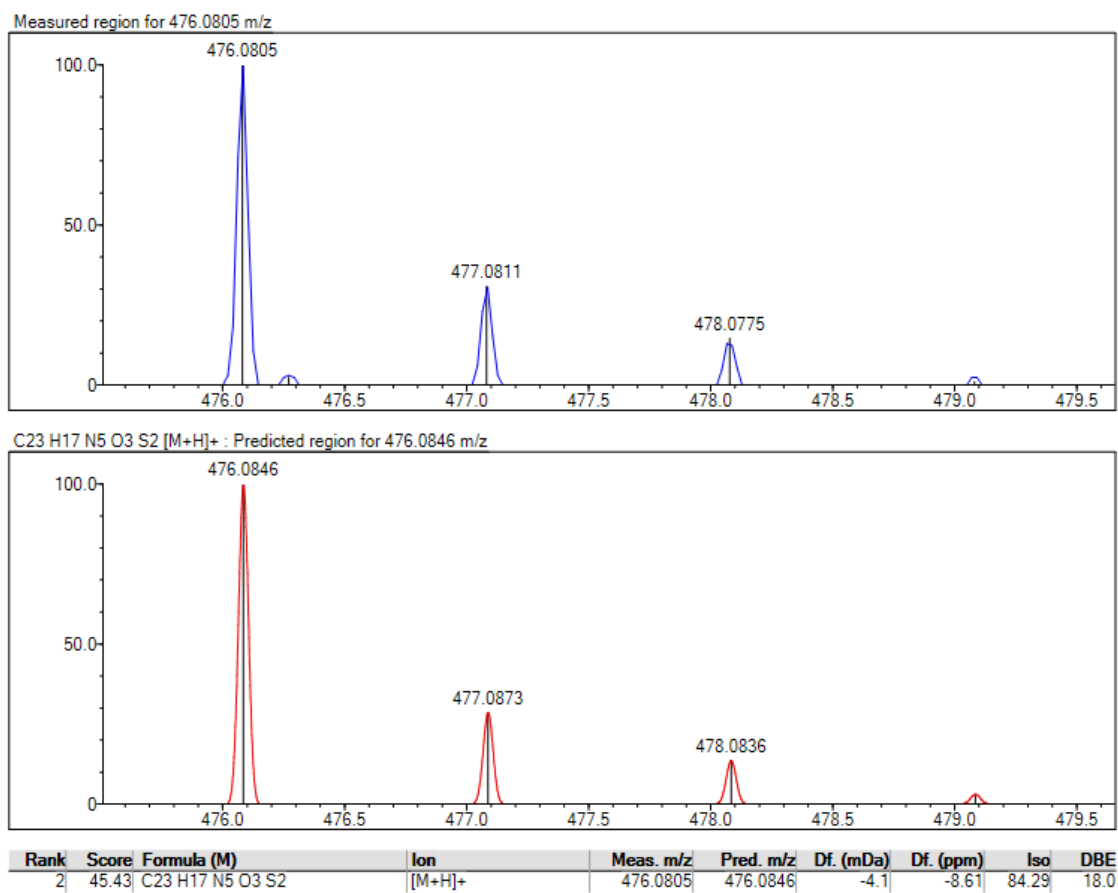
Figure 5.62. *Mass spectrum of compound 6c*

5.2. Chemical Synthesis Evaluation

The compounds in the study were obtained by a four-steps synthetic procedure. In the first step, 8-hydroxyquinoline was reacted with ethyl bromoacetate (**method A**) in order to introduce an ethyl acetate group. In this nucleophilic substitution reaction, the reaction is carried out by increasing the nucleophilic power of the nucleophilic O atom with potassium carbonate. In the later step, acylhydrazine was produced after hydrazine monohydrate addition (**method B**). Thirdly, the produced hydrazide was cyclized into 1,3,4-oxadiazole using carbon disulfide compound (**method C**). Finally, two different substitution reaction (SN_2) procedures have been performed to synthesize the final products. The first one was performed in potassium carbonate and acetone at room temperature (**method D**) while the other was in sodium hydroxide and acetonitrile at 100° C (**method F**). The reason behind using two different procedures in the last step is explained by the reaction's low rate in acetone and potassium carbonate. The reaction proceeded at a higher rate using acetonitrile and strong base. According to SciFinder database, all final products were found original except for compound **4b** that had been previously evaluated as metallocarboxy peptidase inhibitor [146]. Structures of the obtained 5-[(quinolin-8-yloxy)methyl]-1,3,4-oxadiazole-2-(substituted) thiol derivatives have been verified using NMR and HRMS spectral methods.

Figure 5.63. *Schematic representation of the synthetic pathways*

Reaction conditions: a) ethyl bromoacetate, K_2CO_3, acetone, reflux; b) hydrazine monohydrate, ethanol, r.t; c) CS_2, KOH, ethanol, reflux; d) substituted phenacyl bromide derivatives in K_2CO_3, acetone, r.t, or in acetonitrile, NaOH; e) 2-chloro-*N*-(substituted)phenylacetamide derivatives, acetonitrile, NaOH, reflux; f) 2-chloro-*N*-(substituted) thiazole derivatives, NaOH acetonitrile .

	R₁				R₂			R₃	
4a	**4b**	**4c**	**4d**	**5a**	**5b**	**5c**	**6a**	**6b**	**6c**
-H	4-CH₃	4-OCH₃	2,5-di-OCH₃	4-Cl	4-F	4-OCH₃	4,5-di-CH₃	4-CH₃, 5-COOEt	4-phenyl

5.3. Chemical Analysis Results Evaluation

5.3.1. IR analysis results

The IR analysis was used to characterize the main functional groups in the synthesized products.

IR analysis of the compounds (**4a-4d**) showed characteristic absorption band at 1643-1676 cm^{-1} because of carbonyl (C=O) group. For amide containing structures (**5a-5c, 6a-6c**), the N-H band observed at 3100-3300 cm^{-1} while the carbonyl group detected at 1670-1707 cm^{-1}.

C-H stretching of sp^2 hybridized carbons observed above 3000 cm^{-1}, while the sp^3 hybridized carbons recognized in the region 2885-2990 cm^{-1}.

The signals at 1228-1284 cm^{-1} were indicative of the aromatic C-O stretching of oxadiazole ring. The peaks that occurred in 1170-1000 cm^{-1} indicated the aliphatic C-O.

5.3.2. Mass spectrometry

Mass spectra of all final compounds were taken using high resolution mass-spectrometry device in accordance with ESI method. The peak of the M+1 ion was detected in the mass spectra of all compounds according to their molecular weights [147].

5.3.3. ^{1}H-NMR analysis results

^{1}H-NMR analysis was conducted using Bruker UltraShield 400 MHz. All samples were dissolved in DMSO-d_6 that appeared as a quintet at 2.5 ppm in all spectra. A strong singlet appeared in all of the compounds' spectra at around 3.34 ppm which indicates protons of water.

All compounds are composed of 1,3,4-oxadiazole ring connected by a quinolin-8-yloxy methyl group at the 5th position. Various derivatives were designed by changing the groups attached to the thiol group at position 2 of the 1,3,4-oxadiazole ring.

When the ^{1}H-NMR spectra of the compounds were examined, the C_7, C_4 and C_2 protons of the quinoline ring were observed as doublets or doublet of the doublets within (7.29-7.45), (8.34-8.38) and (8.77-8.95) ppm ranges, respectively. Whereas C_3-H, C_5-H and C_6-H appeared as multiplate within (7.5-7.63) range. Except for substituted phenyl acetamide containing structures, the protons of the oxymethylene group connected to quinoline-C_8 were recognized as singlets in (5.60-5.61) ppm. In substituted phenyl acetamide containing structures, oxymethylene protons were detected in (4.55-4.85) ppm as singlets. The methylene's protons attached to phenyl acyl group in compounds **4a-4c**

were shown as singlets in (4.90-5.16) ppm. Whereas the methylene attached to the acetamide group was shielded to (3.90- 4.46) in **5a-c** and **6a-c** compounds. In **4b**, phenyl-CH$_3$ protons were detected at 2.40 ppm as singlets; however, the methyloxy protons were within the downfield in compound **4c** due to the deshielding effect of the oxygen atom.

5.3.4. ^{13}C NMR analysis results

^{13}C-NMR analysis was performed using Bruker UltraShield instrument using DMSO-d_6 as solvent at 100 MHz. The solvent peak appeared as septet at around 39.95 ppm. Each sample required 1 hour to be analyzed. The chemical shift of the oxymethylene carbon and thiomethylene were displayed in the upfield region in (56-70) ppm and (32-45) ppm, respectively. The carbonyl carbon was the most deshielded in all compounds. The carbonyl carbon in the amide groups was shown in the range of (164-173) ppm while it was deshilded to (190-192) ppm in non-amidic structures. All aromatic carbons were seen within the range of 111-165 ppm.

5.4. *In-vitro* Anticholinesterase Inhibition Results

The cholinesterase inhibitory activities of the final products were investigated by the colorimetric method developed by Ellman *et al.* in 1961 [148]. The method mainly depends on the measurements of the yellow color produced from dithiobisnitrobenzoate ion reaction with thiocholine released after the hydrolysis of acetylthiocholine. The resulted absorbance change that reflects the enzyme activity is detected at 412 nm.
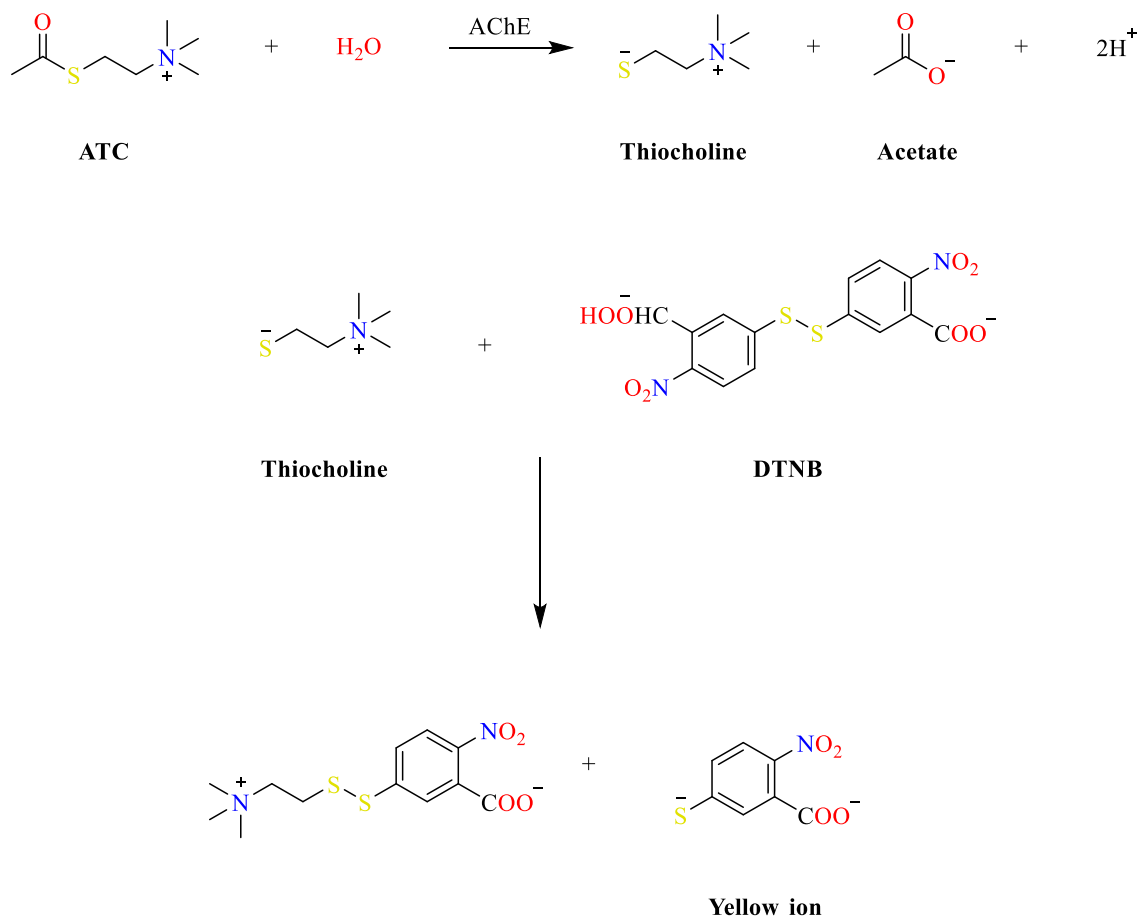
Figure 5.64. *Chemical mechanism of Ellman's method*

All the synthesized compounds in this thesis were found to have a higher inhibition profile on AChE compared to BuChE. Except for compound **4d**, all compounds exhibited an inhibition percentage higher than 50% at 10^{-3} M concentration compared to donepezil as shown in **Table 2**.

Interestingly, all acetamide-containing structures (**5a-c** and **6a-c)** have displayed inhibitory percentages higher than 75% at 10^{-3} M for AChE. When the concentrations were reduced to 10^{-4} M, compounds **5a**, **5c** and **6a** indicated more than 80% activity. It was also observed that all 1-(substituted phenyl)-2-[[5-((quinolin-8-yloxy)methyl)-1,3,4-oxadiazol-2-yl]thio]ethan-1-one compounds showed low activity against AChE enzyme.

After the preliminary screening, compounds **5a**, **5c** and **6a** were chosen to calculate their IC_{50} values for acetylcholinesterase. The inhibition values of these compounds were tested at $10^{-5}–10^{-9}$ M concentrations against AChE along with the reference drug donepezil. The IC_{50} value was recorded as 0.0201 μM for donepezil whereas the IC_{50} values of **5a,** **5c** and **6a** were calculated as 0.033 μM, 0.096 μM and 0.177 μM,

106

respectively. The most potent compound among this series **5a** ($IC_{50} = 0.033\ \mu M$) was that having 4-chlorophenyl acetamide substitution attached by the thioether bridge to the fifth position of 1,3,4-oxadiazole. Replacing the chlorine at the para position of compound **5a** by methoxy group **5c** ($IC_{50} = 0.096\ \mu M$) resulted in three folds decrease of the inhibitory activity while replacing it with fluorine **5b** resulted in non-significant activity. Further replacement of the 4-chlorophenyl acetamide in **5a** by 4,5-dimehylthiazole **6a** led to a decrease in inhibitory activity ($IC_{50} = 0.177\ \mu M$). Other thiazole substitutions were relatively inactive.

The synthesized compounds and standard drug tacrine were studied on BuChE at concentrations 10^{-3} M and 10^{-4} M. The results revealed that **5a, 5c** and **6a** resulted in an enzyme inhibition of more than 50% at 10^{-3} M. However, the inhibition percentages were reduced to less than 35% 10^{-4} M; thus, they were not tested at lower concentrations.

Table 2. *Inhibition results of the cholinesterase*

Code	AChE % Inhibition		AChE IC_{50} (μM)	BuChE % Inhibition		BuChE IC_{50} (μM)	Selectivity	SI*
	10^{-3} M	10^{-4} M		10^{-3} M	10^{-4} M			
4a	**66.532 ±1.267**	39.461 ±0.836	>100	25.821 ±0.832	20.611 ±0.754	>1000	AChE	>10
4b	**76.098 ±1.191**	41.690 ±1.234	>100	29.748 ±0.736	22.598 ±0.957	>1000	AChE	>10
4c	**64.562 ±0.937**	40.751 ±0.958	>100	22.830 ±0.961	18.448 ±0.884	>1000	AChE	>10
4d	42.837 ±1.022	37.828 ±0.877	>1000	32.454 ±0.827	27.962 ±0.997	>1000	-	-
5a	**94.662 ±1.654**	**90.709 ±2.136**	**0.033 ±0.001**	**61.088 ±0.903**	31.035 ±1.057	>100	AChE	>3030.303
5b	**81.769 ±2.036**	42.302 ±0.832	>100	30.320 ±1.155	21.219 ±0.763	>1000	AChE	>10
5c	**93.952 ±1.788**	**87.276 ±1.923**	**0.096 ±0.004**	**57.464 ±0.869**	23.892 ±0.747	>100	AChE	>1041.667
6a	**88.312 ±2.228**	**82.065 ±1.045**	**0.177 ±0.007**	**54.615 ±0.641**	20.464 ±0.957	>100	AChE	>564.97
6b	**79.406 ±1.455**	39.467 ±0.799	>100	33.934 ±0.825	29.657 ±0.873	>1000	AChE	>10
6c	**83.823 ±1.058**	47.975 ±0.817	>100	32.162 ±1.288	27.338 ±0.930	>1000	AChE	>10
Donepezil	99.156 ±1.302	97.395 ±1.255	0.0201 ±0.0010	-	-	-	AChE	-
Tacrine	-	-	-	99.827 ±1.378	98.651 ±1.402	0.0064 ±0.0002	BuChE	-

*SI: selectivity Index (SI=IC_{50} BuChE/ IC_{50} AChE)

5.5. *In-vitro* Monoamine Oxidase Inhibition Results

MAO isoenzymes inhibitory activities of the synthesized compounds were performed using 10-acetyl-3,7-dihydroxyphenoxazine (Amplex Red™) that oxidizes into the fluorescent compound, resorufin. The assay mainly depends on the horseradish peroxidase and H_2O_2 to oxidize the non-fluorescent Amplex Red to the highly fluorescent resorufin [149].

The screening results for MAO-A inhibitory potential at 10^{-3} M showed an inhibition percentage ranging from 26% to 39% in comparison with moclobemide (94%) and clorgyline (96%). Meanwhile, the range was between 30% and 48% for MAO-B inhibition activity at the same concentration. When the concentrations were reduced to 10^{-4} M, the % inhibition against MAO-A and MAO-B were 20-31% and 20-35%, respectively. Therefore, further investigations at lower concentrations have been omitted due to the weak inhibitory action of the compounds. The results are displayed in **Table 3.**

Table 3. *% Inhibition of the synthesized compounds against MAO-A and MAO-B enzymes*

Compound	MAO-A % inhibition		MAO-B % inhibition	
	10^{-3} M	10^{-4} M	10^{-3} M	10^{-4} M
4a	29.421±0.922	23.751±0.732	41.787±0.933	29.361±0.836
4b	38.911±0.949	20.248±0.857	45.408±1.275	30.733±0.920
4c	26.308±0.758	22.812±0.790	40.967±1.098	35.964±1.154
4d	30.134±0.836	20.435±0.846	48.048±1.348	31.012±0.830
5a	37.875±0.902	31.928±1.128	31.855±0.862	27.457±0.764
5b	30.590±0.777	27.116±0.875	36.223±0.935	20.628±0.622
5c	27.056±0.859	23.564±0.836	30.714±0.914	26.267±0.875
6a	39.621±0.921	31.355±1.044	40.695±1.262	33.018±1.091
6b	31.764±0.720	27.486±0.751	46.414±1.146	30.126±0.861
6c	35.599±1.246	29.804±0.880	43.768±1.451	28.430±0.728
Moclobemide	94.121±2.760	82.143±2.691	-	-
Clorgyline	96.940± 1.250	91.308± 1.305	-	-
Selegiline	-	-	98.258±1.052	96.107±1.165

5.6. Physicochemical Properties Evaluation

SwissADME online tool was used to determine physicochemical descriptors, pharmacokinetic properties and medicinal chemistry friendliness of the active compounds. Log P values that indicate the lipophilicity *via* partition coefficient between octanol and water of **5a**, **5c** and **6a** were found 3.52, 2.99 and 3.12, respectively. The topological polar surface area (TPSA) of the structures was high which anticipate the inferior BBB permeation of the compounds. The synthesized compounds were designed to treat AD by targeting AChE and MAO in the central nervous system, therefore a high BBB permeability is required. Compounds **5a** and **5c** are predicted to have a high gastrointestinal absorption ability, while thiazole-containing structure **6a** has lower bioavailability. The number of hydrogen bond acceptors (HBA) in all active structures was 6 or 7 whereas only one hydrogen bond donor (HBD) was detected. **5a** and **5c** structures showed no deviation from Lipinski, Ghose, Veber, Egan and Muegge rules that indicate the drug-likeness properties. **6a** deviated from these rules due to its high TPSA.

The prediction of the physicochemical parameters for the active compounds and the reference drug donepezil are illustrated in **Table 4**.

Table 4. *In-silico physicochemical parameters of the compounds*

	MW (g/mol)	HBA	HBD	TPSA (Å²)	Log P	GI abs.	DL	BBB perm.
5a	426.88	6	1	115.44	3.52	High	5/5	No
5c	422.46	7	1	124.67	2.99	High	5/5	No
6a	427.50	7	1	156.57	3.12	Low	2/5	No
Donepezil	379.49	4	0	38.77	4.00	High	5/5	Yes

MW, molecular weight; **HBA**, the number of hydrogen bond acceptor; **HBD**, the number of hydrogen bond donor; **TPSA**, the topological polar surface area; **Log P**, partition coefficient (Consensus Log $P_{o/w}$); **GI abs**, gastrointestinal absorption; **DL,** drug likeness (including Lipinski, Ghose, Veber, Egan and Muegge rules); **BBB perm.**, the Blood-Brain Barrier permeability.

5.7. Molecular Docking Study Results

5.7.1. Acetylcholinesterase enzyme binding sites

According to protein data bank resources, AChE structure has been identified from eight different eukaryote species using X-ray diffraction methods. These eukaryotes include Tetronarce californica, Mus musculus, Homo sapiens, Dendroaspis angusticeps, Anopheles gambiae, Drosophila melanogaster, Electrophorus electricus and Bungarus

fasciatus. In this work, a high-resolution crystal structure (2.35 Å resolution) of *human* acetylcholinesterase (Homo sapiens) co-crystallized with donepezil (PDB ID: *4EY7*) has been used to perform the molecular modeling study. The crystal structure of acetylcholinesterase is defined as two subunits A and B as shown in (**Figure 5.55**) [143].
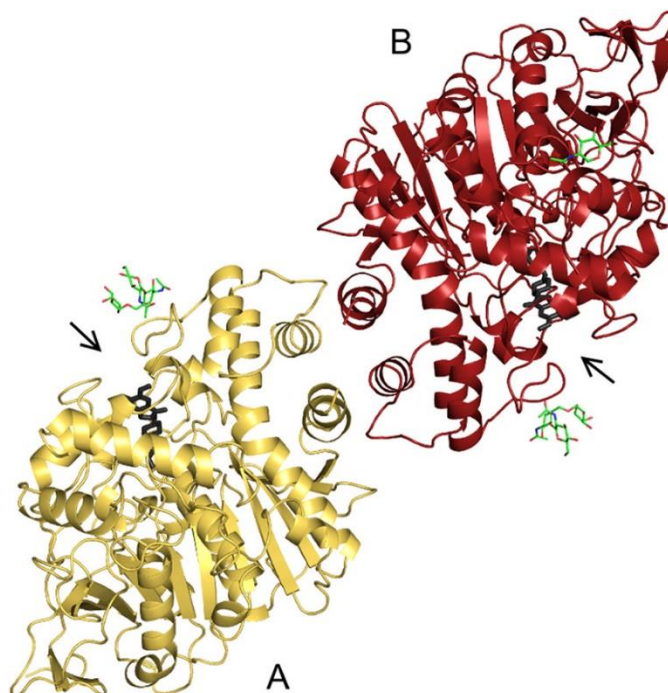
Figure 5.65. *Crystallographic structure of human acetylcholinesterase combined with donepezil*

According to the X-ray analysis, AChE active site is mainly composed of two main binding regions including the peripheral anionic site (PAS) and catalytic active site (CAS). The catalytic active site is distinguished as a narrow, long, hydrophobic gorge with about 20 Å length incorporating the acyl binding site that holds Phe295 and Phe297 amino acids, the active center bearing Glu202, Glu450 fragments, the hydrophobic subsite having Tyr337, Tyr133, Trp86 and Phe338 residues, the oxyanion binding site which contains Gly120, Gly121 and Gly123 residues and a catalytic triad of Ser203-His447-Glu334 amino acids [150-152] . Likewise, the peripheral anionic site (PAS) is mainly constituted of aromatic residues Tyr72, Tyr124, Trp286, Tyr341, and Asp74 affording a binding site for allosteric inhibitors besides its recognition function for acetylcholine at the gorge rim [153].

Molecular docking studies of recombinant *human* AChE (*rh*AChE) with donepezil revealed that the drug's benzyl ring stacks against Trp86 with the additional ability to

interact with two amino acids of the catalytic triad Ser203 and His447 in the CAS. It has been also observed that donepezil's piperidine ring retains the potential to form water-mediated hydrogen bonds with Tyr341 and Tyr377 at the CAS [154], whereas the indanone part makes strong hydrophobic interactions with Trp286 in the PAS. Thus, the selective AChE inhibitor donepezil interacts with both CAS and PAS sites [143, 155].

It has been evidenced that the peripheral anionic site of AChE regulates the enzyme expression and promotes the deposition of amyloid plaques. Therefore, enzyme inhibitors that have the ability to interact with the PAS amino acids are predicted to attenuate amyloid plaques deposition resulting in a neuroprotective effect [156]. Recent studies have attempted to develop dual-binding site inhibitors targeting both the catalytic (CAS) and the peripherical anionic (PAS) domains pursuing simultaneous prevention of acetylcholine degradation and AChE-induced Aβ aggregation [22].

Molecular docking studies have concluded the most significant binding clues to acquiring highly potent AChE inhibitors. These interactions include π-π overlapping with Trp86 at the CAS and Trp286 at the PAS [157].

Therefore, the binding modes of the most potent derivatives **5a**, **5c** and **6a** were analyzed to determine their binding features with *h*AChE.

5.7.2. Molecular docking of compound 5a

The results of the molecular docking study of compound **5a** with AChE revealed that there were five π–π interactions between **5a** and AChE. Three of them were between the quinoline ring of the ligand and Trp286 in the PAS region and the other two were between the phenyl ring and Trp86 within the CAS. The compound has also performed two halogen interactions between the chloro-substitution and Tyr133 and Gly120. Another two ar-H interactions have been shown according to the 3D model representation. The first one was performed between quinoline C_3-H and Ser293 whereas the other was displayed between the oxygen in the ether bridge and Tyr341. The two-dimensional (3D) and three-dimensional (2D) pose illustrations are displayed in (**Figure 5.56**) and (**Figure 5.57**).
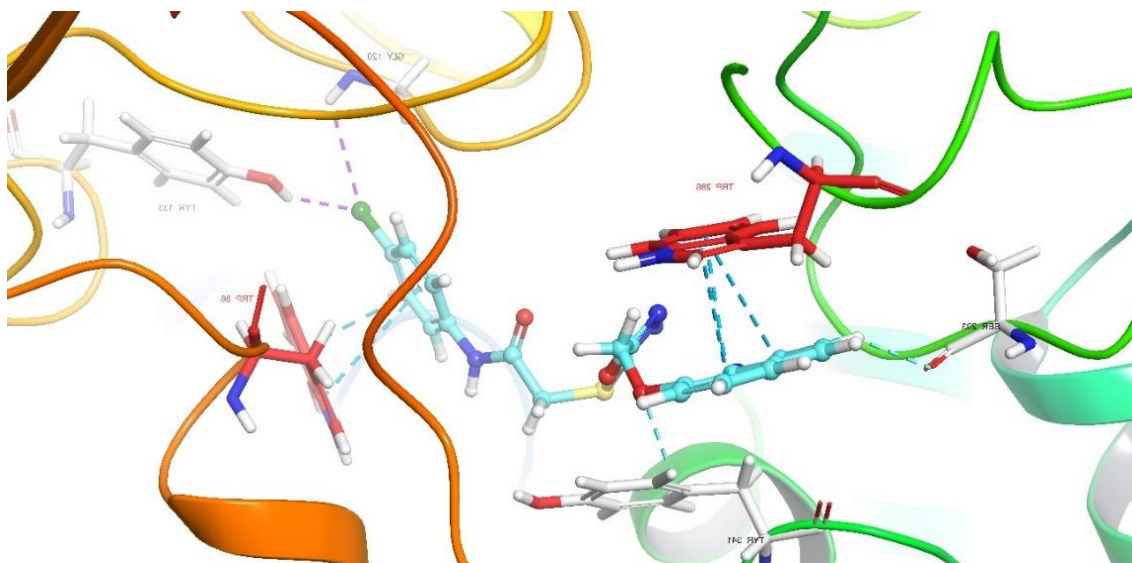
Figure 5.66 *Three-dimensional interactions of compound **5a** at the binding region (PBDID: 4EY7).*

Blue carbons: compound **5a**; white carbons: binding site residues; cyan dashes: aromatic
H-bond; blue dashes: π–π interaction; purple dashes: halogen interaction
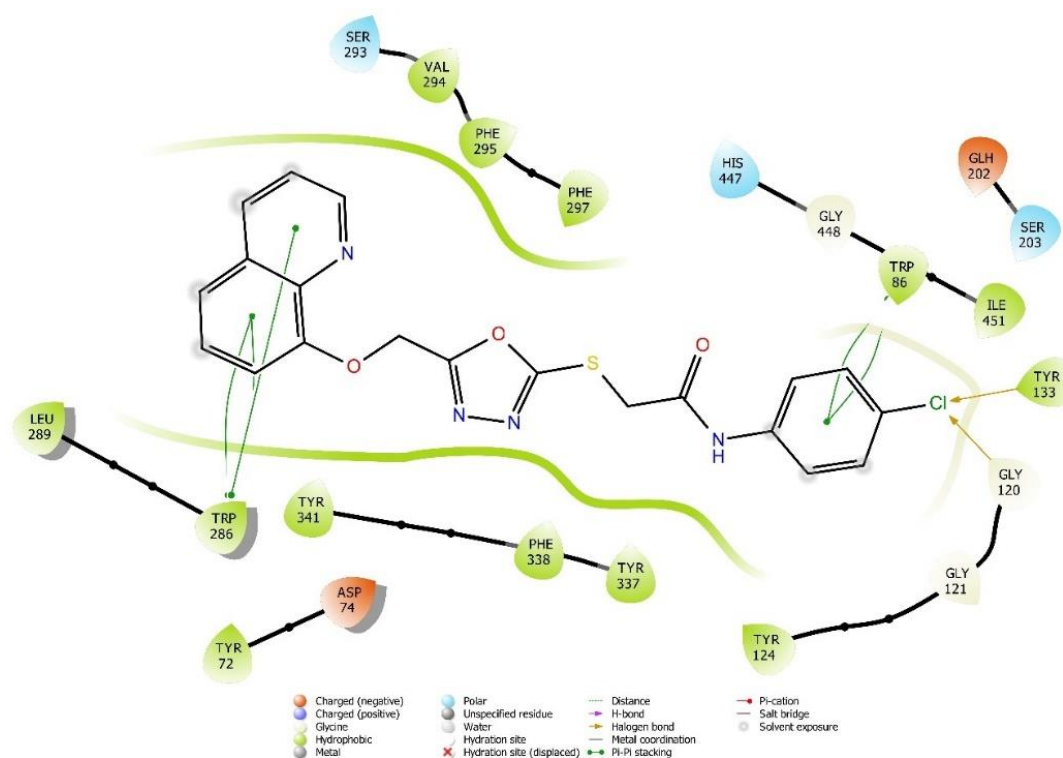
Figure 5.67. *Two-dimensional interactions of compound **5a** at the binding region (PBDID: 4EY7)*

5.7.3. Molecular docking of compound 5c

According to molecular docking study results, like compound **5a**, compound **5c** allowed five π–π interactions. Two of them were performed between the quinoline ring and Trp86. While the oxadiazole ring displayed two π–π stacking interactions with Tyr337 and Tyr341. Another π–π stacking was observed between the phenyl ring and Trp286. Interestingly, the phenyl ring has shown additional two Ar-H interactions between the phenyl H_2, H_4 and Tyr341, and Arg296. The quinoline C_2-H interacted with Ser125 by Ar-H interaction. The positioning was also strengthened by the hydrogen bonding between Phe295 and the carbonyl group. The interactions of compound **5c** with the active site residues are illustrated in (**Figure 5.58**) and (**Figure 5.59**).
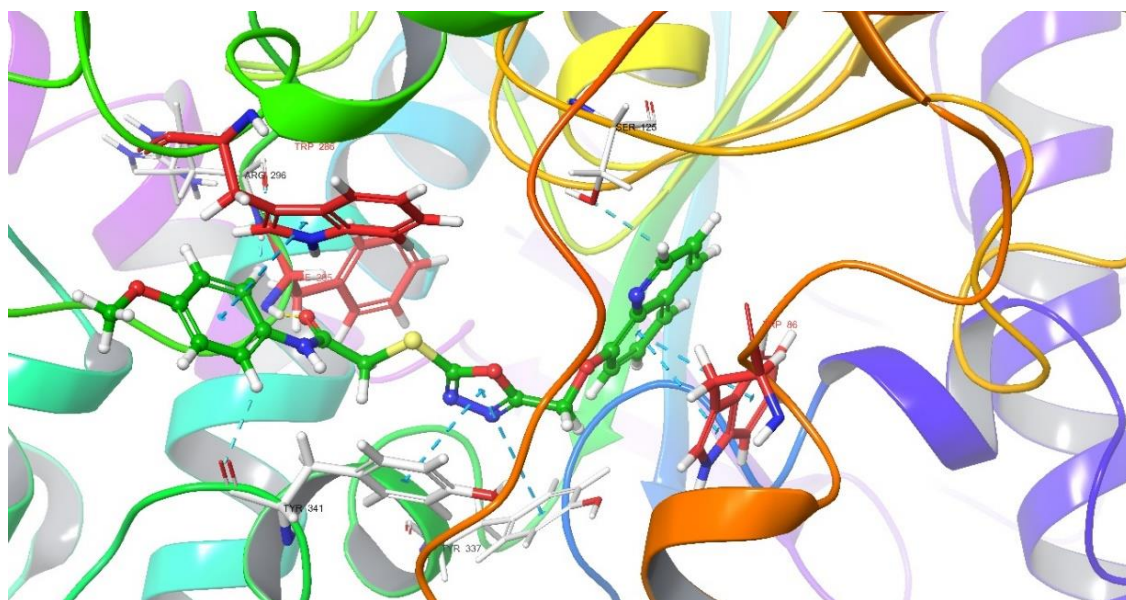
Figure 5.68. *Three-dimensional interactions of compound 5c at the binding region (PBDID: 4EY7)*

113
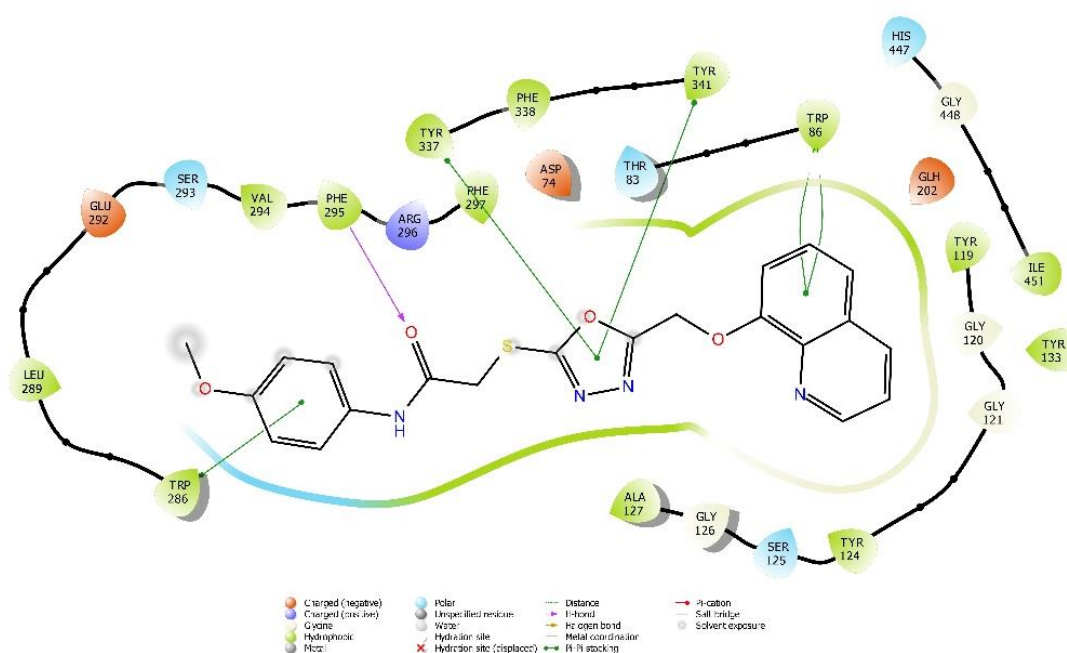
Figure 5.69. *Two-dimensional interactions of compound **5c** at the binding region (PBDID: 4EY7)*

5.7.4. Molecular docking of compound 6a

According to molecular modeling results, it has been observed that the quinoline ring is in interaction with the indole residue of Trp86 by π-π interaction. Another π-π interaction is detected between the oxadiazole ring and Tyr341. Also, the carbonyl moiety of the structure interacts with Phe295 forming a hydrogen interaction. Besides, the quinoline C_3-H and C_6-H create Ar-H interactions with Tyr133 and His447, respectively. The interactions of compound **6c** with the active site are illustrated in (**Figure 5.60**) and (**Figure 5.61**).
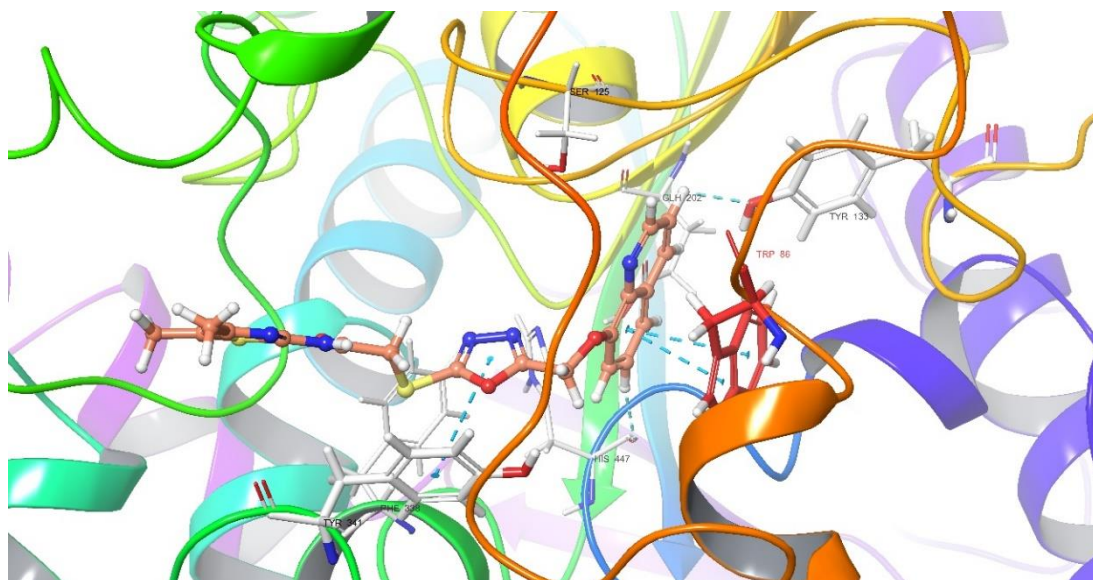
Figure 5.70. *Three-dimensional interactions of compound **6a** at the binding region (PBDID: 4EY7)*
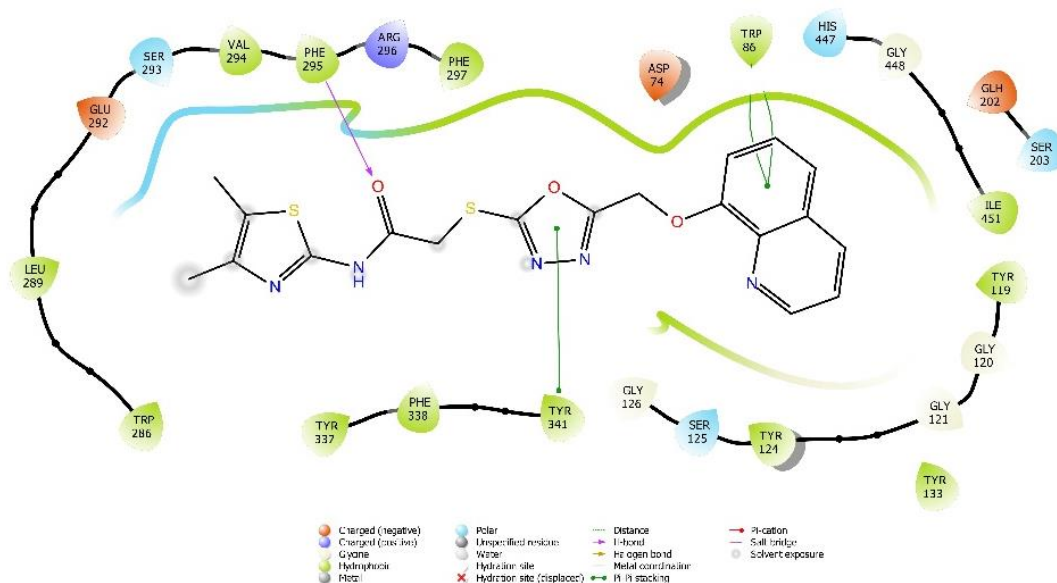
Figure 5.71. *Two-dimensional interactions of compound **6a** at the binding region (PBDID: 4EY7)*

5.7.5. Molecular docking results evaluation

According to the aforementioned results, compounds **5a, 5c** and **6a** showed the ability to interact with Trp86 and Tyr341 similarly to the reference drug donepezil. Compounds **5a** and **5c** bearing 4-chloro and 4-methoxy substitution on the acetanilide part displayed another fundamental interaction with Trp286 in the PAS. Both **5c** and **6a** compounds exhibited the potential to interact with Phe295. **6a** provided crucial interactions with one part of the catalytic triad amino acids His447. All the previous interactions have been performed by the potent AChE inhibitor,

donepezil. Therefore, it is anticipated that **5a,5c** and **6a** compounds retain high inhibitory action against AChE similar to donepezil.

It has also revealed that **5a** and **6a** possess the potential to interact with Tyr133 that participate in the accommodation of these compounds similar to that involved in huperzine A interaction with AChE [158].

Interestingly, compound **5a** has the ability to bind with Gly120 which is considered a part of the glycine loop that constitutes the gorge walls beside the catalytic serine. This interaction may affect the glycine loop's conformation which is considered one of the key determinants in the huperzine active center geometry [152].

It has been also demonstrated that Tyr337 is involved in the compound **5c** interactions with the enzyme playing a central role in its positioning in the same manner as huperzine A and tacrine [158]. Besides, it is predicted that Ser125 stabilizes the compound **5c** in the pocket in a similar way to aflatoxins stabilization in the CAS [159]. It is also suggested that the compound **5c** positioning is strengthened by the bonding with Arg296 [160].

Based on these findings, *in-vitro* enzyme study outcomes have consorted with *in-silico* study results.

5.8. Structure-Activity Relationship Evaluation
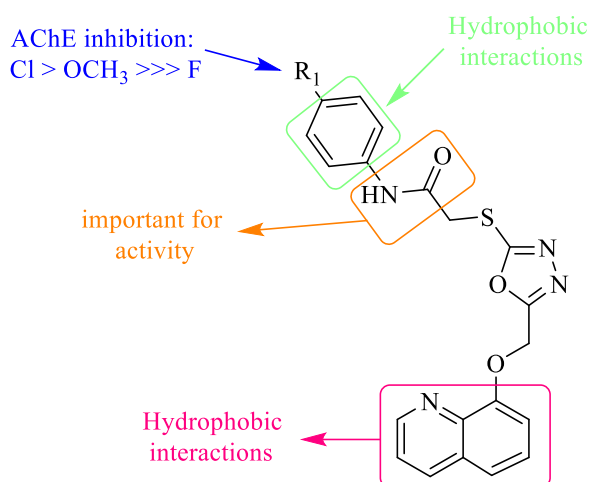
Figure 5.72. *Structure-activity relationship*

Based on activity results and molecular docking studies, the preliminary structure-activity relationship might be explained in multiple points. Firstly, the presence of the quinoline ring bears significant importance in the activity explained by its ability to perform hydrophobic interactions within the binding site of the AChE enzyme. Secondly, the replacement of the amide group between the thioether bridge and the aromatic ring by a carbonyl group results in a marked decrease in the compound's potency. Furthermore, 4-substituted phenyl exhibits a notable inhibitory action due to its ability to interact with the binding site by π-π interactions; Thus, replacing the 4-substituted phenyl with 4,5-substituted thiazole-2-yl produces a pronounce declining in the activity. Nevertheless, phenyl substitution with 4-chloro and 4-methoxy groups indicates a superior inhibition towards AChE [161], conversely, the introduction of a fluorine atom at the para position of the phenyl ring might dramatically reduce the inhibitory activity.

6. CONCLUDING REMARKS AND FUTURE RECOMMENDATIONS

In considering the design of novel anticholinesterase and monoamine oxidase inhibitors, a series of quinoline-oxadiazole hybrids have been synthesized and evaluated as potential candidates to tread AD. The 1,3,4-oxadiazole ring was closed by reacting 2-(quinolin-8-yloxy) acetohydrazide with carbon disulfide under basic conditions. The final products were attained using two different SN_2 reaction procedures. The first one was proceeded using acetone and the weak base potassium carbonate at ambient temperature while the other was performed in acetonitrile and the strong base sodium hydroxide at reflux temperature. The second method introduced a higher reaction rate and enhanced yield. The final products were analyzed using spectrometric analysis methods. Regarding anticholinesterase inhibition, compounds **5a, 5c** and **6a** were the most potent structures against AChE with 0.033 µM, 0.096 µM and 0.177 µM, respectively, while none of the synthesized structures showed a significant inhibitory action against BuChE. The compounds were also screened for their ability to inhibit MAO-A and MAO-B enzymes. The inhibition percentages were less than 50% at 10^{-3} and 10^{-4} therefore the compounds' IC_{50}s were not calculated. The physicochemical properties of **5a, 5c** and **6a** were calculated in comparison to donepezil. Besides, the binding modes of the potent structures with AChE were studied using molecular modeling methods. By combining the activity results with molecular docking findings, the higher potency of compound **5a** was explained by its ability to interact with the critical amino acid residues in the active site similarly to donepezil. It was also revealed that **5c** retains the ability to bind with the PAS and CAS of AChE enzyme. Dual inhibition of AChE by **5c** expects its additional neuroprotective effect through decreasing amyloid plaques deposition. Structural-activity relationship was also explained.

For future works, further modifications of compound **5c** as a dual inhibitor for AChE are recommended. The modifications might be done be implemented by introducing further substitution to the quinoline expecting better interactions within the binding site.

REFERENCES

[1] Weller, J., Budson, A. (2018). Current understanding of Alzheimer's disease diagnosis and treatment. *F1000Res,* 7.

[2] (2021): Dementia. World Health Organization., https://www.who.int/news-room/fact-sheets/detail/dementia (Accessed 3 April 2022).

[3] Revadigar, V., Ghalib, R.M., Murugaiyah, V., Embaby, M.A., Jawad, A., Mehdi, S.H., Hashim, R., Sulaiman, O. (2014). Enzyme Inhibitors Involved in the Treatment of Alzheimer's Disease, *Drug Design and Discovery in Alzheimer's Disease* (p. 142-198).

[4] (2020). 2020 Alzheimer's disease facts and figures. *Alzheimers Dement.,* https://www.ncbi.nlm.nih.gov/pubmed/32157811 (Accessed 3 April 2022).

[5] Qiu, C., Kivipelto, M., von Strauss, E. (2022). Epidemiology of Alzheimer's disease: occurrence, determinants, and strategies toward intervention. *Dialogues Clin. Neurosci.,* 11 (2), 111-128.

[6] Abeysinghe, A., Deshapriya, R., Udawatte, C. (2020). Alzheimer's disease; a review of the pathophysiological basis and therapeutic interventions. *Life Sci.,* 256, 117996.

[7] Imbimbo, B.P., Lombard, J., Pomara, N. (2005). Pathophysiology of Alzheimer's disease. *Neuroimaging Clin. N. Am.,* 15 (4), 727-753, ix.

[8] Sanabria-Castro, A., Alvarado-Echeverria, I., Monge-Bonilla, C. (2017). Molecular Pathogenesis of Alzheimer's Disease: An Update. *Ann Neurosci,* 24 (1), 46-54.

[9] Ferreira, J.P.S., Albuquerque, H.M.T., Cardoso, S.M., Silva, A.M.S., Silva, V.L.M. (2021). Dual-target compounds for Alzheimer's disease: Natural and synthetic AChE and BACE-1 dual-inhibitors and their structure-activity relationship (SAR). *Eur. J. Med. Chem.,* 221, 113492.

[10] Tatulian, S.A. (2022). Challenges and hopes for Alzheimer's disease. *Drug Discov Today,* 27 (4), 1027-1043.

[11] Goedert, M., Spillantini, M.G., Crowther, R.A. (1991). Tau proteins and neurofibrillary degeneration. *Brain Pathol.,* 1 (4), 279-286.

[12] Feng, Y., Wang, X. (2012). Antioxidant therapies for Alzheimer's disease. *Oxid. Med. Cell. Longev.,* 2012, 472932.

[13] Pizzinat, N., Copin, N., Vindis, C., Parini, A., Cambon, C. (1999). Reactive oxygen species production by monoamine oxidases in intact cells. *Naunyn Schmiedebergs Arch. Pharmacol.,* 359 (5), 428-431.

[14] Shih, J.C., Thompson, R.F. (1999). Monoamine oxidase in neuropsychiatry and behavior. *Am. J. Hum. Genet.,* 65 (3), 593-598.

[15] Yeung, A.W.K., Georgieva, M.G., Atanasov, A.G., Tzvetkov, N.T. (2019). Monoamine Oxidases (MAOs) as Privileged Molecular Targets in Neuroscience: Research Literature Analysis. *Front. Mol. Neurosci.,* 12, 143.

[16] Saura, J., Luque, J.M., Cesura, A.M., Prada, M.D., Chan-Palay, V., Huber, G., Löffler, J., Richards, J.G. (1994). Increased monoamine oxidase b activity in plaque-associated astrocytes of Alzheimer brains revealed by quantitative enzyme radioautography. *Neuroscience,* 62 (1), 15-30.

[17] Riederer, P. (2004). Monoamine Oxidase-B Inhibition in Alzheimer's Disease. *Neurotoxicology,* 25 (1-2), 271-277.

[18] Manzoor, S., Hoda, N. (2020). A comprehensive review of monoamine oxidase inhibitors as Anti-Alzheimer's disease agents: A review. *Eur. J. Med. Chem.,* 206, 112787.

[19] Pohanka, M. (2011). Cholinesterases, a target of pharmacology and toxicology. *Biomed. Pap. Med. Fac. Univ. Palacky Olomouc Czech. Repub.,* 155 (3), 219-229.

[20] Saxena, M., Dubey, R. (2019). Target Enzyme in Alzheimer's Disease: Acetylcholinesterase Inhibitors. *Curr. Top. Med. Chem.,* 19 (4), 264-275.

[21] Hampel, H., Mesulam, M.M., Cuello, A.C., Farlow, M.R., Giacobini, E., Grossberg, G.T., Khachaturian, A.S., Vergallo, A., Cavedo, E., Snyder, P.J., Khachaturian, Z.S. (2018). The cholinergic system in the pathophysiology and treatment of Alzheimer's disease. *Brain,* 141 (7), 1917-1933.

[22] Li, Q., He, S., Chen, Y., Feng, F., Qu, W., Sun, H. (2018). Donepezil-based multi-functional cholinesterase inhibitors for treatment of Alzheimer's disease. *Eur. J. Med. Chem.,* 158, 463-477.

[23] Greig, N.H., Lahiri, D.K., Sambamurti, K. (2002). Butyrylcholinesterase: an important new target in Alzheimer's disease therapy. *Int. Psychogeriatr.,* 14 Suppl 1, 77-91.

[24] Diamant, S., Podoly, E., Friedler, A., Ligumsky, H., Livnah, O., Soreq, H. (2006). Butyrylcholinesterase attenuates amyloid fibril formation in vitro. *Proc. Natl. Acad. Sci. U. S. A.,* 103 (23), 8628-8633.

[25] Crismon, M.L. (1994). Tacrine: first drug approved for Alzheimer's disease. *Ann. Pharmacother.,* 28 (6), 744-751.

[26] Hollmann, P. (2022). Update: FDA approval of Biogen's aducanumab. *Geriatr. Nurs.,* 43, 318-319.

[27] (2021): How Is Alzheimer's Disease Treated?. NIH National Institute on Aging (NIA).

[28] Bartorelli, L., Giraldi, C., Saccardo, M., Cammarata, S., Bottini, G., Fasanaro, A.M., Trequattrini, A. (2005). Effects of switching from an AChE inhibitor to a dual AChE-BuChE inhibitor in patients with Alzheimer's disease. *Curr. Med. Res. Opin.,* 21 (11), 1809-1817.

[29] Nordberg, A., Ballard, C., Bullock, R., Darreh-Shori, T., Somogyi, M. (2013). A review of butyrylcholinesterase as a therapeutic target in the treatment of Alzheimer's disease. *Prim. Care Companion CNS Disord.,* 15 (2).

[30] Singh, M., Kaur, M., Kukreja, H., Chugh, R., Silakari, O., Singh, D. (2013). Acetylcholinesterase inhibitors as Alzheimer therapy: from nerve toxins to neuroprotection. *Eur. J. Med. Chem.,* 70, 165-188.

[31] Jana, A., Bhattacharjee, A., Das, S.S., Srivastava, A., Choudhury, A., Bhattacharjee, R., De, S., Perveen, A., Iqbal, D., Gupta, P.K., Jha, S.K., Ojha, S., Singh, S.K., Ruokolainen, J., Jha, N.K., Kesari, K.K., Ashraf, G.M. (2022). Molecular Insights into Therapeutic Potentials of Hybrid Compounds Targeting Alzheimer's Disease. *Mol. Neurobiol., 1-7.*

[32] Dorababu, A. (2022). Promising heterocycle-based scaffolds in recent (2019-2021) anti-Alzheimer's drug design and discovery. *Eur. J. Pharmacol.,* 920, 174847.

[33] Oliveira, C., Bagetta, D., Cagide, F., Teixeira, J., Amorim, R., Silva, T., Garrido, J., Remiao, F., Uriarte, E., Oliveira, P.J., Alcaro, S., Ortuso, F., Borges, F. (2019). Benzoic acid-derived nitrones: A new class of potential acetylcholinesterase inhibitors and neuroprotective agents. *Eur. J. Med. Chem.,* 174, 116-129.

[34] Yun, Y., Yang, J., Miao, Y., Wang, X., Sun, J. (2020). Synthesis and biological evaluation of 4-arylcoumarins as potential anti-Alzheimer's disease agents. *Bioorg. Med. Chem. Lett.,* 30 (4), 126900.

[35] Umar, T., Shalini, S., Raza, M.K., Gusain, S., Kumar, J., Seth, P., Tiwari, M., Hoda, N. (2019). A multifunctional therapeutic approach: Synthesis, biological evaluation, crystal structure and molecular docking of diversified 1H-pyrazolo[3,4-b]pyridine derivatives against Alzheimer's disease. *Eur. J. Med. Chem.,* 175, 2-19.

[36] Zhu, D., Chen, M., Li, M., Luo, B., Zhao, Y., Huang, P., Xue, F., Rapposelli, S., Pi, R., Wen, S. (2013). Discovery of novel N-substituted carbazoles as neuroprotective agents with potent anti-oxidative activity. *Eur. J. Med. Chem.,* 68, 81-88.

[37] Kosak, U., Strasek, N., Knez, D., Jukic, M., Zakelj, S., Zahirovic, A., Pislar, A., Brazzolotto, X., Nachon, F., Kos, J., Gobec, S. (2020). N-alkylpiperidine carbamates as potential anti-Alzheimer's agents. *Eur. J. Med. Chem.,* 197, 112282.

[38] Wichur, T., Wieckowska, A., Wieckowski, K., Godyn, J., Jonczyk, J., Valdivieso, A.D.R., Panek, D., Pasieka, A., Sabate, R., Knez, D., Gobec, S., Malawska, B. (2020). 1-Benzylpyrrolidine-3-amine-based BuChE inhibitors with anti-aggregating, antioxidant and metal-chelating properties as multifunctional agents against Alzheimer's disease. *Eur. J. Med. Chem.,* 187, 111916.

[39] Turkan, F., Cetin, A., Taslimi, P., Gulcin, I. (2018). Some pyrazoles derivatives: Potent carbonic anhydrase, alpha-glycosidase, and cholinesterase enzymes inhibitors. *Arch. Pharm. (Weinheim),* 351 (10), e1800200.

[40] Yurttaş, L., Özkay, Y., Karaca Gençer, H., Acar, U. (2015). Synthesis of Some New Thiazole Derivatives and Their Biological Activity Evaluation. *Journal of Chemistry,* 2015, 1-7.

[41] Anjali, J., Sen, A., Malla, R.R. (2021). Chemistry of Oxadiazole Analogues: Current Status and Applications. *Russ. J. Bioorganic Chem.,* 47 (3), 670-680.

[42] Kumari, S., Kumar, R., Mazumder, A., Salahuddin, Saxena, S., Sharma, D., Joshi, S., Abdullah, M.M. (2021). Recent updates on Synthetic Strategies and Biological Potential of 1,3,4-oxadiazole: Review. *Lett. Org. Chem.,* 19.

[43] Verma, G., Khan, M.F., Akhtar, W., Alam, M.M., Akhter, M., Shaquiquzzaman, M. (2019). A Review Exploring Therapeutic Worth of 1,3,4-Oxadiazole Tailored Compounds. *Mini Rev. Med. Chem.,* 19 (6), 477-509.

[44] Siwach, A., Verma, P.K. (2020). Therapeutic potential of oxadiazole or furadiazole containing compounds. *BMC Chem,* 14 (1), 70.

[45] Mei, W.-w., Ji, S.-s., Xiao, W., Wang, X.-d., Jiang, C.-s., Ma, W.-q., Zhang, H.-y., Gong, J.-x., Guo, Y.-w. (2017). Synthesis and biological evaluation of

benzothiazol-based 1,3,4-oxadiazole derivatives as amyloid β-targeted compounds against Alzheimer's disease. *Monatsh. Chem.,* 148 (10), 1807-1815.

[46] Saitoh, M., Kunitomo, J., Kimura, E., Hayase, Y., Kobayashi, H., Uchiyama, N., Kawamoto, T., Tanaka, T., Mol, C.D., Dougan, D.R., Textor, G.S., Snell, G.P., Itoh, F. (2009). Design, synthesis and structure-activity relationships of 1,3,4-oxadiazole derivatives as novel inhibitors of glycogen synthase kinase-3beta. *Bioorg. Med. Chem.,* 17 (5), 2017-2029.

[47] Onishi, T., Iwashita, H., Uno, Y., Kunitomo, J., Saitoh, M., Kimura, E., Fujita, H., Uchiyama, N., Kori, M., Takizawa, M. (2011). A novel glycogen synthase kinase-3 inhibitor 2-methyl-5-(3-{4-[(S)-methylsulfinyl]phenyl}-1-benzofuran-5-yl)-1,3,4-oxadiazole decreases tau phosphorylation and ameliorates cognitive deficits in a transgenic model of Alzheimer's disease. *J. Neurochem.,* 119 (6), 1330-1340.

[48] Lo Monte, F., Kramer, T., Gu, J., Brodrecht, M., Pilakowski, J., Fuertes, A., Dominguez, J.M., Plotkin, B., Eldar-Finkelman, H., Schmidt, B. (2013). Structure-based optimization of oxadiazole-based GSK-3 inhibitors. *Eur. J. Med. Chem.,* 61, 26-40.

[49] Wang, M., Liu, T., Chen, S., Wu, M., Han, J., Li, Z. (2021). Design and synthesis of 3-(4-pyridyl)-5-(4-sulfamido-phenyl)-1,2,4-oxadiazole derivatives as novel GSK-3beta inhibitors and evaluation of their potential as multifunctional anti-Alzheimer agents. *Eur. J. Med. Chem.,* 209, 112874.

[50] Elghazawy, N.H., Zaafar, D., Hassan, R.R., Mahmoud, M.Y., Bedda, L., Bakr, A.F., Arafa, R.K. (2022). Discovery of New 1,3,4-Oxadiazoles with Dual Activity Targeting the Cholinergic Pathway as Effective Anti-Alzheimer Agents. *ACS Chem. Neurosci.,* 13 (8), 1187-1205.

[51] Karabelyov, V., Kondeva-Burdina, M., Angelova, V.T. (2021). Synthetic approaches to unsymmetrical 2,5-disubstituted 1,3,4-oxadiazoles and their MAO-B inhibitory activity. A review. *Bioorg. Med. Chem.,* 29, 115888.

[52] Tok, F., Ugras, Z., Saglik, B.N., Ozkay, Y., Kaplancikli, Z.A., Kocyigit-Kaymakcioglu, B. (2021). Novel 2,5-disubstituted-1,3,4-oxadiazole derivatives as MAO-B inhibitors: Synthesis, biological evaluation and molecular modeling studies. *Bioorg. Chem.,* 112, 104917.

[53] Yadav, P., Shah, K. (2021). Quinolines, a perpetual, multipurpose scaffold in medicinal chemistry. *Bioorg. Chem.,* 109, 104639.

[54] Weyesa, A., Mulugeta, E. (2020). Recent advances in the synthesis of biologically and pharmaceutically active quinoline and its analogues: a review. *RSC Adv,* 10 (35), 20784-20793.

[55] Moor, L.F.E., Vasconcelos, T.R.A., da, R.R.R., Pinto, L.S.S., da Costa, T.M. (2021). Quinoline: An Attractive Scaffold in Drug Design. *Mini Rev. Med. Chem.,* 21 (16), 2209-2226.

[56] Vandekerckhove, S., D'Hooghe, M. (2015). Quinoline-based antimalarial hybrid compounds. *Bioorg. Med. Chem.,* 23 (16), 5098-5119.

[57] Muruganantham, N., Sivakumar, R., Anbalagan, N., Gunasekaran, V., Leonard, J.T. (2004). Synthesis, anticonvulsant and antihypertensive activities of 8-substituted quinoline derivatives. *Biol. Pharm. Bull.,* 27 (10), 1683-1687.

[58] Marella, A., Tanwar, O.P., Saha, R., Ali, M.R., Srivastava, S., Akhter, M., Shaquiquzzaman, M., Alam, M.M. (2013). Quinoline: A versatile heterocyclic. *Saudi Pharm. J.,* 21 (1), 1-12.

[59] Jain, S., Chandra, V., Kumar Jain, P., Pathak, K., Pathak, D., Vaidya, A. (2019). Comprehensive review on current developments of quinoline-based anticancer agents. *Arab. J. Chem.,* 12 (8), 4920-4946.

[60] Koga, H., Itoh, A., Murayama, S., Suzue, S., Irikura, T. (1980). Structure-activity relationships of antibacterial 6,7- and 7,8-disubstituted 1-alkyl-1,4-dihydro-4-oxoquinoline-3-carboxylic acids. *J. Med. Chem.,* 23 (12), 1358-1363.

[61] Musiol, R., Jampilek, J., Buchta, V., Silva, L., Niedbala, H., Podeszwa, B., Palka, A., Majerz-Maniecka, K., Oleksyn, B., Polanski, J. (2006). Antifungal properties of new series of quinoline derivatives. *Bioorg. Med. Chem.,* 14 (10), 3592-3598.

[62] Liu, Z.C., Wang, B.D., Yang, Z.Y., Li, Y., Qin, D.D., Li, T.R. (2009). Synthesis, crystal structure, DNA interaction and antioxidant activities of two novel water-soluble Cu2+ complexes derived from 2-oxo-quinoline-3-carbaldehyde Schiff-bases. *Eur. J. Med. Chem.,* 44 (11), 4477-4484.

[63] Salahuddin, Mazumder, A., Yar, M.S., Mazumder, R., Chakraborthy, G.S., Ahsan, M.J., Rahman, M.U. (2017). Updates on synthesis and biological activities of 1,3,4-oxadiazole: A review. *Synth. Commun.,* 47 (20), 1805-1847.

[64] Ajani, O.O., Iyaye, K.T. (2020). Recent advances on oxadiazole motifs: Synthesis, reactions and biological activities. *Mediterranean Journal of Chemistry,* 10 (5).

[65] Saha, R., Tanwar, O., Marella, A., Alam, M.M., Akhter, M. (2013). Recent updates on biological activities of oxadiazoles. *Mini Rev. Med. Chem.,* 13 (7), 1027-1046.

[66] Bostrom, J., Hogner, A., Llinas, A., Wellner, E., Plowright, A.T. (2012). Oxadiazoles in medicinal chemistry. *J. Med. Chem.,* 55 (5), 1817-1830.

[67] Lima, L.M., Barreiro, E.J. (2005). Bioisosterism: a useful strategy for molecular modification and drug design. *Curr. Med. Chem.,* 12 (1), 23-49.

[68] Maryan, L., Marta, M., Myroslava, K., Iryna, D., Stefan, H., Taras, C., Ihor, C., Vasyl, M. (2020). Approaches for synthesis and chemical modification of non-condensed heterocyclic systems based on 1,3,4-oxadiazole ring and their biological activity: A review. J. Appl. Pharm. Sci. 10(10)*, 151-165.*

[69] Patel, K.D., Prajapati, S.M., Panchal, S.N., Patel, H.D. (2014). Review of Synthesis of 1,3,4-Oxadiazole Derivatives. *Synth. Commun.,* 44 (13), 1859-1875.

[70] Hetzheim, A., Möckel, K. (1967). Recent Advances in 1, 3, 4-Oxadiazole Chemistry, *Advances in Heterocyclic Chemistry Volume 7,* (p. 183-224).

[71] Hoggarth, E. (1952). 938. 2-Benzoyldithiocarbazinic acid and related compounds. *J. Chem. Soc., (Resumed),* 4811-4817.

[72] Young, R.W., Wood, K.H. (2002). The Cyclization of 3-Acyldithiocarbazate Esters1. *J. Am. Chem. Soc.,* 77 (2), 400-403.

[73] Kuo, S.C., Wu, C.H., Huang, L.J., Yamamoto, K., Yoshina, S. (1981). Synthesis and antimicrobial Activity of methyl 5-nitro-3,4-diphenylfuran-2-carboxylate and related compounds. *Chem. Pharm. Bull. (Tokyo),* 29 (3), 635-645.

[74] Joshi, S., Karnik, A.V. (2006). Facile Conversion of Acyldiithiocarbazinate Salts to 1,3,4-Oxadiazole Derivatives under Microwave Irradiation. *Synth. Commun.,* 32 (1), 111-114.

[75] Soleiman-Beigi, M., Aryan, R., Yousofizadeh, M., Khosravi, S. (2013). A Combined Synthetic and DFT Study on the Catalyst-Free and Solvent-Assisted Synthesis of 1,3,4-Oxadiazole-2-thiol Derivatives. *J. Chem.,* 2013, 1-6.

[76] Tang, W., Yu, H., Cai, C., Zhao, T., Lu, C., Zhao, S., Lu, X. (2020). Solvent effects on a derivative of 1,3,4-oxadiazole tautomerization reaction in water: A reaction density functional theory study. *Chem. Eng. Sci.,* 213, 115380.

[77] Futaki, K., Tosa, S. (1960). Studies on the Synthesis of 3-Alkyl-5, 6, 7, 8-tetrahydro-s-triazolo [4, 3-b] [1, 2, 4] triazine-6, 7-diones. *Chem. Pharm. Bull. (Tokyo),* 8 (10), 908-912.

[78] Košmrlj, J., Kočevar, M., Polanc, S. (1996). A Mild Approach to 1,3,4-Oxadiazoles and Fused 1,2,4-Triazoles. Diazenes as Intermediates? *Synlett,* 1996 (07), 652-654.

[79] Yang, S.J., Lee, S.H., Kwak, H.J., Gong, Y.D. (2013). Regioselective synthesis of 2-amino-substituted 1,3,4-oxadiazole and 1,3,4-thiadiazole derivatives via reagent-based cyclization of thiosemicarbazide intermediate. *J. Org. Chem.,* 78 (2), 438-444.

[80] Shelke, S., Mhaske, G., Gadakh, S., Gill, C. (2010). Green synthesis and biological evaluation of some novel azoles as antimicrobial agents. *Bioorg. Med. Chem. Lett.,* 20 (24), 7200-7204.

[81] Nesynov, E.P., Grekov, A.P. (1964). The chemistry of 1,3,4-oxadiazole derivatves. *Russ. Chemi. Rev.,* 33, 508-514.

[82] Rivera, N.R., Balsells, J., Hansen, K.B. (2006). Synthesis of 2-amino-5-substituted-1,3,4-oxadiazoles using 1,3-dibromo-5,5-dimethylhydantoin as oxidant. *Tetrahedron Lett.,* 47 (28), 4889-4891.

[83] Dolman, S.J., Gosselin, F., O'Shea, P.D., Davies, I.W. (2006). Superior reactivity of thiosemicarbazides in the synthesis of 2-amino-1,3,4-oxadiazoles. *J. Org. Chem.,* 71 (25), 9548-9551.

[84] Guin, S., Rout, S.K., Ghosh, T., Khatun, N., Patel, B.K. (2012). A one pot synthesis of [1,3,4]-oxadiazoles mediated by molecular iodine. *RSC Advances,* 2 (8)

[85] Sainsbury, M. (1964). Five-Membered Heterocyclic Compounds with Three Hetero-Atoms in the Ring, *Rodd's Chemistry of Carbon Compounds,* (p. 1-209).

[86] Mashraqui, S.H., Ghadigaonkar, S.G., Kenny, R.S. (2006). An Expeditious and Convenient One Pot Synthesis of 2,5-Disubstituted-1,3,4-oxadiazoles. *Synth. Commun.,* 33 (14), 2541-2545.

[87] Link, H. (1978). Synthese von 1, 3, 4-Oxadiazolen und 4, 5-Dihydro-1, 2, 4-triazinen aus 3-Dimethylamino-2, 2-dimethyl-2H-azirin und Carbohydraziden. *Helv. Chim. Acta,* 61 (7), 2419-2427.

[88] Rigo, B., Caullez, P., Fasseur, D., Couturier, D. (1988). Acid Catalyzed Cyclization of Bis Silyl Diacylhydrazines: A New 1, 3, 4-Oxadiazole Synthesis. *Synth. Commun.,* 18 (11), 1247-1251.

[89] Yang, R., Dai, L. (2002). Hypervalent iodine oxidation of N-acylhydrazones and N-phenylsemicarbazone: an efficient method for the synthesis of derivatives of

1,3,4-oxadiazoles and .DELTA.3-1,3,4-oxadiazolines. *J. Org. Chem.,* 58 (12), 3381-3383.

[90] Jedlovská, E., Leško, J. (1994). A Simple One-Pot Procedure for the Synthesis of 1,3,4-Oxadiazoles. *Synth. Commun.,* 24 (13), 1879-1885.

[91] Oussaid, B., Moeini, L., Martin, B., Villemin, D., Garrigues, B. (1995). Improved Synthesis of Oxadiazoles Under Microwave Irradiation. *Synth. Commun.,* 25 (10), 1451-1459.

[92] Isobe, T., Ishikawa, T. (1999). 2-Chloro-1,3-dimethylimidazolinium Chloride. 2. Its Application to the Construction of Heterocycles through Dehydration Reactions. *J. Org. Chem.,* 64 (19), 6989-6992.

[93] Tandon, V.K., Chhor, R.B. (2001). An Efficient One Pot Synthesis of 1,3,4-Oxadiazoles. *Synth. Commun.,* 31 (11), 1727-1732.

[94] Ma, H.-Y., Zha, Z.-G., Zhang, Z.-L., Meng, L., Wang, Z.-Y. (2013). Electrosynthesis of oxadiazoles from benzoylhydrazines. *Chin. Chem. Lett.,* 24 (9), 780-782.

[95] Yu, W., Huang, G., Zhang, Y., Liu, H., Dong, L., Yu, X., Li, Y., Chang, J. (2013). I2-mediated oxidative C-O bond formation for the synthesis of 1,3,4-oxadiazoles from aldehydes and hydrazides. *J. Org. Chem.,* 78 (20), 10337-10343.

[96] Pouliot, M.F., Angers, L., Hamel, J.D., Paquin, J.F. (2012). Synthesis of 1,3,4-oxadiazoles from 1,2-diacylhydrazines using [Et2NSF2]BF4 as a practical cyclodehydration agent. *Org. Biomol. Chem.,* 10 (5), 988-993.

[97] Mazouz, F., Lebreton, L., Milcent, R., Burstein, C. (1990). 5-Aryl-1,3,4-oxadiazol-2(3H)-one derivatives and sulfur analogues as new selective and competitive monoamine oxidase type B inhibitors. *Eur. J. Med. Chem.,* 25 (8), 659-671.

[98] Mazouz, F., Gueddari, S., Burstein, C., Mansuy, D., Milcent, R. (1993). 5-[4-(benzyloxy)phenyl]-1,3,4-oxadiazol-2(3H)-one derivatives and related analogues: new reversible, highly potent, and selective monamine oxidase type B inhibitors. *J. Med. Chem.,* 36 (9), 1157-1167.

[99] Rehman, A., Fatima, A., Abbas, N., Abbasi, M.A., Khan, K.M., Ashraf, M., Ahmad, I., Ejaz, S.A. (2013). Synthesis, characterization and biological screening of 5-substituted-1, 3, 4-oxadiazole-2yl-N-(2-methoxy-5-chlorophenyl)-2-sulfanyl acetamide. *Pak. J. Pharm. Sci,* 26 (2), 345-352.

[100] Siddiqui, S.Z., Rehman, A., Abbasi, M.A., Abbas, N., Khan, K.M., Ashraf, M., Ejaz, S.A. (2013). Synthesis, characterization and biological screening of N-substituted derivatives of 5-benzyl-1, 3, 4-oxadiazole-2yl-2″-sulfanyl acetamide. *Pak. J. Pharm. Sci,* 26 (3), 455-463.

[101] Kamal, A., Shaik, A.B., Reddy, G.N., Kumar, C.G., Joseph, J., Kumar, G.B., Purushotham, U., Sastry, G.N. (2013). Synthesis, biological evaluation, and molecular modeling of (E)-2-aryl-5-styryl-1,3,4-oxadiazole derivatives as acetylcholine esterase inhibitors. *Med. Chem. Res.,* 23 (4), 2080-2092.

[102] Rehman, A.-u., Nafeesa, K., Abbasi, M.A., Siddiqui, S.Z., Rasool, S., Shah, S.A.A., Ashraf, M., Browder, C. (2018). Synthesis of new heterocyclic 3-piperidinyl-1,3,4-oxadiazole derivatives as potential drug candidate for the treatment of Alzheimer's disease. *Cogent Chem.,* 4 (1). 1472197.

[103] Ibrar, A., Khan, A., Ali, M., Sarwar, R., Mehsud, S., Farooq, U., Halimi, S.M.A., Khan, I., Al-Harrasi, A. (2018). Combined in Vitro and in Silico Studies for the Anticholinesterase Activity and Pharmacokinetics of Coumarinyl Thiazoles and Oxadiazoles. *Front Chem,* 6, 61.

[104] Abbasi, M.A., Ramzan, M.S., Aziz ur, R., Siddiqui, S.Z., Shah, S.A.A., Hassan, M., Seo, S.Y., Ashraf, M., Mirza, B., Ismail, H. (2019). N-(5-Methyl-1,3-Thiazol-2-yl)-2-{[5-((Un)Substituted-Phenyl)1,3,4-Oxadiazol-2-yl]Sulfanyl}acetamides. Unique Biheterocycles as Promising Therapeutic Agents. *Russ. J. Bioorganic Chem.,* 44 (6), 801-811.

[105] Ramzan, M.S., Abbasi, M.A., Ur-Rehman, A., Siddiqui, S.Z., Shah, S.A.A., Ashraf, M., Lodhi, M.A., Khan, F.A., Mirza, B. (2018). Synthesis of 2-{[5-(aralkyl/aryl)-1,3,4-oxadiazol-2-yl]sulfanyl}-N-(4-methyl-1,3-thiazol-2-yl)acetamides: Novel bi-heterocycles as potential therapeutic agents. *Trop. J. Pharm. Res.,* 17 (5).

[106] Tripathi, P.N., Srivastava, P., Sharma, P., Seth, A., Shrivastava, S.K. (2019). Design and development of novel N-(pyrimidin-2-yl)-1,3,4-oxadiazole hybrids to treat cognitive dysfunctions. *Bioorg. Med. Chem.,* 27 (7), 1327-1340.

[107] Mishra, P., Sharma, P., Tripathi, P.N., Gupta, S.K., Srivastava, P., Seth, A., Tripathi, A., Krishnamurthy, S., Shrivastava, S.K. (2019). Design and development of 1,3,4-oxadiazole derivatives as potential inhibitors of acetylcholinesterase to ameliorate scopolamine-induced cognitive dysfunctions. *Bioorg. Chem.,* 89, 103025.

[108] Bingul, M., Saglam, M.F., Kandemir, H., Boga, M., Sengul, I.F. (2019). Synthesis of indole-2-carbohydrazides and 2-(indol-2-yl)-1,3,4-oxadiazoles as antioxidants and their acetylcholinesterase inhibition properties. *Monatsh. Chem.,* 150 (8), 1553-1560.

[109] Jain, A., Piplani, P. (2020). Design, synthesis and biological evaluation of triazole-oxadiazole conjugates for the management of cognitive dysfunction. *Bioorg. Chem.,* 103, 104151.

[110] Tripathi, A., Choubey, P.K., Sharma, P., Seth, A., Saraf, P., Shrivastava, S.K. (2020). Design, synthesis, and biological evaluation of ferulic acid based 1,3,4-oxadiazole hybrids as multifunctional therapeutics for the treatment of Alzheimer's disease. *Bioorg. Chem.,* 95, 103506.

[111] Mirzazadeh, R., Asgari, M.S., Barzegari, E., Pedrood, K., Mohammadi-Khanaposhtani, M., Sherafati, M., Larijani, B., Rastegar, H., Rahmani, H., Mahdavi, M., Taslimi, P., Uc, E.M., Gulcin, I. (2021). New quinoxalin-1,3,4-oxadiazole derivatives: Synthesis, characterization, in vitro biological evaluations, and molecular modeling studies. *Arch. Pharm. (Weinheim),* 354 (9), e2000471.

[112] Choubey, P.K., Tripathi, A., Tripathi, M.K., Seth, A., Shrivastava, S.K. (2021). Design, synthesis, and evaluation of N-benzylpyrrolidine and 1,3,4-oxadiazole as multitargeted hybrids for the treatment of Alzheimer's disease. *Bioorg. Chem.,* 111, 104922.

[113] George, N., Sabahi, B.A., AbuKhader, M., Balushi, K.A., Akhtar, M.J., Khan, S.A. (2022). Design, synthesis and in vitro biological activities of coumarin linked 1,3,4-oxadiazole hybrids as potential multi-target directed anti-Alzheimer agents. *J. King Saud Univ. Sci.,* 34 (4) 101977.

[114] Harfenist, M., Heuser, D.J., Joyner, C.T., Batchelor, J.F., White, H.L. (1996). Selective inhibitors of monoamine oxidase. 3. Structure-activity relationship of tricyclics bearing imidazoline, oxadiazole, or tetrazole groups. *J. Med. Chem.,* 39 (9), 1857-1863.

[115] Ke, S., Li, Z., Qian, X. (2008). 1,3,4-Oxadiazole-3(2H)-carboxamide derivatives as potential novel class of monoamine oxidase (MAO) inhibitors: synthesis, evaluation, and role of urea moiety. *Bioorg. Med. Chem.,* 16 (16), 7565-7572.

[116] Distinto, S., Meleddu, R., Yanez, M., Cirilli, R., Bianco, G., Sanna, M.L., Arridu, A., Cossu, P., Cottiglia, F., Faggi, C., Ortuso, F., Alcaro, S., Maccioni, E. (2016).

Drug design, synthesis, in vitro and in silico evaluation of selective monoaminoxidase B inhibitors based on 3-acetyl-2-dichlorophenyl-5-aryl-2,3-dihydro-1,3,4-oxadiazole chemical scaffold. *Eur. J. Med. Chem.,* 108, 542-552.

[117] Pflegr, V., Stepankova, S., Svrckova, K., Svarcova, M., Vinsova, J., Kratky, M. (2022). 5-Aryl-1,3,4-oxadiazol-2-amines Decorated with Long Alkyl and Their Analogues: Synthesis, Acetyl- and Butyrylcholinesterase Inhibition and Docking Study. *Pharmaceuticals (Basel),* 15 (4), 400.

[118] McKenna, M.T., Proctor, G.R., Young, L.C., Harvey, A.L. (1997). Novel tacrine analogues for potential use against Alzheimer's disease: potent and selective acetylcholinesterase inhibitors and 5-HT uptake inhibitors. *J. Med. Chem.,* 40 (22), 3516-3523.

[119] Carlier, P.R., Chow, E.S., Han, Y., Liu, J., El Yazal, J., Pang, Y.P. (1999). Heterodimeric tacrine-based acetylcholinesterase inhibitors: investigating ligand-peripheral site interactions. *J. Med. Chem.,* 42 (20), 4225-4231.

[120] Camps, P., Formosa, X., Galdeano, C., Munoz-Torrero, D., Ramirez, L., Gomez, E., Isambert, N., Lavilla, R., Badia, A., Clos, M.V., Bartolini, M., Mancini, F., Andrisano, V., Arce, M.P., Rodriguez-Franco, M.I., Huertas, O., Dafni, T., Luque, F.J. (2009). Pyrano[3,2-c]quinoline-6-chlorotacrine hybrids as a novel family of acetylcholinesterase- and beta-amyloid-directed anti-Alzheimer compounds. *J. Med. Chem.,* 52 (17), 5365-5379.

[121] Fernandez-Bachiller, M.I., Perez, C., Gonzalez-Munoz, G.C., Conde, S., Lopez, M.G., Villarroya, M., Garcia, A.G., Rodriguez-Franco, M.I. (2010). Novel tacrine-8-hydroxyquinoline hybrids as multifunctional agents for the treatment of Alzheimer's disease, with neuroprotective, cholinergic, antioxidant, and copper-complexing properties. *J. Med. Chem.,* 53 (13), 4927-4937.

[122] Szymanski, P., Laznickova, A., Laznicek, M., Bajda, M., Malawska, B., Markowicz, M., Mikiciuk-Olasik, E. (2012). 2,3-dihydro-1H-cyclopenta[b]quinoline derivatives as acetylcholinesterase inhibitors-synthesis, radiolabeling and biodistribution. *Int. J. Mol. Sci.,* 13 (8), 10067-10090.

[123] Khorana, N., Changwichit, K., Ingkaninan, K., Utsintong, M. (2012). Prospective acetylcholinesterase inhibitory activity of indole and its analogs. *Bioorg. Med. Chem. Lett.,* 22 (8), 2885-2888.

[124] Wang, X.Q., Xia, C.L., Chen, S.B., Tan, J.H., Ou, T.M., Huang, S.L., Li, D., Gu, L.Q., Huang, Z.S. (2015). Design, synthesis, and biological evaluation of 2-arylethenylquinoline derivatives as multifunctional agents for the treatment of Alzheimer's disease. *Eur. J. Med. Chem.,* 89, 349-361.

[125] Zaib, S., Rizvi, S.U., Aslam, S., Ahmad, M., Ali Abid, S.M., Al-Rashida, M., Iqbal, J. (2015). Quinolinyl-thienyl chalcones as monoamine oxidase inhibitors and their in silico modeling studies. *Med. Chem.,* 11 (6), 580-589.

[126] Mantoani, S.P., Chierrito, T.P., Vilela, A.F., Cardoso, C.L., Martinez, A., Carvalho, I. (2016). Novel Triazole-Quinoline Derivatives as Selective Dual Binding Site Acetylcholinesterase Inhibitors. *Molecules,* 21 (2), 193.

[127] Xia, C.L., Wang, N., Guo, Q.L., Liu, Z.Q., Wu, J.Q., Huang, S.L., Ou, T.M., Tan, J.H., Wang, H.G., Li, D., Huang, Z.S. (2017). Design, synthesis and evaluation of 2-arylethenyl-N-methylquinolinium derivatives as effective multifunctional agents for Alzheimer's disease treatment. *Eur. J. Med. Chem.,* 130, 139-153.

[128] Shah, M.S., Najam-Ul-Haq, M., Shah, H.S., Farooq Rizvi, S.U., Iqbal, J. (2018). Quinoline containing chalcone derivatives as cholinesterase inhibitors and their in silico modeling studies. *Comput. Biol. Chem.,* 76, 310-317.

[129] Khan, N.A., Khan, I., Abid, S.M.A., Zaib, S., Ibrar, A., Andleeb, H., Hameed, S., Iqbal, J. (2018). Quinolinic Carboxylic Acid Derivatives as Potential Multi-target Compounds for Neurodegeneration: Monoamine Oxidase and Cholinesterase Inhibition. *Med. Chem.,* 14 (1), 74-85.

[130] Wu, G., Gao, Y., Kang, D., Huang, B., Huo, Z., Liu, H., Poongavanam, V., Zhan, P., Liu, X. (2018). Design, synthesis and biological evaluation of tacrine-1,2,3-triazole derivatives as potent cholinesterase inhibitors. *Medchemcomm.,* 9 (1), 149-159.

[131] Huang, W., Liang, M., Li, Q., Zheng, X., Zhang, C., Wang, Q., Tang, L., Zhang, Z., Wang, B., Shen, Z. (2019). Development of the "hidden" multifunctional agents for Alzheimer's disease. *Eur. J. Med. Chem.,* 177, 247-258.

[132] Youdim, M.B.H. (2022). Site-activated multi target iron chelators with acetylcholinesterase (AChE) and monoamine oxidase (MAO) inhibitory activities for Alzheimer's disease therapy. *J. Neur. Transm. (Vienna),* 1-7.

[133] Yurttaş, L., Kubilay, A., Evren, A.E., Kısacık, İ., Karaca Gençer, H. (2020). Synthesis of some novel 3,4,5-trisubstituted triazole derivatives bearing quinoline

ring and evaluation of their antimicrobial activity. *Phosphorus, Sulfur Silicon Relat. Elem.,* 195 (9), 767-773.

[134] Yurttaş, L., Bülbül, E.F., Tekinkoca, S., Demirayak, Ş. (2017). Antimicrobial activity evaluation of new 1,3,4-oxadiazole derivatives. *Acta. Pharm. Sci.,* 55 (2).

[135] Kaplancikli, Z.A., Yurttas, L., Ozdemir, A., Turan-Zitouni, G., Iscan, G., Akalin, G., Abu Mohsen, U. (2014). Synthesis, anticandidal activity and cytotoxicity of some tetrazole derivatives. *J. Enzyme Inhib. Med. Chem.,* 29 (1), 43-48.

[136] Yurttas, L., Ozkay, Y., Akalin-Ciftci, G., Ulusoylar-Yildirim, S. (2014). Synthesis and anticancer activity evaluation of N-[4-(2-methylthiazol-4-yl)phenyl]acetamide derivatives containing (benz)azole moiety. *J. Enzyme Inhib. Med. Chem.,* 29 (2), 175-184.

[137] Zheng, Q.Z., Zhang, X.M., Xu, Y., Cheng, K., Jiao, Q.C., Zhu, H.L. (2010). Synthesis, biological evaluation, and molecular docking studies of 2-chloropyridine derivatives possessing 1,3,4-oxadiazole moiety as potential antitumor agents. *Bioorg. Med. Chem.,* 18 (22), 7836-7841.

[138] Saglik, B.N., Ilgin, S., Ozkay, Y. (2016). Synthesis of new donepezil analogues and investigation of their effects on cholinesterase enzymes. *Eur. J. Med. Chem.,* 124, 1026-1040.

[139] Demirayak, Ş., Şahin, Z., Ertaş, M., Bülbül, E.F., Bender, C., Biltekin, S.N., Berk, B., Sağlık, B.N., Levent, S., Yurttaş, L. (2019). Novel thiazole-piperazine derivatives as potential cholinesterase inhibitors. *J. Heterocycl. Chem.,* 56 (12), 3370-3386.

[140] Osmaniye, D., Evren, A.E., Saglik, B.N., Levent, S., Ozkay, Y., Kaplancikli, Z.A. (2022). Design, synthesis, biological activity, molecular docking, and molecular dynamics of novel benzimidazole derivatives as potential AChE/MAO-B dual inhibitors. *Arch. Pharm. (Weinheim),* 355 (3), e2100450.

[141] Saglik, B.N., Kaya Cavusoglu, B., Osmaniye, D., Levent, S., Acar Cevik, U., Ilgin, S., Ozkay, Y., Kaplancikli, Z.A., Ozturk, Y. (2019). In vitro and in silico evaluation of new thiazole compounds as monoamine oxidase inhibitors. *Bioorg. Chem.,* 85, 97-108.

[142] Daina, A., Michielin, O., Zoete, V. (2017). SwissADME: a free web tool to evaluate pharmacokinetics, drug-likeness and medicinal chemistry friendliness of small molecules. *Sci. Rep.,* 7 (1), 1-13.

[143] Cheung, J., Rudolph, M.J., Burshteyn, F., Cassidy, M.S., Gary, E.N., Love, J., Franklin, M.C., Height, J.J. (2012). Structures of human acetylcholinesterase in complex with pharmacologically important ligands. *J. Med. Chem.,* 55 (22), 10282-10286.

[144] Ahmed, M., Sharma, R., Nagda, D.P., Jat, J.L., Talesara, G.L. (2006). Synthesis and antimicrobial activity of succinimido(2-aryl-4-oxo-3-{[(quinolin-8-yloxy)acetyl]amino}-1,3-thiazolidin-5-yl)acetates. *ARKIVOC,* 2006 (11), 66-75.

[145] Saeed, A., Perveen, F., Abbas, N., Jamal, S., Floerke, U. (2015). Synthesis, Structure and Quantum Mechanical Calculations of Methyl 2-(5-((Quinolin-8-yloxy)-methyl)-1, 3, 4-oxadiazol-2-ylthio)-acetate. *Chin. J. Chem.,* 34 (6).

[146] Fernandez, D., Aviles, F.X., Vendrell, J. (2009). Aromatic organic compounds as scaffolds for metallocarboxypeptidase inhibitor design. *Chem. Biol. Drug Des.,* 73 (1), 75-82.

[147] Glish, G.L., Vachet, R.W. (2003). The basics of mass spectrometry in the twenty-first century. *Nat. Rev. Drug Discov.,* 2 (2), 140-150.

[148] Ellman, G.L., Courtney, K.D., Andres, V., Featherstone, R.M. (1961). A new and rapid colorimetric determination of acetylcholinesterase activity. *Biochem. Pharmacol.,* 7 (2), 88-95.

[149] Ramsay, R.R., Tipton, K.F. (2017). Assessment of Enzyme Inhibition: A Review with Examples from the Development of Monoamine Oxidase and Cholinesterase Inhibitory Drugs. *Molecules,* 22 (7), 1192.

[150] Imramovsky, A., Stepankova, S., Vanco, J., Pauk, K., Monreal-Ferriz, J., Vinsova, J., Jampilek, J. (2012). Acetylcholinesterase-inhibiting activity of salicylanilide N-alkylcarbamates and their molecular docking. *Molecules,* 17 (9), 10142-10158.

[151] Silman, I., Sussman, J.L. (2008). Acetylcholinesterase: how is structure related to function. *Chem. Biol. Interact.,* 175 (1-3), 3-10.

[152] Ordentlich, A., Barak, D., Kronman, C., Flashner, Y., Leitner, M., Segall, Y., Ariel, N., Cohen, S., Velan, B., Shafferman, A. (1993). Dissection of the human acetylcholinesterase active center determinants of substrate specificity. Identification of residues constituting the anionic site, the hydrophobic site, and the acyl pocket. *J. Biol. Chem.,* 268 (23), 17083-17095.

[153] Dvir, H., Silman, I., Harel, M., Rosenberry, T.L., Sussman, J.L. (2010). Acetylcholinesterase: from 3D structure to function. *Chem. Biol. Interact.,* 187 (1-3), 10-22.

[154] Ghosh, S., Jana, K., Ganguly, B. (2019). Revealing the mechanistic pathway of cholinergic inhibition of Alzheimer's disease by donepezil: a metadynamics simulation study. *Phys. Chem. Chem. Phys.,* 21 (25), 13578-13589.

[155] Makarian, M., Gonzalez, M., Salvador, S.M., Lorzadeh, S., Hudson, P.K., Pecic, S. (2022). Synthesis, kinetic evaluation and molecular docking studies of donepezil-based acetylcholinesterase inhibitors. *J. Mol. Struct.,* 1247.

[156] Pohanka, M. (2012). Acetylcholinesterase inhibitors: a patent review (2008 - present). *Expert Opin. Ther. Pat.,* 22 (8), 871-886.

[157] Lu, S.H., Wu, J.W., Liu, H.L., Zhao, J.H., Liu, K.T., Chuang, C.K., Lin, H.Y., Tsai, W.B., Ho, Y. (2011). The discovery of potential acetylcholinesterase inhibitors: a combination of pharmacophore modeling, virtual screening, and molecular docking studies. *J. Biomed. Sci.,* 18, 8.

[158] Ariel, N., Ordentlich, A., Barak, D., Bino, T., Velan, B., Shafferman, A. (1998). The 'aromatic patch' of three proximal residues in the human acetylcholinesterase active centre allows for versatile interaction modes with inhibitors. *Biochem. J.,* 335 (Pt 1), 95-102.

[159] de Almeida, J., Dolezal, R., Krejcar, O., Kuca, K., Musilek, K., Jun, D., Franca, T.C.C. (2018). Molecular Modeling Studies on the Interactions of Aflatoxin B1 and Its Metabolites with Human Acetylcholinesterase. Part II: Interactions with the Catalytic Anionic Site (CAS). *Toxins (Basel),* 10 (10), 389.

[160] Sahin, Z., Ertas, M., Bender, C., Bulbul, E.F., Berk, B., Biltekin, S.N., Yurttas, L., Demirayak, S. (2018). Thiazole-substituted benzoylpiperazine derivatives as acetylcholinesterase inhibitors. *Drug Dev Res.,* 79 (8), 406-425.

[161] Singh, Y.P., Tej, G., Pandey, A., Priya, K., Pandey, P., Shankar, G., Nayak, P.K., Rai, G., Chittiboyina, A.G., Doerksen, R.J., Vishwakarma, S., Modi, G. (2020). Design, synthesis and biological evaluation of novel naturally-inspired multifunctional molecules for the management of Alzheimer's disease. *Eur. J. Med. Chem.,* 198, 112257.

CURRICULUM VITAE

Name and Surname : Sana SAFFOUR

Place of Birth : Homs, Syria

Email : sasaffour@gamil.com

ORCID : 0000-0001-8124-9315

Education:

Bachelor's degree : Hashemite University, Faculty of Pharmaceutical

Sciences, Zarqaa, Jordan, May 2019

Languages: : Arabic (mother tongue), English, Turkish, French

Articles:

Shahin, R., Shaheen, O., El-Dahiyat, F., Habash, M., & Saffour, S. (2017). Research advances in kinase enzymes and inhibitors for cardiovascular disease treatment. *Future Science OA*, *3*(4), FSO204.

Projects:

Synthesis of novel 1,3,4-oxadiazole and carbothioamide derivatives and evaluation of their anticancer activities. Anadolu University, Publication and Research Incentive Projects, 2022-2023.

Awards:

Master's Scholarship by the Turkish Government (YTB), 2019, Turkey.

Bachelor's Scholarship by the German government and Saïd Foundation (DAFI), 2014, Jordan.